Metabolism regulates cell fate in lymphocytes and progenitor cells

Submitted in partial fulfillment of the
requirements for the degree of
Doctor of Philosophy
under the Executive Committee
of the Graduate School of Arts and Sciences

COLUMBIA UNIVERSITY

2018

Abstract

Metabolism regulates cell fate in lymphocytes and progenitor cells
Radomir Kratchmarov

Self-renewal mediates homeostasis across mammalian organ systems as the cellular components of mature tissues are continually replaced in the face of wear and tear, injury, infection, and malignancy. The hematopoietic and immune systems are crucial for organismal longevity and rely on the ability of progenitor cells to bifurcate in fate to produce mature terminally differentiated progeny while self-renewing to maintain more quiescent progenitors. Asymmetric cell division is associated with self-renewal of lymphocytes and hematopoietic progenitors, but the mechanisms underlying the cell biology of these processes remain incompletely understood. Here we show that metabolic signals in the form of differential anabolism and catabolism regulate asymmetric division and cell fate bifurcations. Key transcription factors, including TCF1 and IRF4 in lymphocytes and IRF8 in hematopoietic progenitors, occupy regulatory nodes where signals associated with metabolism and traditional cell fate determinants converge. Notably, anabolic PI3K/mTOR signaling was required for terminal differentiation of both lymphocytes and hematopoietic progenitors through the regulation of a constellation of nutrient uptake, mitochondrial turnover, reactive oxygen species production, and autophagy. Further, we found that antigen receptor signaling in lymphocytes organizes a cell-intrinsic polarity pathway of asymmetric intracellular membrane trafficking that is regulated by PI3K activity and associated with terminal differentiation. These results support a model wherein cell fate bifurcations are organized by metabolic signaling at the population and subcellular level to ensure self-renewal of progenitor and memory populations.

TABLE OF CONTENTS

List of Charts, Graphs, Illustrations

Acknowledgements

The success of my time as a PhD student would not have been possible without the help of my colleagues, friends, and family. From the time that Steve welcomed me to his lab, I was surrounded by insightful colleagues who spent many hours working with me and did not hesitate to help when asked. I am grateful to Simone Nish for teaching me key techniques in immunology and helping me to get started in the lab. I want to thank Will Adams for working with me on several important projects and for making the atmosphere in the lab light and coffee-filled. I am also grateful for the friendship and help of all the other members of the Reiner lab - Wendy Lin, Bonnie Yen, Yen-hua Chen, Nyanza Rothman, and Amelie Collins. My thesis committee, Ron Liem, Nick Arpaia, and Lei Ding, gave wonderful and insightful advice that has helped us to complete manuscripts and allowed me to finish my graduate work in a timely fashion. Lastly, I want to thank Steve for welcoming me to the lab and teaching me to think differently and not be afraid to challenge the status quo in a field. I have had a wonderful time working with everyone these past three years.

I am also indebted to my friends, both in New York City and in other places. While I cannot name everyone here, I am grateful for their friendship, and lasting friendships such as these are what make the rigors of graduate work possible. I would also like to thank Sarah Karinja for being my partner throughout my time as an MD/PhD student. As always, I am grateful for my family who have stood by me throughout the fun and the difficult times and always let me know that I can come home whenever I want. This dissertation is dedicated to our family.

Introduction

Organismal homeostasis is inherently linked to cellular turnover and pattern formation. Tissues continually replace their cellular components in the face of external stimuli, aging, and normal wear-and-tear. Stem and progenitor cells of the different organ systems differentiate to populate the mature cell compartment and maintain organ function during turnover. However, this differentiation is balanced with self-renewal to maintain a pool of multi-potent cells that retain the capacity to proliferate and replenish the mature cells. Self-renewal is therefore critical for maintenance of dynamic tissues and organs over time, including the hematopoietic and immune systems.

Hematopoietic progenitor cells differentiate and diverge in fate to populate the mature blood lineages during pattern formation, normal organismal homeostasis, and infection/cancer. Similarly, following clonal selection, naïve lymphocytes differentiate into diverse effector cells, e.g T follicular helper cells and T helper cells, or germinal center B cells and plasmablasts, as well as quiescent memory cells. To prevent exhaustion and collapse of these systems in the face of a continual need to create mature, terminal cells, mechanisms have evolved to balance these differentiation programs.

While it is well-established that individual clones of the hematopoietic and immune systems generate intraclonal diversity during differentiation, the mechanisms underlying these cell fate bifurcations are controversial, with alternate stochastic and deterministic models having been proposed (reviewed in (Reiner and Adams, 2014)). Further, development and differentiation of hematopoietic progenitors has also remained controversial, with models supporting either step-wise bifurcative

developmental trees or stochasticity and lineage biasing (Hoppe et al., 2016; Naik et al., 2013; Pei et al., 2017).

Under stochastic models, activated clones proliferate and generate a heterogeneous population of cells with differential biases toward one fate; differentiation then proceeds along a linear path toward a single fate (Buchholz et al., 2013; Duffy et al., 2012; Gerlach et al., 2013). Averaging of these linear paths across the total population of clones would then produce the heterogeneous response observed *in vivo*. For B and T cells, these fate differences have been postulated to involve TCR/BCR signal strength (Taylor et al., 2015; Tubo et al., 2013). These studies have been based in part on a substantial body of mathematical modeling owing to difficulties with barcoding techniques and tracking of single cell progeny *in vivo*.

Asymmetric cell division has been described across numerous metazoan species and enables a cell to generate divergent progeny that either remain quiescent or undergo terminal differentiation (Morrison and Kimble, 2006). Deterministic fate maps involving asymmetric division describe the developmental pathways in many model systems including *C. elegans.* Evidence for asymmetric division in the hematopoietic and immune systems has been provided in infection, malignancy, and at steady state (Chang et al., 2007; Dey-Guha et al., 2011; Pham et al., 2015; Ting et al., 2012; Wu et al., 2007; Zimdahl et al., 2014). T cells undergoing the first division *in vitro* and *in vivo* can divide asymmetrically, apportioning unequal amounts of receptors, transporters, and adhesion molecules between the first two daughter cells (Chang et al., 2007; 2011; Pollizzi et al., 2016; Verbist et al., 2016). These instances of asymmetric division are organized by external polarity cues in the form of contact with an antigen presenting cell

and were postulated to impart differential capacities on the proximal and distal daughter cells to become effector and memory cells respectively. Further, cancer stem-like cells and hematopoietic progenitors divide asymmetrically depending on extrinsic signaling factors as well as intrinsic signaling (Dey-Guha et al., 2011; Habib et al., 2013; Wu et al., 2007).

While asymmetric division in mammalian lymphocytes and hematopoietic cells has been described by many groups, its requirement for cell fate and development has remained enigmatic. One candidate mechanism, the polarity network family of proteins (PAR), was first described in *C. elegans* and constitutes an ancient group of symmetry-breaking cytosolic proteins that have been implicated in asymmetric division and pattern formation of lower-order metazoa (Goldstein and Macara, 2007). However, initial work in mammalian systems has yielded only partial or incompletely penetrant phenotypes in both hematopoietic cells and lymphocytes (Hawkins et al., 2013; Metz et al., 2015; 2016; Sengupta et al., 2011). Thus, cell intrinsic mechanisms that organize cellular polarity and symmetry-breaking in higher-order mammals remain unclear.

Emerging evidence implicates the metabolic state of hematopoietic cells and lymphocytes as a determinant of cell fate (Chandel et al., 2016; Ito and Ito, 2016). Naive and quiescent memory lymphocytes employ a program of catabolic metabolism, including mitochondrial oxidative phosphorylation (Ox-Phos), fatty acid β-oxidation, and autophagy, for homeostasis and self-renewal. In contrast, activation and proliferation of effector T cells and plasmablasts requires anabolic metabolism, including PI3K/Akt/mTOR activity, aerobic glycolysis, and induction of the Warburg effect – the preferential use of aerobic glycolysis despite oxygen abundance (Buck et al., 2017).

Phospholipid signaling activated by growth factor receptor tyrosine kinases and PI3K has also been implicated in polarity and immune synapse formation (Le Floc'h et al., 2013).

This thesis characterizes the role of asymmetric metabolic signaling in cell fate decisions for model lymphocyte systems as well as a hematopoietic progenitor population. The results described herein are consistent with a model where PI3K activity organizes a polarity pathway involving membrane and organelle traffic that regulates a key node governing transcriptional and metabolic control of cell fate decisions.

Chapter 1: Effector Th1 CD4+ T cell differentiation mediated by PI3K

Portions of this Chapter have been adapted from the following manuscripts:

Nish SA, Zens K, **Kratchmarov R**, Lin WH, Adams WC, Chen YH, Yen B, Rothman NJ, Bhandoola A, Xue HH, Farber D, Reiner SL. (2016). CD4+ T Cell Effector Commitment Coupled to Self-renewal by Asymmetric Cell Divisions. *Journal of Experimental Medicine.* 214: 1-10. doi.org/10.1084/jem.20161046.

Kratchmarov R, Nish SA, Lin WHW, Adams WC, Chen YH, Yen B, Rothman NJ, Klein U, and Reiner SL. (2017). IRF4 Couples Anabolic Metabolism to Th1 Cell Fate Determination. *Immunohorizons.* 1(7):156-161.

Abstract

During infection, activated CD4+ T cell clones proliferate and diverge in fate to produce terminally differentiated effector cells as well as self-renewing memory cells that respond to future infections. Cellular metabolism can determine a lymphocyte's fate and function. In this study, we characterized the role of PI3K signaling in driving terminal differentiation of Th1 type CD4+ T cells. PI3K was required for terminal Th1 differentiation, as indicated by repression of the transcription factor TCF1, induction of Blimp1 expression, and cytokine production. Terminal differentiation was associated with elevated mTOR activity. Furthermore, we show that IRF4, a transcription factor that mediates metabolic reprograming, promotes Th1 differentiation and anabolic metabolism. IRF4-deficient CD4+ T cells exhibited defective repression of TCF1 and impaired induction of Th1-associated markers including CD25 and T-bet, a master regulator of Th1 differentiation. IRF4-deficient CD4+ T cells also underwent a shift toward catabolic metabolism, with reduced PI3K/mTOR activation, deficient nutrient

uptake, and increased mitochondrial clearance. Taken together, these results indicate that PI3K and IRF4 are essential for the anabolic metabolism that directs determined Th1 differentiation. Our findings support a model wherein certain key transcription factors couple metabolic state with gene expression networks to regulate cell fate bifurcations.

Introduction

Following TCR stimulation, naïve CD4+ T cells undergo clonal expansion and differentiate into distinct helper T cell subsets as well as long-lived memory cells that mount responses upon re-exposure to the pathogen. This heterogeneity in cell fate is essential for both combating current pathogens and preserving future immune function for the life of the organism. Memory T cells are found in distinct subsets based on distinct effector function and homing capacity (Masopust et al., 2001; Reinhardt et al., 2001; Sallusto et al., 2004). Notably, these distinct subsets exhibit significant clonal overlap, indicative of a common naïve cell ancestor (Becattini et al., 2015).

Different cytokines, including IL-4, IL-12, and IL-17, modulate effector cell differentiation to tailor the response to a given microbial pathogen. The Th1 subset is defined by expression of the lineage-determining transcription factor T-bet and the capacity to secrete effector molecules including IFN-γ and TNF-α (Zhu et al., 2010). Different transcription factors control the differentiation of CD4+ subsets, and IRF4 is important for Th2, Th9, Th17, Tfh, and Treg CD4+ responses (Bollig et al., 2012; Brüstle et al., 2007; Staudt et al., 2010; Tominaga et al., 2003; Zheng et al., 2009). The role of IRF4 in Th1 CD4+ differentiation is less clear (Lohoff et al., 2004; 2002; Tominaga et al., 2003), though recent work indicates a role for IRF4 in Th1 responses both *in vitro* and *in vivo* (Mahnke et al., 2016). IRF4 is also critical for effector CD8+ T cell differentiation where it modules metabolic pathways (Man et al., 2013; Yao et al., 2013).

Studies in both CD4+ and CD8+ T cells indicate that IRF4 functions as a regulator of the metabolic reprograming necessary for effector T cell function (Huber and Lohoff, 2014). Activated CD4+ T cells upregulate biosynthetic and bioenergetic

pathways necessary for proliferation, cytokine production, and migration (Pollizzi and Powell, 2014). Terminally differentiated Th1 CD4+ T cells have increased anabolic demands and preferentially employ aerobic glycolysis, as this subset proliferates extensively and engages lipid biosynthesis and cytokine production (Gerriets et al., 2015; Michalek et al., 2011). This anabolic program is mediated primarily by the kinases PI3K and mammalian target of rapamycin (mTOR). Conversely, memory CD4+ and CD8+ T cells as well as Treg cells are primarily catabolic and rely on lipid oxidation and mitochondrial oxidative phosphorylation for ATP production (O'Sullivan et al., 2014; Pearce et al., 2009; van der Windt et al., 2013). The efficient induction of these anabolic and catabolic metabolic programs are critical for CD4+ T cell fate determination. Anabolic signaling itself directs the terminal differentiation and loss of self-renewal capacity in CD8+ T cells as well as B lymphocytes, likely through regulation of key transcription factors, such as FOXO1, that control both gene expression networks and cellular metabolic profiles (Lin et al., 2015).

It has become increasingly apparent that metabolic signals are critical for directing the fate of lymphocytes. Fate-determining transcription factor expression can both regulate and receive input from the cellular metabolic state. To further understand how transcription factor expression is coupled to metabolic reprograming for cell fate determination, we explored whether PI3K signaling coordinately regulates TCF1 and IRF4 expression during Th1 differentiation as a mechanism for cellular differentiation.

Results

PI3K signaling drives mTOR activation, TCF1 silencing, and Th1 cell differentiation

Cytokine receptor binding interfaces with intracellular signaling networks. Previous work indicates that IL-2 may drive the down-regulation of the transcription factor TCF1 in CD4+ T cells, a transcriptional change associated with terminal effector cell differentiation (Wu et al., 2015). To determine the role for Th1-inducing cytokines in mediating TCF1-downregulation, we activated naïve CD4+ T cells with plate-bound anti-CD3 and anti-CD28 in the presence of either IL-2 or IL-12 (Figure 1.1A). We found that both cytokines could independently drive TCF1 repression in the context of TCR stimulation, suggesting that cytokine signals can initiate terminal differentiation. Interestingly, this repression was dependent on intact PI3K signaling as treatment with the small molecule LY294002, a pan PI3K inhibitor, resulted in maintenance of TCF1 expression despite IL-2/IL-12 stimulation.

PI3K/mTOR activity is important for driving repression of TCF1 in CD8+ T cells and Pax5 in B cells (Lin et al., 2015), and is induced by IL-2 signaling (Ray et al., 2015). We found that inhibition of PI3K in the context of TCR stimulation prevented repression of TCF1, across cell divisions as proliferating cells remained largely TCF1-high (Figure 1.1B). Th1 differentiation was also impaired in the context of PI3K inhibition, as activated cells failed to upregulated the cytokine IFN-γ and cytolytic granule component GranzymeB (Figure 1.1B). Moreover, PI3K inhibition decreased cellular proliferation following TCR stimulation and abrogated Blimp-1 induction, a key regulator of terminal differentiation (Crotty et al., 2010) (Figure 1.1C). Finally, inhibition of PI3K decreased

mTOR activity in proliferating cells, as determined by phosphorylation of the ribosomal subunit S6, confirming that increased anabolic signaling accompanies proliferation and terminal differentiation (Figure 1.1D).

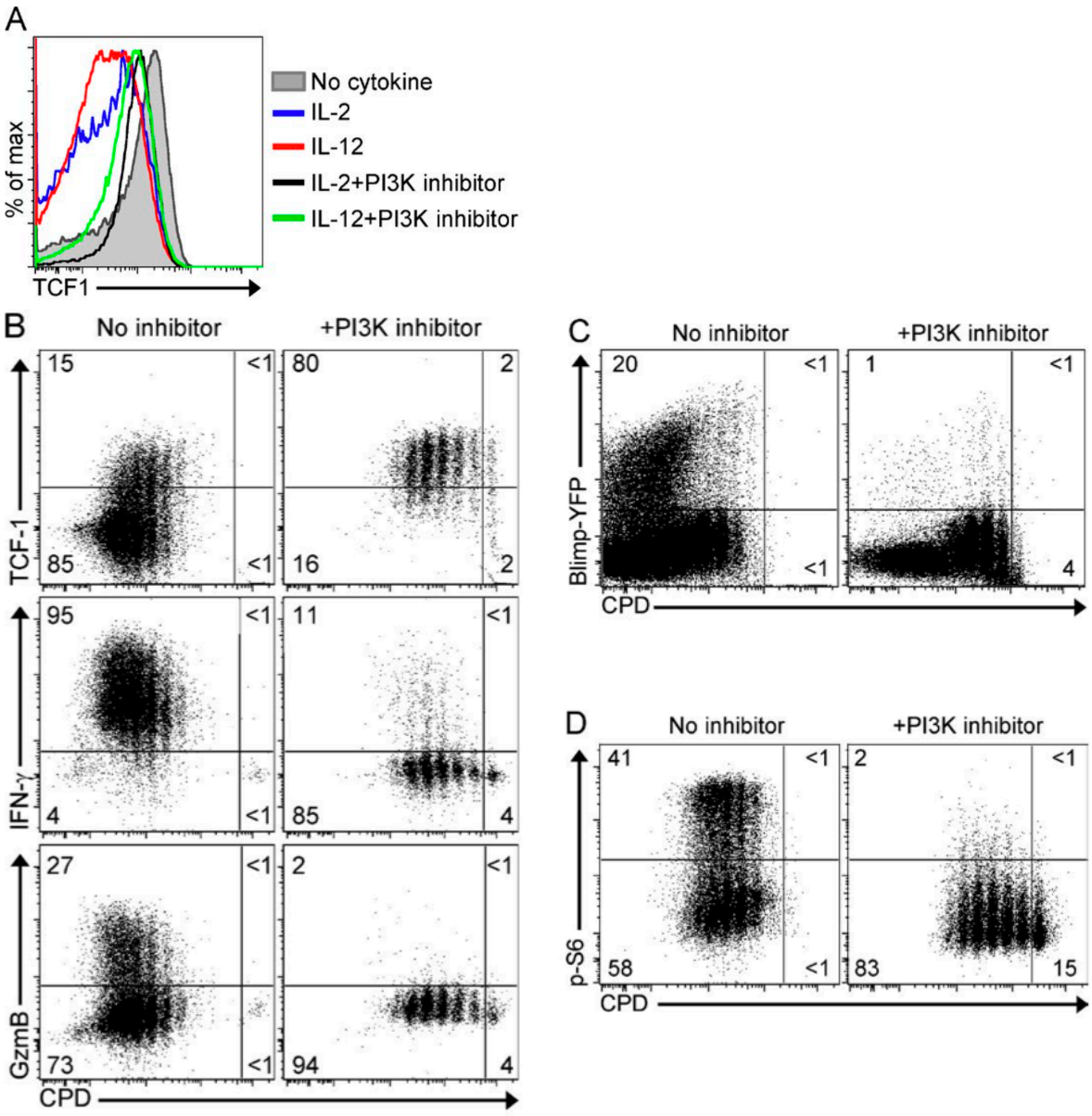

Figure 1.1. PI3K signaling driving TCF1 repression and Th1 effector differentiation. (A) TCF1 expression in CD4+ T cells stimulated for 5 d with anti-CD3/CD28 in the presence of IL-2 or IL-12, without or with 5 μM PI3K inhibitor. Results are representative of at least three independent expreiments. (B) CPD versus TCF1, granzyme B (GzmB), and IFN-γ in CD4+ T cells stimulated for 5 d in Th1 cell–inducing conditions (IL-2 and IL-12) with or without PI3K inhibitor. Plots are representative of 3 or more independent experiments. (C) CPD versus Blimp-1–YFP expression in CD4+ T cells stimulated with or without PI3K inhibitor. Data are representative of three independent experiments. (D) CPD versus phospho-S6 (p-S6) in CD4+ T cells with or without PI3K inhibitor. Data are representative of three independent experiments.

Impaired Th1 differentiation in IRF4-KO CD4+ T cells

IRF4 is thought to function downstream of PI3K/mTOR activation in activated T cells to direct metabolic reprograming for terminal differentiation (Yao et al., 2013). To explore the role of IRF4 in Th1-type CD4+ T cell responses, we first determined whether Th1 effector cell differentiation required IRF4 expression. Naïve wild-type (WT) or IRF4-KO CD4+ T cells were labeled with a proliferation dye and TCR-stimulated under Th1-skewing conditions (IL-2 / IL-12) *in vitro*. We then assayed cytokine production and cytotoxicity by flow cytometry following PMA/ionomycin stimulation to determine whether IRF4-KO cells were functional deficient (Figure 1.2A). Indeed, compared to WT cells lower percentages of IRF4-KO CD4+ T cells produced IFN-γ, granzyme B, and TNF-α, indicating decreased effector function. Next, the expression of key transcription factors was assayed by flow cytometry after 4 days of culture. After several (3-4) divisions, two populations marked by differential (high / low) TCF1 expression emerged (Figure 1.2B). TCF1-high cells have Tfh and memory developmental potential, while TCF1-low cells undergo irreversible Th1-type terminal differentiation (Choi et al., 2015; Nish et al., 2017b; Wu et al., 2015; Xu et al., 2015b). Differentiation of the TCF1-low effector cell subset was decreased in IRF4-KO CD4+ T cell cultures (Figure 1.2B). Concurrently, expression of the Th1-master regulator T-bet as well as the high affinity IL-2 receptor CD25, a marker of activation, was also decreased (Figure 1.2B). Expression of CD62L, a chemokine receptor important for lymphoid tissue homing, was increased on IRF4-KO CD4+ T cells, further indicating decreased terminal differentiation (Figure 1.2B). Transduction of IRF4-deficient cells with T-bet-GFP retrovirus failed to rescue defects in TCF1 silencing and cytokine induction (Figure 1.2B). These results,

together with recent studies of IRF4 deficient cells using *Listeria* infection (Mahnke et al., 2016), suggest that IRF4 is required for the induction of optimal Th1 differentiation. The inability of T-bet overexpression to rescue terminal Th1 differentiation further suggests that IRF4 does not function solely as an inducer of Th1-specific genes.

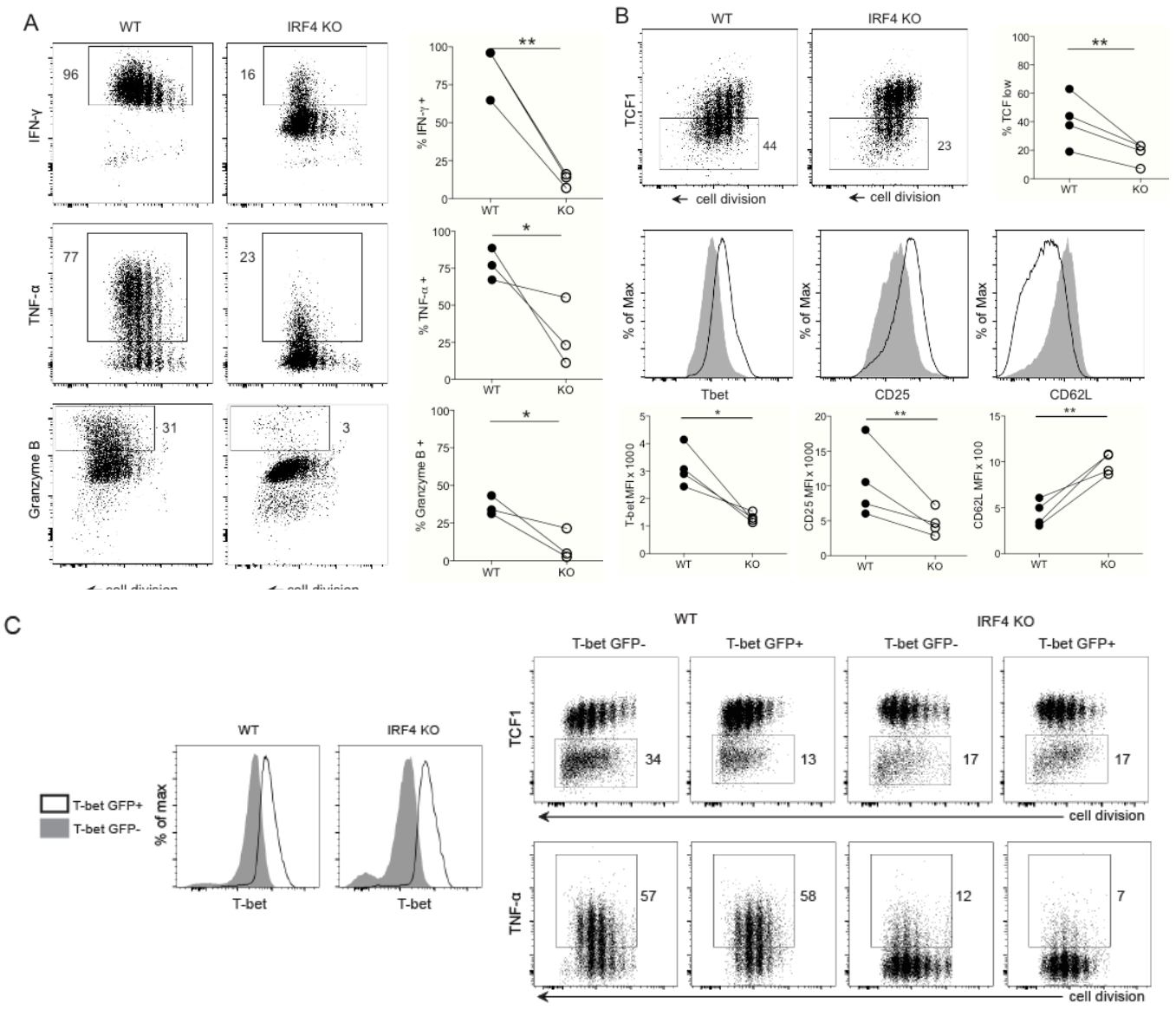

Figure 1.2. IRF4 is required for efficient Th1 CD4+ effector cell differentiation. (A) CD4+ T cells labeled with CPD, stimulated with anti-CD3/CD28 + IL-2/IL-12, and re-stimulated with PMA/ionomycin on day 4. Representative FACS plots of indicated protein versus CPD (left panels). Quantification of the percent positive population in WT and IRF4-KO CD4+ T cells (right panels). (B) Representative FACS plots of TCF1 expression versus CPD in Th1-inducing conditions (top left and middle panels). Quantification of TCF1-low population in WT and IRF4-KO CD4+ T cells (top right panel). Representative histograms of T-bet, CD25, and CD62L expression (middle row). Quantification of protein expression in WT and IRF4-KO CD4+ T cells (bottom row). (C) Increased T-bet protein expression in WT and IRF4-KO CD4+ T cells following transduction with T-bet–GFP retrovirus (left panels). Expression of TCF1 (upper right panels) and TNF-**α** (lower right panels) by CD4+ T cells transduced (GFP+) or untransduced (GFP-) with T-bet–GFP retrovirus, at day 4 post-activation. Plots are representative of three independent experiments. * $p<0.05$ ** $p<0.01$ Paired t test.

Deficient anabolic signaling following TCR stimulation in IRF4KO CD4+ T cells

Terminally differentiated effector CD4+ T cells require metabolic reprogramming to promote efficient effector function (Gerriets et al., 2015; Macintyre et al., 2014; Michalek et al., 2011). As IRF4 is important for effector CD8+ T cell anabolic pathways, we sought to determine the role of IRF4 in CD4+ T cell metabolism. TCR stimulation of CD4+ T cells induced robust PI3K/mTOR activation, indicated by phosphorylation of ribosomal subunit S6 (Figure 1.3A). Notably, IRF4-KO CD4+ T cells had decreased PI3K/mTOR activity, indicating that IRF4 is important for sustained PI3K signaling following TCR stimulation (Figure 1.3A). Deficient mTOR activation was evident in both early and late division cells and maintained throughout the duration of the experiment, suggesting that IRF4 plays a primary role in supporting PI3K/mTOR activation. Despite the impairment in phosphorylation of S6, levels of FoxO1 phosphorylation (another target of PI3K signaling) appeared normal in IRF4-deficient cells (Figure 1.3A), which is consistent with the ability of IRF4-deficient B cells to undergo inducible nuclear displacement of FoxO1 (Lin et al., 2015). While initial CD28 co-receptor stimulation directly induces PI3K activation (Powell et al., 1999), these results indicate that downstream transcription factors, including IRF4, are critical for maintaining anabolic kinase activity.

T cell subsets with self-renewal capacity preferentially employ mitochondrial oxidative metabolism and have elevated catabolic signaling mediated by AMPK (Pearce et al., 2009). Furthermore, autophagy as well as mitophagy, the selective clearance of damaged mitochondria, are critical for memory T cell formation (Adams et al., 2016; Xu et al., 2014). This constellation of catabolic processes opposes terminal effector cell

differentiation (Adams et al., 2016). As IRF4-KO CD4+ T cells have decreased anabolic activity following TCR stimulation and decreased terminal differentiation, we sought to determine if increased catabolic signaling would be apparent in an *in vitro* assay of autophagy/mitophagy (Adams et al., 2016). We found that the cellular progeny of IRF4-deficient cells exhibited enhanced clearance of aged mitochondria (Figure 1.3B), an index of catabolic mitophagy, which may predict a diminished likelihood of differentiation. Differences in the levels of aged mitochondria were evident beginning at the second division and persisted throughout later divisions (Figure 1.3B), further suggesting a primary role for IRF4 in sustaining nutritive signaling. Despite enhanced mitochondrial elimination, proliferating IRF4-deficient CD4+ T cells also had lower total mitochondrial content and lower mitochondrial membrane potential (Figure 1.3B).

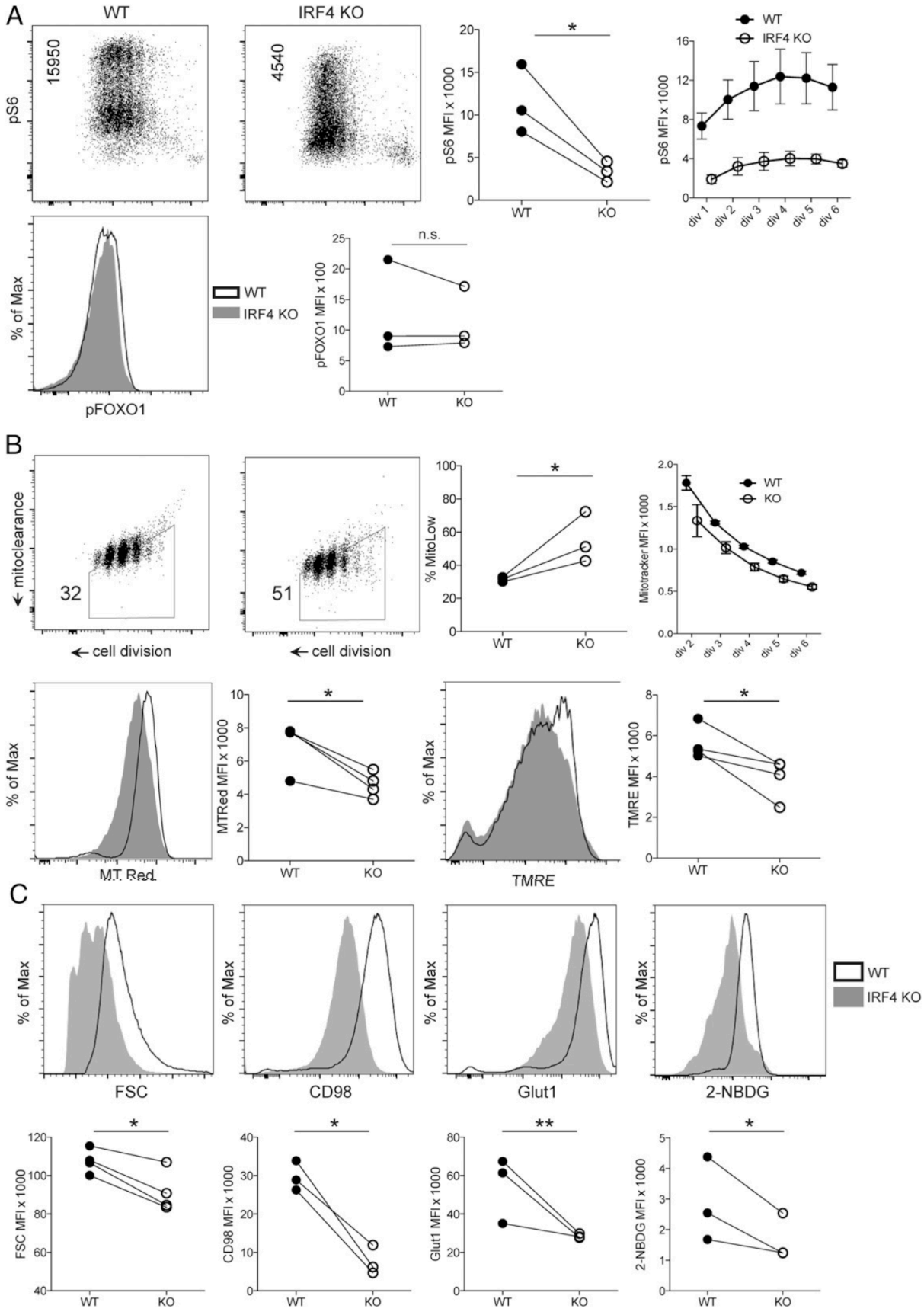

Figure 1.3. IRF4 is required for anabolic induction of CD4+ T cells.

Figure 1.3. IRF4 is required for anabolic induction of CD4+ T cells.
(A) CD4+ T cells analyzed by phospho-flow cytometry for mTOR activity (pS6) (upper left and middle left panels). FACS plot statistic indicates mean fluorescence intensity (MFI) of phospho-S6. Quantification of phospho-S6 levels (upper middle right panel). MFI of phospho-S6 at the indicated cell divisions (upper right panel). Error bars denote SEM. Representative histogram of p-FoxO1 levels in WT and IRF4-KO CD4+ T cells (lower left panel). Quantification of phospho-FoxO1 MFI (lower right panel). (B) WT and IRF4-KO CD4+ T cells pulse-labeled with CPD and MitoTracker Green, followed by TCR stimulation and flow cytometry analysis after 66 h (upper left and middle left panels). MitoTracker fluorescence (y-axis) decreases with each cell division (x-axis) as the pulse-labeled mitochondria age and are passively apportioned, as well as actively cleared by mitophagy. Frequency statistic indicates the percentage of cells in the MitoTracker-low trapezoidal gate. Quantification of the frequency of cells in the MitoTracker-low gate (upper middle right panel). MFI of pulsed MitoTracker fluorescence at the indicated cell divisions (upper right panel). Error bars denote SEM. Lower: Representative histograms of total mitochondrial content measured by MitoTracker Red, and mitochondrial membrane potential measured by TMRE. Quantification of MitoTracker Red MFI (lower middle left panel) Quantification of TMRE MFI (lower right panel). (C) Representative line graphs of CD4+ T cells labeled with CPD, stimulated in Th1 conditions, and analyzed by flow cytometry on day 4 of culture for forward scatter (FSC; cell size), expression of the indicated nutrient transporters (CD98 and Glut1), and glucose uptake (2-NBDG) (upper panels). Quantification of the indicated flow cytometry parameters for WT and IRF4-KO CD4+ T cells (lower panels). * $p<0.05$, ** $p<0.01$. n.s. not significant. Paired t test.

T cell activation induces an anabolic program of cell growth that depends on nutrient uptake. IRF4 mediates this metabolic reprogramming in CD8+ T cells, including anabolic nutrient transporter expression (Man et al., 2013). Following TCR stimulation, WT CD4+ T cells proliferated and increased cell size, indicative of blasting and anabolic signaling; however, IRF4-KO CD4+ T cells showed decreased blasting potential as indicated by forward scatter measurements (Figure 1.3C). In WT cells, Glut1, the primary inducible glucose transporter for CD4+ T cells, and CD98, an amino acid transporter, were both upregulated following TCR stimulation (Macintyre et al., 2014; Sinclair et al., 2013). However, Glut1 and CD98 expression was substantially decreased on IRF4-KO CD4+ T cells compared to WT (Figure 1.3C). We then assessed glucose uptake using the fluorescent glucose analog 2-NBDG (Figure 1.3C). Activated, proliferating CD4+ T cells imported more 2-NBDG than undivided cells for both WT and knockout cells. However, IRF4-KO CD4+ T cells showed a severe deficit in 2-NBDG uptake compared to WT cells. These results indicate that IRF4 is required for upregulation of nutrient transporters in CD4+ T cells during Th1 differentiation and suggest that defects in anabolism underlie the deficient terminal differentiation of Th1 effector cells in the absence of IRF4.

Conclusion

The emerging role of fate-determining transcription factors as regulators of selective metabolism constitutes a mechanism that may link bioenergetics and cell fate. Cell fate decisions in lymphocytes require the coordination of transcription factor networks with metabolic state. Our results indicate that PI3K and IRF4 occupy a key node in CD4+ T cell differentiation with the bifunctional capacity to both regulate expression of canonical Th1 transcription factors/receptors and modulate metabolic pathways. The coordinated activity of IRF4 in these spheres allows for the coupling of metabolic state to gene expression networks necessary for cell fate bifurcation.

It was previously shown that IRF4 acts downstream of mTOR signaling in T cells (Yao et al., 2013). Our current results indicate that sustained mTOR activation itself also requires IRF4 function, consistent with a feed-forward, feed-back relationship that characterizes bistable systems. As such, perturbations of either upstream signaling or downstream processes of anabolism can skew the cellular metabolic profile. By licensing upstream nutritive signaling, nutrient uptake and utilization, and rewiring the transcriptional circuitry of cell fate, IRF4 couples metabolic and lineage choice.

Mitochondrial biogenesis and fusion, which accompanies the autophagy of older mitochondria in physiological memory T cells, is essential for optimal oxidative metabolism and T cell memory (Buck et al., 2016). We found that IRF4-deficient cells exhibit a reduction in total mitochondrial content and mitochondrial membrane potential, despite enhanced mitochondrial turnover, suggesting that the severity of nutrient deprivation in the absence of IRF4 may prevent basal biogenesis of new mitochondria to offset the elimination of aged organelles. The resultant defects in mitochondrial

function would therefore be consistent with recent findings that oxidative metabolism is reduced in IRF4-deficient CD4+ T cells (Mahnke et al., 2016). Defective oxygen consumption of IRF4-deficient CD4+ T cells might therefore reflect severe catabolic metabolism rather than a role for IRF4 in mitochondrial biogenesis directly.

Our results suggest that IRF4 does not direct two parallel but unrelated processes, i.e. Th1 gene induction and anabolic metabolism. Instead, defective anabolism in IRF4-deficient cells is analogous to glucose scarcity, which is directly responsible for defective Th1 differentiation and function (Gerriets et al., 2015; Michalek et al., 2011). Anabolic metabolism, mediated in part by IRF4, could drive Th1 differentiation through its ability to support silencing of TCF1, a negative regulator of T-bet induction (Choi et al., 2015; Wu et al., 2015). It remains unclear whether IRF4 and anabolic signaling mediate silencing of TCF1 solely through Akt-mediated inactivation of FoxO1, or if other gene regulatory mechanisms are involved. Taken together, this study demonstrates that PI3K signaling and IRF4 expression are required for efficient TCF1 repression, via an anabolic signaling mechanism which balances the opposing cell fates of differentiation and self-renewal.

Methods

Mice and *in vitro* Th1 culture

Wild type C57BL/6 and IRF4 KO (Klein et al., 2006) littermate mice served as sources of CD4+ T cells. Both male and female mice were used at age 8-10 weeks, and mice were housed in specific-pathogen-free conditions. All experiments were conducted in accordance with National Institutes of Health and Columbia University Institutional Animal Care and Use Committee guidelines. All efforts were made to minimize animal suffering and the number of animals used. Naïve CD4+ T cells were purified from spleens by magnetic cell separation (Miltenyi Biotech) and subsequently labeled with the cell proliferation dye (CPD) Cell Trace Violet (Thermo Fisher). $5x10^5$ cells were seeded in 48-well tissue culture plates pre-coated with anti-CD3 (1ug/ml) and anti-CD28 (1ug/mL) in Iscoves Modified Eagle Medium (Corning) supplemented with 10% FBS, IL-2 (20 IU/ml), and IL-12 (10 ng/ml). For experiments with retroviral expression of Tbet-GFP, cells were activated for at least 36 hours before spin infection, as previously described (can use the Adams citation). Following spin infection, cells were returned to the original culture media and cultured for an additional 48 hours before flow cytometric analysis.

Flow cytometry

Staining for flow cytometry analysis was performed as described (Lin et al., 2015). For phospho-flow cytometry, samples were first fixed with 4% paraformaldehyde for 15 minutes followed by permeablization with ice-cold methanol for 5 minutes before antibody staining. Cytokine production was assayed following PMA (50ng/mL) and ionomycin (1ug/mL) re-stimulation for 4 hours. Antibodies used in this study include

CD25 (PC61; Biolegend), CD62L (MEL-14; BD Biosciences), CD98 (RI388; Biolegend), anti-Glut1 (EPR3915; Abcam), T-bet (4B10; Biolegend), TCF1 (C63D9; Cell Signaling Technology), Phospho-S6 (S235/236; Cell Signaling Technology), GranzymeB (GB11, Biolegend), IFN-γ (XMG1.2, BD Biosciences), TNF-α (MPG-XT22, BD Biosciences), and goat anti-rabbit AlexaFluor 647 secondary (Thermo Fischer). Flow cytometry samples were acquired on a BD LSRII or BD Fortessa, and analysis was performed with FlowJo software (Treestar, San Carlos, CA). Glucose uptake following TCR stimulation was measured by incubating cells in 2-NBDG (Cayman; 100 μM) for 45 minutes at 37 °C in glucose free RPMI supplemented with 10% dialyzed FBS. Mitoclearance was assessed by labeling naïve CD4+ T cells with Mitotracker Green (Thermo Fisher; 200nM per 1x10^6 cells) followed by two washes with complete media. Cells were then labeled with Cell Trace Violet and activated in Th1-inducing conditions. Clearance of mitochondrial fluorescence represents the sum of passive dilution during cell division plus active destruction through autophagy. Total mitochondrial mass and mitochondrial membrane potential were determined by labeling cells with Mitotracker Red or TMRE (Thermo Fischer), respectively, according to the manufacturer's instructions.

Statistical analyses

Statistical analyses were performed using GraphPad Prism (version 6). P-values and significance cut-offs are specified in each figure legend.

Chapter 2: Asymmetric metabolic signaling regulates autophagy and mitochondrial stasis to determine lymphocyte cell fate

Portions of this Chapter have been adapted from the following manuscript:

Adams WC*, Chen YH*, **Kratchmarov R***, Yen B, Nish SA, Lin WH, Rothman NJ, Luchsinger L, Klein U, Busslinger M, Rathmell JC, Snoeck HW, and Reiner SL. (2016). Anabolism-associated Mitochondrial Stasis Driving Lymphocyte Differentiation over Self-renewal. *Cell Reports.* 17: 3142–3152. doi:10.1016/j.celrep.2016.11.065.

* These authors contributed equally.

Abstract

The mechanisms that orchestrate divergent cell fate amongst the cellular progeny of activated lymphocyte clones remain controversial. Recently, we showed that metabolic signals can direct the acquisition of effector versus memory fates in B and T cells, but the underlying cellular biology of this process has not been fully explored. To dissect the subcellular pathways involved, we assessed the role of mitochondrial turnover and autophagy, two key metabolic signaling nodes, in lymphocyte differentiation. Pharmacological or genetic perturbation of Drp1, a protein required for mitochondrial fission and mitophagy, resulted in increased terminal effector differentiation of both B and T cells with a concomitant increase in production of mitochondrial reactive oxygen species. Further, we observed unequal elimination of aged mitochondria between differentiating and self-renewing lymphocytes, at both the population and clonal level. Asymmetric elimination correlated with asymmetric autophagy at the single cell level, as well as effector versus memory cell fate *in vivo*. Additionally, we show that PI3K activity is required for mediating differential metabolic

signals at the subcellular level, in part through regulation of asymmetric autophagosome localization. These results suggest that asymmetric PI3K signals affect key subcellular organelles and their associated metabolic pathways to mediate cell fate bifurcations in lymphocytes.

Introduction

Adaptive immunity involves the clonal selection of B and T lymphocytes wherein activated progenitor cells differentiate to produce functionally distinct progeny. The differentiation pattern of a naïve lymphocyte involves PI3K-driven changes in transcription factor expression and the development of both effector and memory cells, which uniquely retain the ability to self-renew. The process of lymphocyte differentiation is inherently linked to cell division, and asymmetric cell division offers a mechanism by which one cell may generate divergent progeny (Morrison and Kimble, 2006). Daughter cells of activated, dividing clones may self-renew due to unequal transmission of PI3K signaling (Lin et al., 2015). In both B cells and T cells, this divergence in cell fate occurs after several rounds of cell division. Activated progenitors that have undergone several divisions can give rise to asymmetric daughter cells, with unequal anabolic PI3K/mTOR activation and asymmetric inactivation of the transcription factor FOXO1 (Lin et al., 2015). As such, the balance of cellular anabolism and catabolism is coupled to the transcriptional control of lymphocyte differentiation.

Metabolic signals from the kinases PI3K/mTOR and AMPK reciprocally regulate nutrient uptake and autophagy, the catabolic process of cellular self-digestion that mediates proteostasis and digestion of macromolecules (Green et al., 2011). PI3K/mTOR activity represses autophagy while promoting anabolic pathways, including glycolysis and biosynthesis. Conversely, AMPK induces autophagy and inhibits mTOR (Gwinn et al., 2008; Inoki et al., 2003). Both memory B and T cells require autophagy for their formation and/or survival (Chen et al., 2014; Xu et al., 2014).

Cellular metabolism and metabolic signaling converges on mitochondria. As such, mitochondrial content and quality control is critical for both cellular metabolism and intracellular signaling pathways (Chandel, 2015). Mitochondrial mass and reactive oxygen species (mROS) production modulate hematopoietic cell fate (Owusu-Ansah and Banerjee, 2009) and direct activated B cells toward plasmablast or germinal center fate (Jang et al., 2015). mROS themselves can increase PI3K signaling and thus alter cell fate (Chen et al., 2008; Yalcin et al., 2010) while also being implicated in effector T cell differentiation (Sena et al., 2013) and NK cell memory formation (O'Sullivan et al., 2015). Mitochondrial turnover in the form of fission, fusion, and mitophagy, is critical for maintaining a functional pool of healthy organelles (Mishra and Chan, 2014). Notably, in stem-like cells, aged mitochondria are differentially inherited during asymmetric divisions that ensure acquisition of healthy mitochondria by more stem-like daughters (Katajisto et al., 2015). Here, we sought to dissect the coupling of discordant lymphocyte fate outcomes to cell biological signaling at the interface of PI3K, mitochondria, and autophagy.

Results

Unequal Clearance of Aged Mitochondria Modulates B and T Cell Fate

We first explored the role of mitochondrial quality control in lymphocyte cell fate bifurcations using *in vitro* models of terminal differentiation. B cells stimulated with LPS undergo terminal differentiation, as evidenced by repression of the lineage determining transcription factor Pax5 and upregulation of IRF4 (Lin et al., 2015). Similarly, CD8+ T cells undergo differentiation coupled to irreversible silencing of the transcription factor TCF1 following peptide-based TCR stimulation (Lin et al., 2016). As these differentiation programs are linked to PI3K signaling, we assessed the role of mitochondrial clearance through genetic and pharmacological approaches to interfere with Dynamin-related protein 1 (Drp1), a protein essential for mitochondrial fission and autophagy (Mishra and Chan, 2014). Transduction of activated B and T cells with retrovirus encoding dominant-negative (DN) Drp1, or pharmacological inhibition of Drp1 with mDivi-1, both led to enhanced plasmablast and effector T cell differentiation, respectively, as indexed by Pax5 and TCF1 repression (Figure 2.1A). In addition, DN Drp1 transduction and mDivi-1 treatment induced a reciprocal increase in IRF4 expression in B cells (Figure 2.1A). These results suggest that mitochondrial turnover and/or clearance is required for regulating the balance of effector and memory cell differentiation.

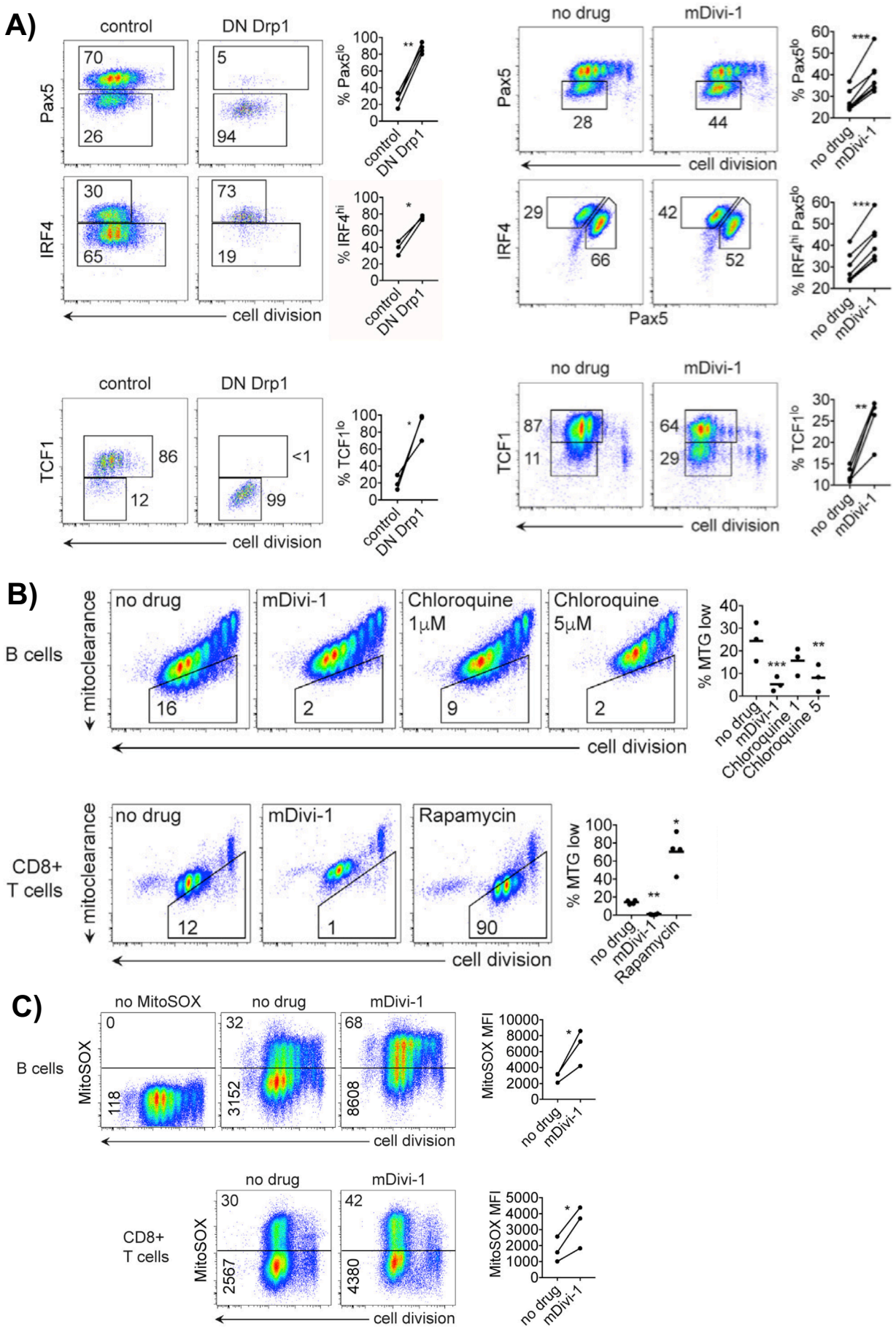

Figure 2.1. Inhibition of mitochondrial turnover drives terminal lymphocyte differentiation.

Figure 2.1. Inhibition of mitochondrial turnover drives terminal lymphocyte differentiation. (A) Upper left: Pax5 and IRF4 expression by B cells labeled with CTV and activated with LPS and transduced with retrovirus (RV) encoding dominant-negative (DN) Drp1 at 36 hrs post-stimulation. Graphs denote the frequency of Pax5-lo (n = 4; ** p<0.01 Paired t test) and IRF4-hi (n = 3; * p<0.05. Paired t test) cells among B cells transduced with control or DN Drp1 RV. Lower left: TCF1 expression by CTV-labeled CD8+ T cells stimulated with anti-CD3/CD28 antibodies and IL-2 for 36 hr, then transduced with control or DN Drp1. Graph indicates the frequency of TCF1-lo T cells among cells transduced with control or DN Drp1 RV (n = 3; * p<0.05 Paired t test). Upper right: CTV-labeled B cells from wild-type mice were stimulated with LPS in the absence or presence of mDivi-1. Graphs indicate the frequency of Pax5-lo and Pax5-lo/IRF4-hi B cells (n = 7; *** p<0.001. Paired t test). Lower right: CTV-labeled P14 transgenic CD8+ T cells were stimulated with gp33-41 and IL-2 for 4 days in the absence or presence of mDivi-1. Graph indicates the frequency of TCF1-lo T cells among cells activated in the absence or presence of mDivi-1 (n = 5; **p<0.01. Paired t test). (B) Mitoclearence assay. MitoTracker Green FM (MTG)-pulsed labeled B cells (top row) and P14 CD8+ T cells (bottom row) were activated as in (A). Cells were cultured in the absence or presence of mDivi-1, Chloroquine, or rapamycin as indicated. Y-axis reflects dilution plus elimination of pre-labeled (pulsed) mitochondria, termed mitoclearance, in relation to cell division (x axis). Graph statistics denote frequency of cells within trapezoidal MTG-low gate (n = 3; *p<0.05 ** p<0.01 ***p < 0.001 for indicated treated groups compared to no drug control group, repeated-measures one-way ANOVA). (C) CTV-labeled B cells (upper row) and P14 CD8+ T cells (lower row) stimulated with LPS or gp33-41 peptide and IL-2, in the absence or presence of mDivi-1 and analyzed for mitochondrial ROS (mROS) production by MitoSOX staining. Horizontal numbers denote the frequency of cells within gate. Vertical numbers denote MFI of all cells. Graphs display MitoSOX MFI among cells stimulated with or without mDivi-1 (n = 3; * p< 0.05. Paired t test).

Mitochondrial turnover, mediated by fission and fusion, facilitates the degradation of aged and dysfunctional mitochondria through a specific form of macro-autophagy termed ‘mitophagy’ (Eiyama and Okamoto, 2015). We sought to determine whether inhibition of Drp1 activity promotes terminal lymphocyte differentiation by altering mitochondrial clearance. A fluorescence-based, pulse chase method was developed to quantify clearance of aged mitochondria in relation to cell division through flow cytometry (Figure 2.1B). Prior to activation, lymphocytes were pulsed with a fluorescent mitochondrial dye to label the total mitochondrial content of the naïve B or T cells. Following activation, dilution of the mitochondrial dye, as quantified by flow cytometry, provided a readout of both passive apportioning and active degradation of the original mitochondrial population (Figure 2.1B). Treatment with mDivi-1 increased stasis of aged (pulse-labeled) mitochondria, as seen by greater maintenance of pulsed fluorescent dye. This stasis was comparable to that observed following treatment with the general macro-autophagy inhibitor chloroquine and opposite that following treatment with an inducer of autophagy (rapamycin) (Figure 2.1B). Notably, inhibition of mitochondrial fission following treatment with mDivi-1 also increased production of mROS by both B and CD8+ T cells (Figure 2.1C). Taken together, these results suggest that lymphocytes actively turn over their mitochondria pool following activation and that stasis of aged mitochondria is associated with terminal lymphocyte differentiation.

Unequal clearance of aged mitochondria during T and B cell differentiation *in vivo*

To determine whether mitochondrial clearance was associated with lymphocyte cell fate during the response to infection *in* vivo, we assessed CD8+ and CD4+ T cell

differentiation following infection. Because inheritance of aged mitochondria was evident for at least six cell generations (Figure 2.1B), we reasoned that unequal inheritance could be associated with cell fate bifurcations *in vivo*. At 3 days following infection with *L. monocytogenes* expressing gp33, terminally differentiated CD8+ KLRG1+ T cells, which are phenotypically TCF1-low (Lin et al., 2016), were enriched with aged mitochondria (Figure 2.2). At 4 days following respiratory infection with influenza virus, CD4+ Th1 effector cells (largely TCF1-low) left the draining lymph node to populate the lung, while self-renewing TCF1-hi central memory cells recirculated through non-draining nodes (Nish et al., 2017b). Effector cells in the lung were enriched for the stasis of aged mitochondria (Figure 2.2). Self-renewing CD4+ T cells localized to the non-draining lymph node were reciprocally enriched for heightened clearance of aged mitochondria (Figure 2.2). Taken together, these results indicate that lymphocyte progeny destined for terminal differentiation *in vivo* are marked by the stasis of aged mitochondria.

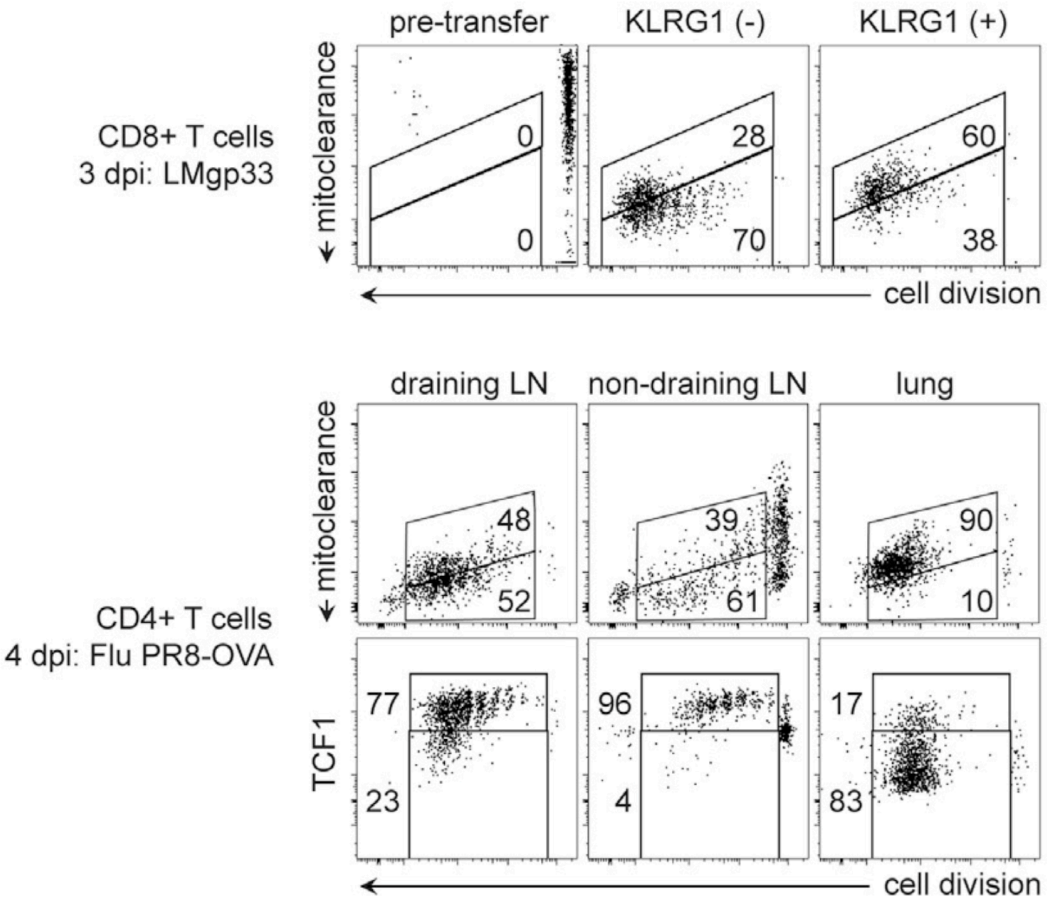

Figure 2.2 Mitochondrial stasis marks lymphocyte progeny destined for terminal differentiation *in vivo.* CTV and MTG pulse-labeled P14 CD8+ T cells (top row) and OT-II CD4+ T cells (bottom panels) were adoptively transferred into congenically disparate recipients challenged with Listeria (LMgp33) or PR8-OVA influenza virus, respectively. For CD8+ T cells, the left plot depicts cell division versus mitoclearance for non-transferred cells as a control for initial MTG fluorescence. Middle and right plots show mitoclearance by P14 CD8+ donor T cells for KLRG1- (TCF1-hi) and KLRG1+ (TCF1-lo) populations at 3 days post Listeria challenge. Results are representative of two independent experiments. For CD4+ T cells, the upper row depicts cell division versus mitoclearance in draining lymph nodes (LNs), non-draining LNs, and lung tissue; the bottom row depicts cell division versus TCF1 expression. Numbers are the frequency within gates encompassing divided cells. Results are representative of two independent experiments.

Asymmetric elimination of aged mitochondria during late cytokinesis

Unequal inheritance of aged mitochondria by different subsets at the population level could reflect signaling and turnover of organelles in interphase cells. However, given the uniform nature of the stimuli used in our modeled differentiation systems, we reasoned that it was unlikely for individual interphase cells to undergo asynchronous, divergent metabolic signaling. We therefore assessed the localization of aged mitochondria in mitotic cells using confocal microscopy, speculating that asymmetric division could facilitate the observed differences. However, we found that the subcellular distribution of aged mitochondria was generally symmetric in metaphase and early telophase cells (Figure 2.3A). In cytokinetic daughter cell pairs, however, the inheritance of aged mitochondria was frequently discordant (Figure 2.3A). Furthermore, in live cell imaging assays, we observed cytokinetic daughter cell pairs with stable discordant levels of aged mitochondria over extended periods of time (Figure 2.3B). This localization and inheritance pattern suggested that differential apportioning of aged mitochondria is not the principal mechanism for establishing asymmetry in lymphocytes, despite prior reports in stem-like cells (Katajisto et al., 2015), but rather that inequality was associated with clearance/degradation during cytokinesis.

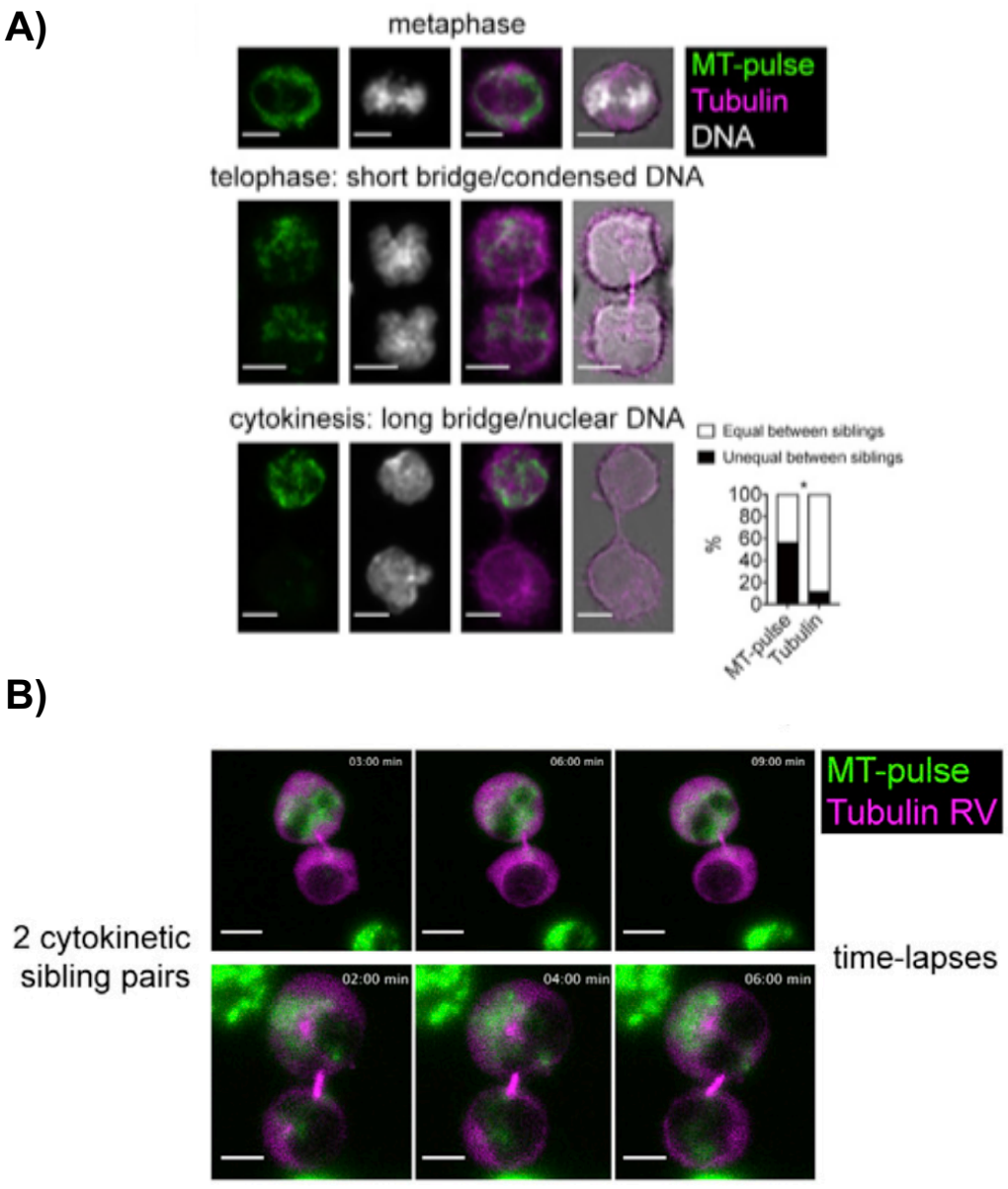

Figure 2.3 Asymmetric elimination of aged mitochondria during late cytokinesis. (A). MitoTracker Red FM (MTR)-pulsed, LPS-stimulated B cells fixed after 44 hr and stained with DNA dye and anti-tubulin antibodies. One representative metaphase (symmetric), telophase (symmetric), and cytokinetic (asymmetric) event is shown. Results are representative of 3 independent experiments. (Pooled number of events: metaphase, n = 11 cells; telophase, n = 8 sibling pairs; cytokinesis, n = 18 sibling pairs). The graph depicts the percentage of sibling cell pairs with equal or unequal ratios of MTR and tubulin (*$p < 0.05$, Fisher's exact test). (B) Live cell imaging of LPS-stimulated B cells transduced with mCherry-alpha-tubulin RV and pulsed labeled with MTG 16 hr prior to imaging. 2 representative time lapse series are shown. Frames, left to right, represent 3-min (upper row) and 2-min (lower row) intervals. Scale bars, 5 um.

Notably, the clearance of aged (pulse-labeled) mitochondria was also coordinate with the clearance of aged (pulse-labeled) lysosomes (Figure 2.4A), suggesting that stasis of membrane bound organelles is implicated in homeostatic pathways associated with degradation. To determine whether unequal mitochondrial clearance correlated with cell fate, we sorted self-renewing Pax5(hCD2)-hi and terminally differentiated Pax5(hCD2)-lo cells from the same range of late cell divisions, and stained mitochondria alongside lysosomes or autophagosomes to obtain a quantitative measure of mitophagy. Lysosomes were labeled with the fluorescent dye Lysotracker Deep Red, while CytoID, a fluorescent probe (Enzo Life Sciences) that specifically labels autophagosomes, was used to visualize autophagy (Chan et al., 2012; Guo et al., 2015). Steady state co-localization of mitochondria with lysosomal or autophagic puncta was infrequent. However, co-localization was more frequently observed in self-renewing cells that had maintained Pax5 expression (Figure 2.4B). Additionally, mDivi-1 treatment, which reduced mitoclearance by flow cytometry (Figure 2.1A), decreased the steady-state incidence of co-localization between mitochondrial and lysosomes in Pax5hi cells (Figure 2.4B). Taken together, these results suggest that the stasis of aged mitochondria is a feature of terminal differentiation in T and B cells.

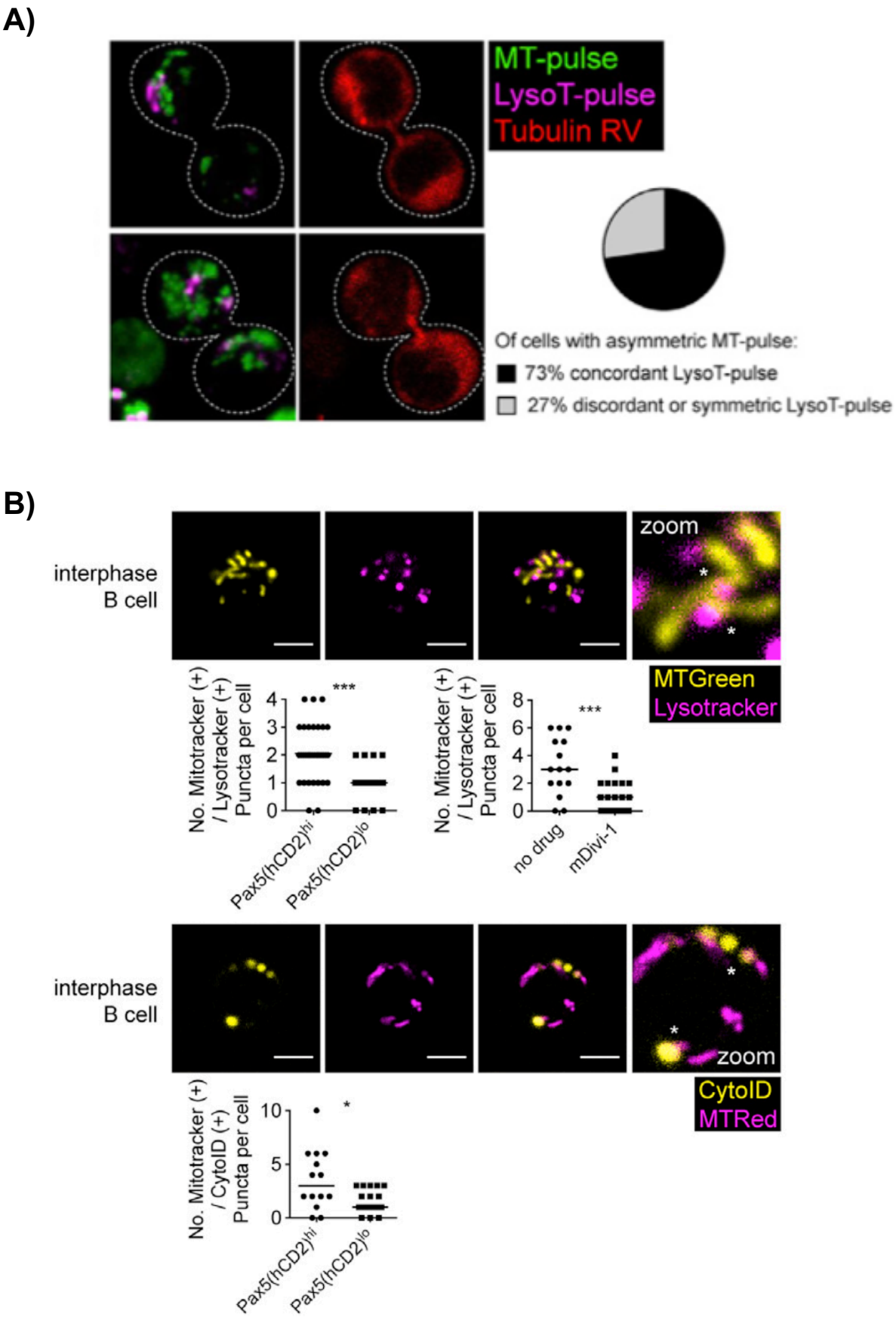

Figure 2.4. Unequal mitochondrial clearance is associated with differential mitophagy.

Figure 2.4. Unequal mitochondrial clearance is associated with differential mitophagy. (A). Live cell imaging of LPS-stimulated B cells transduced with mCherry-alpha-tubulin RV and co-pulsed with Mitotracker Green (MTG) and LysoTracker 16 hr prior to imaging. Images show 2 representative cytokinetic daughter cell pairs. Of the cells imaged, 73% had concordant asymmetric MTG and LysoTracker abundance (n = 11 sibling pairs). (B) Live cell imaging of mitophagy in activated B cells. Pax5-hCD2 reporter B cells were stimualted for 3 days with LPS and sorted based on surface hCD2 expression. Cells were then labeled with MTG and LysoTracker DeepRed (top panels) or CytoID and MTR. Steady-state mitophagy was determined by co-localization of mitochondrial puncta with LysoTracker or CytoID puncta. Top left graph indicates the number of co-localized MTG/LysoTracker DeepRed puncta for Pax5-hi (n = 35) and Pax5-lo (n = 17) cells. *** $p<0.001$, Mann-Whitney test. Top right graph indicates the number of co-localized MTG/LysoTracker DeepRed puncta, amongst Pax5-hi cells sorted from cultures stimulated in the absence (n = 15) or presence (n = 21) of mDivi-1. ***$p<0.005$, Mann-Whitney test. Bottom graph indicates the number of co-localized MTR/CytoID puncta amongst Pax5-hi (n = 14) and Pax5-lo (n = 19) cells (*$p < 0.05$, Mann-Whitney test). Scale bars, 5 uM. Fourth panel in each row is a zoomed-in version of the third panel.

Asymmetric localization and inheritance of autophagosomes mediated by PI3K

Our results suggest that differential degradation could contribute to the observed inequalities in inheritance of aged mitochondria. Mitophagy converges with the macroautophagy pathway to direct degradation of bulk substrates (Green et al., 2011). To determine whether asymmetric autophagy mediates unequal mitochondrial elimination, we visualized autophagosomes with fluorescence dyes in mitotic B cells. Crucially, we found that the organelles were strikingly asymmetric in conjoined sibling cells (Figure 2.5). Given that aged mitochondria were generally symmetric in metaphase cells, it remained unclear at what stage in the cell cycle the signaling network that orchestrates this asymmetric autophagy becomes active. We found that asymmetry of autophagosomes was consistent as early as prometaphase (Figure 2.5). These results suggest that asymmetry of signals promoting the formation and/or localization of these degradative organelles occurs early in mitosis.

Formation of the isolation membrane of nascent autophagosomes is directed by Vps34 and inhibited by Class I PI3K/Akt/mTOR signaling. We therefore determined whether inhibition of PI3K activity could perturb autophagosome asymmetry in metaphase and cytokinetic as a candidate signaling machinery for orchestrating polarize inheritance of subcellular organelles related to metabolism. We found that treatment of B cells with LY294002 resulted in a consistent decrease in CytoID fluorescence, consistent with a role for Class III PI3K activity in initiating autophagosome formation. Nevertheless, autophagosome puncta were clearly visualized in both no drug and LY294002-treated cultures and exhibited the same morphology (Figure 2.5). Critically, inhibition of PI3K activity resulted in a more

symmetric distribution of autophagosomes in both metaphase and cytokinetic cells (Figure 2.5). Taken together, these results suggest that asymmetry of the autophagy machinery correlates with unequal degradation of aged mitochondria in dividing lymphocytes, and that this asymmetry pathway may be organized by PI3K.

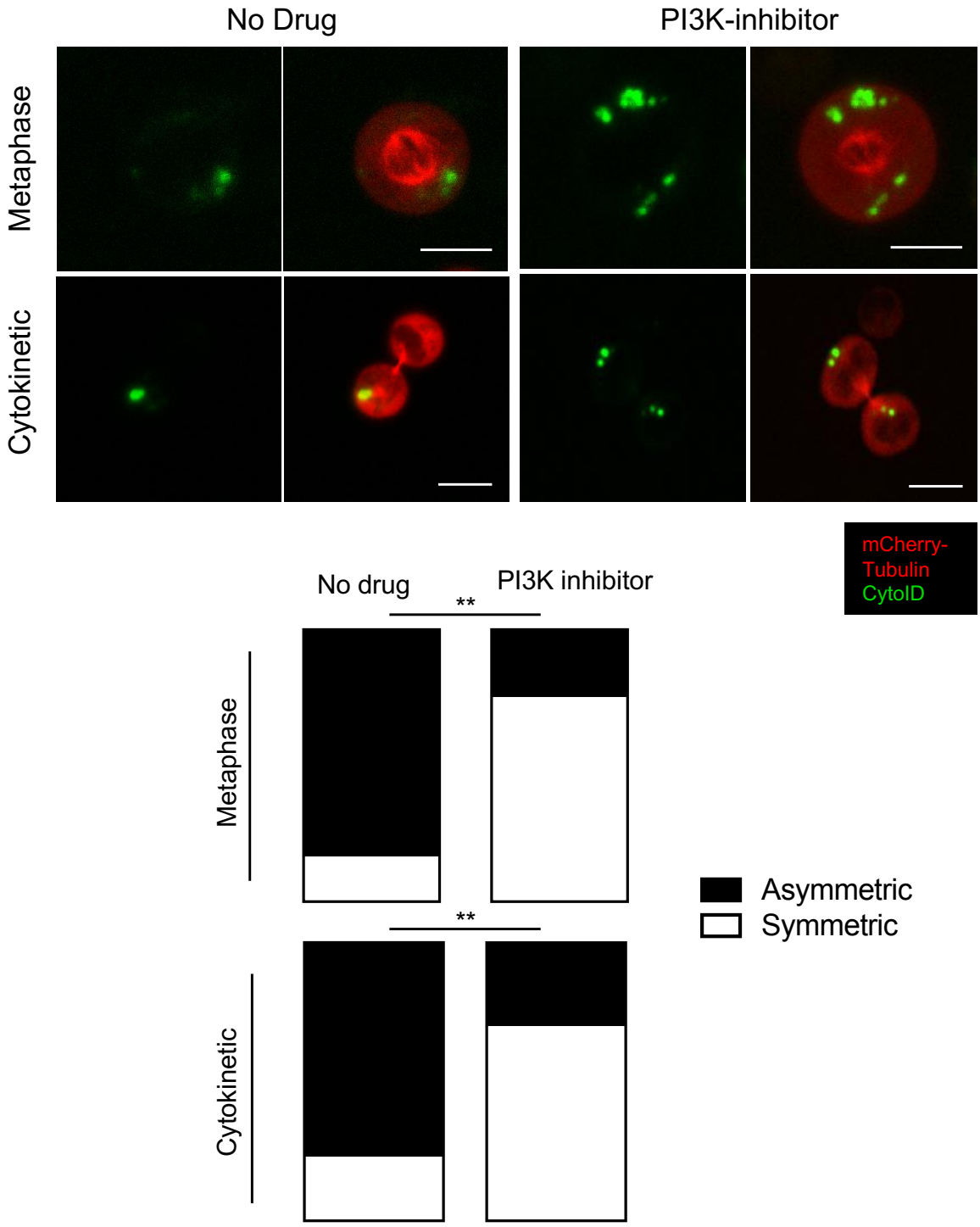

Figure 2.5 PI3K drives asymmetric autophagy in mitotic lymphocytes
Live cell imaging of autophagosome localization in LPS-stimulated B cells transduced with mCherry-tubulin and labeled with CytoID. Cells were stimulated with or without LY2920042. Upper: Representative images of metaphase and cytokinetic cells, with or without inhibitor. Lower: Proportion of asymmetric metaphase cells for No drug (83%) and PI3K inhibitor treatment (25%); proportion of asymmetric cytokinetic cells for No drug (77%) and PI3K inhibitor treatment (30%). ** $p<0.01$. Fisher's Exact Test. Scale Bars 5uM.

Discussion

Mitochondrial quality control and dynamics are key pathways that impinge on cellular and organismal homeostasis. The regulation of these mitochondrial pathways has been associated with normal growth and development, stem cell self-renewal, tissue remodeling, cellular metabolism, and healthy aging (Mishra and Chan, 2014). Clearance of aged mitochondria promotes self-renewal of hematopoietic, muscle, and breast stem cells as well as natural killer cells (García-Prat et al., 2016; Ito et al., 2016; Katajisto et al., 2015; O'Sullivan et al., 2015). Similarly, mitochondrial biogenesis (Bengsch et al., 2016; Scharping et al., 2016) and fusion (Buck et al., 2016; Khacho et al., 2016; Luchsinger et al., 2016) also support self-renewal of hematopoietic, neural, and memory T cells. Mitochondrial dynamics might therefore facilitate cellular self-renewal by eliminating dysfunctional organelles, while concurrently generating new organelles and fusing mitochondria to optimize the efficiency of oxidative metabolism as well as overall mitochondrial fitness. In this study, we show that unequal elimination of aged mitochondria is associated with cell fate bifurcations in lymphocytes and further that perturbation of this homeostatic pathway can alter lymphocyte differentiation. Asymmetric inheritance of autophagosomes, as driven by PI3K signaling earlier in mitosis, is associated with and may drive unequal clearance of mitochondria.

These findings support a model wherein mitochondrial stasis is part of a larger constellation of cellular metabolic signaling and autophagy. which may be associated with differentiation ROS production and inactivation of the key transcription factor FoxO1. Conversely, mitochondrial clearance appears to be part of a larger catabolic constellation of AMPK activation, autophagy, mitochondrial elimination, oxidative metabolism, maintenance of FoxO1 activity, and Pax5 or TCF1 expression. The

metabolic pathways implicated in unequal autophagy and mitochondrial elimination may be inherently bi-stable and thereby support acquisition of distinct cell fates following feedback/feedforward signaling.

MATERIALS AND METHODS

Mice

All animal work was conducted in accordance with Institutional Animal Care and Use Guidelines of Columbia University. Mice were housed in specific-pathogen-free conditions. Both male and female mice were used, and all mice were between 6-8 weeks of age. Strains used include: C57BL/6 (wild type), P14 TCR transgenic (P14) recognizing LCMV peptide gp33-41/Db, OT-II, and Pax5-IRES-hCD2 reporter mice (Fuxa and Busslinger, 2007).

In vitro lymphocyte activation

Spleens from mice of the indicated genotypes were isolated and processed using established protocols. Wild type B cells were enriched from splenocytes using magnetic bead negative selection kits (Miltenyi Biotec). B cells were stimulated with 20ug/mL LPS and polyclonal CD8+ T cells were stimulated with plate-bound anti-CD3/CD28 (1ug/mL) supplemented with 100IU/mL IL2. For experiments with P14 CD8+ T cells, bulk splenocytes were activated with gp33 peptide (1ug/mL) as previously described (Lin et al., 2016). In all experiments, lymphocytes were labeled with Cell Trace Violet (CTV) prior to stimulation according to the manufacturer's instructions to monitor cell division number. Where indicated, cells were treated with LY294002 (pan PI3K-inhibitor, Cell Signaling Technology, used at 2.5-5uM).

Retroviral Transduction

Enriched B cells or CD8+ T cells were stimulated with LPS or plate-bound anti-CD3/anti-CD28 antibodies plus IL-2, respectively, for 36 hr prior to retroviral

transduction. Cells were then re-plated in supernatant collected prior to transduction. Retroviral constructs used were as follows: mCherry-α-tubulin fusion; mouse dominant-negative Drp1(K38A), a gift from David Chan (Addgene plasmid 26049) and subsequently cloned into the MSCV-IRES-Thy1.1 plasmid, a gift from Anjana Rao (Addgene plasmid 17442). Empty MSCV-IRES-Thy1.1 or MSCV-IRES-GFP vectors were used as controls.

In vivo infection

For *in vivo* experiments of CD8+ T cell differentiation, 1-3x10^6 TCF7-GFP reporter P14 CD8+ T cells were adoptively transferred intravenously (i.v.) into allotype-disparate C57Bl/6 wild-type mice, which were subsequently infected with 5x10^3 CFUs of *L. monocytogenes* expressing gp33 (LM-gp33) via i.v. injection. Spleens were harvested at day 4-5 of infection, and CD8+ T cells were then MACS enriched for cell sorting of transferred, TCF7-GFP+ P14 cells. For experiments on tissue homing of Th1 CD4+ T cells, 1-3x10^6 OT-II Thy1.1+ CD4 T cells were purified, pulse-labeled with CTV and MitoTracker Green FM, and then adoptively transferred into Thy1.2+ recipients 24 hr before intranasal infection with 250 50%-tissue culture-infective dose PR8-OVA influenza virus.

FACS staining

Single-cell suspensions were prepared and stained as previously described (Lin et al., 2015). For staining of transcription factors, the eBioscience Foxp3 kit was used. Antibodies used in this study include: IRF4 (3E4 eBioscience), TCF1 (C63D9, Cell

Signaling Technology), and Pax5 (1H9, eBioscience). BD LSRII and Fortessa flow cytometers were used to analyze cells. Data were analyzed using FlowJo (Tree Star).

Organelle Pulse Labeling

Cells were labeled with Cell Trace Violet (CTV; Thermo Fisher Scientific) prior to stimulation to track cell division. Mitochondria were pulse-labeled with MitoTracker Green FM or MitoTracker Red FM (200 nM) at 37 C for 15 min. Lysosomes were labeled with LysoTracker Deep Red (Thermo Fisher Scientific; 50–75 nM) for 30 min at 37 C in media. Autophagosomes were labeled with CytoID (Enzo Life Sciences). Labeling steps were followed by at least two washing steps in cell culture media.

Confocal Microscopy

Immunofluorescence microscopy of mitotic B and T cells was performed as previously described (Lin et al., 2015). Briefly, cells were adhered to poly-l-lysine (Sigma) coated coverslips and fixed with freshly prepared 3.7% paraformaldehyde followed by permeablization with 0.3% Triton X-100. Cells were then blocked in buffer containing 0.01% saponin and 0.25% fish skin gelatin (Sigma) in PBS+ and stained with antibodies to the indicated proteins. Antibodies used include: α-tubulin (YOL1/34, Abcam). All Alexa Fluor dye-conjugated secondary antibodies were obtained from Thermo Fischer. Imaging was performed on Nikon Ti-Eclipse inverted scanning confocal or spinning disk confocal microscopes. Images were processed with ImageJ software. Metaphase cells were identified by the presence of two microtubule organizing centers (MTOC) with opposed spindle poles. Late telophase/cytokinetic cells were identified by the presence

of a characteristic tubulin bridge and cytoplasmic cleft. For quantification of asymmetry in mitotic cells, fluorescent signal was thresholded to remove background, and the integrated fluorescence density in each nascent daughter cell or half of the metaphase plate was calculated. Statistical significance was assessed using GraphPad Prism and specific statistical tests are indicated in each figure legend.

Chapter 3: PI3K organizes a polarity and asymmetry pathway in lymphocytes

Portions of this Chapter have been adapted from the following manuscripts:

Chen YH*, **Kratchmarov R***, Lin WH*, Rothman NJ, Yen B, Adams WC, Nish SA, Rathmell JC, and Reiner, SL. (2017). Asymmetric PI3K Activity in Lymphocytes Organized by a PI3K-mediated Polarity Pathway. *Cell Reports. In revision.*

* These authors contributed equally.

Abstract

Cell intrinsic polarity pathways in lymphocytes have remained enigmatic, though previous work has implicated localized PI3K activity in the formation of the immunological synapse and cytotoxic T cell degranulation. Here, we show that activation of B and T cells induces internalization and polarized inheritance of antigen receptors. Additionally, activated lymphocytes had elevated PI3K signaling which subsequently induced the formation of PIP3 lipid-positive intracellular vesicular structures. Intracellular PIP3 exhibited polarized subcellular organization at the MTOC, co-localizing with antigen receptors. In mitosis, PIP3 and CD3 exhibited concordant asymmetry, with intracellular structures partitioning to the same side of metaphase cells. These results provide evidence for asymmetric, spatially constrained Class I PI3K activity *in vitro* and *in vivo*. Furthermore, we observed polarized regional trafficking and inheritance of the facultative glucose transporter Glut1, the expression of which was found to mark cells destined for terminal differentiation. Critically, perturbation of Class I PI3Kδ activity abrogated terminal effector differentiation and induced a striking loss of receptor and transporter polarity. Taken together, these results suggest that the distinct roles of PI3K signaling in cell growth, regulation of gene expression, and polarity may direct unequal cell fate outcomes.

Introduction

After synapsing with an antigen presenting cell (APC), a selected T cell clone divides to yield a more activated, proliferative, and differentiation-prone daughter cell alongside a less activated and more quiescent sibling cell (Arsenio et al., 2014; Chang et al., 2007; Pollizzi et al., 2016; Verbist et al., 2016). After 3 or 4 more divisions, progenitor cells differentiate and bifurcate in fate to irreversibly determined effector cells with *de novo* silencing of TCF1 expression, alongside self-renewing memory precursor cells that maintain TCF1 expression and the bipotency to yield daughter cells with discordant silencing of TCF1 (Adams et al., 2016; Lin et al., 2015; Lin et al., 2016; Nish et al., 2017b).

It remains unclear how lymphocyte progenitors undergoing these later divisions can organize signals in the absence of a defined external polarity cue. *In vivo*, the first T cell division as well as pre- and intra-germinal center B cell divisions leading to plasma cell selection occur in the context of an extrinsic contact, namely an APC interfacing with a T cell, and antigen or T cell help directing a B cell. Thus, polarity and asymmetry of immune synapse components such as the antigen receptor, integrins, and cytokine receptors preceding a cell division may confer an asymmetry cue to daughter cells. When activated lymphocyte progenitors divide asymmetrically after 4 or more divisions *in vivo*, however, it is not obvious what the polarizing stimulus might be. Furthermore, modeled differentiation conditions *in vitro*, i.e. B cells stimulated with LPS in buoyant media, or T cells stimulated with peptide/immobilized antibodies, induce asymmetric division without a clear extrinsic cue.

To further elucidate the nature of asymmetric fate outcomes in late division lymphocytes, we considered cell-intrinsic mechanisms that do not depend on the polarity network or an extrinsic cue. Endosomal vesicular traffic can direct asymmetric division independent of PAR proteins and engages in crosstalk with Class II PI3K activity (Emery et al., 2005). Furthermore in lymphocytes, endocytosis of antigen receptors sustains activating signals and therefore plays an essential role in anabolic induction and sustained proliferation, *in vitro* and *in vivo* (Chaturvedi et al., 2011; Willinger et al., 2014). Endocytosis and anabolic signals via internalized antigen receptor do not require the continuing presence of an antigen presenting cell and can direct extensive proliferation, differentiation, and memory formation in subsequent generations of cells that had not contacted antigen directly (Kaech and Ahmed, 2001). Furthermore, anabolic signaling in the form of PI3K activity may have evolved to facilitate spatial segregation. Cell migration, axon growth, apico-basal polarity, and asymmetric skin progenitor cell division are all mediated by localized PI3K activation. We therefore assessed whether endocytosis and unequal anabolic signaling to cellular organelles can regulate cell fate decisions in late division lymphocytes.

Results

Compartmentalized PI3K activity associated with CD8+ T cell terminal differentiation

PI3K signaling drives effector CD8+ T cell differentiation and is required for asymmetric divisions that generate sibling cells with TCF1-high and low expression respectively (Lin et al., 2015). In our previous studies, we found that CD8+ T cells repress TCF1 only after several divisions. We therefore became interested in how these later cell generations could maintain polarized anabolic activity in the absence of an obvious external polarity cue. In lymphocytes, the microtubule organizing center (MTOC) is a candidate polarity landmark to orient unequal compartmentalization of signaling in relation to the axis of cell division. PI3K activity directs cellular traffic such as peri-centrosomal recycling, ciliogenesis, actin dynamics at the immune synapse, and Glut1 trafficking (Marat and Haucke, 2016). To assess the relationship between vesicular traffic and the MTOC, we activated P14 CD8+ T cells *in vitro* with gp33 peptide, and imaged cells through confocal IF microscopy at day 3-4 post-activation when cells had undergone several divisions and began to repress TCF1 (Figure 3.1A). As endocytosis is critical for sustained TCR signaling and anabolic activity (Willinger et al., 2014), we first examined the subcellular localization of CD3. Unstimulated T cells had diffuse CD3 expression throughout the plasma membrane. Upon TCR stimulation, CD3 became polarized and localized intracellularly to the MTOC (Figure 3.1A). This polarity was maintained in dividing cells, as CD3 was found to be asymmetric at metaphase during these later divisions. We then examined the subcellular distribution of PIP3, a lipid signaling intermediate generated by active PI3K. We found that PIP3+ membranes were primarily found in discrete puncta that frequently localized to the MTOC of later-division

T cells, in both interphase and metaphase (Figure 3.1B). This localization was concordant with intracellular CD3 polarity. Critically, metaphase cells with asymmetric PIP3 also exhibited concordant CD3 asymmetry (Figure 3.1B). Examination of CD98, a receptor implicated in asymmetric mTOR induction in first-division T cells (Pollizzi et al., 2016; Verbist et al., 2016), revealed that asymmetric localization of CD3 was not accompanied by coordinate asymmetry of CD98 (Figure 3.2) suggesting that receptor/PIP3 asymmetry involves regulated localization rather than non-specific accumulation of bulk membrane domains.

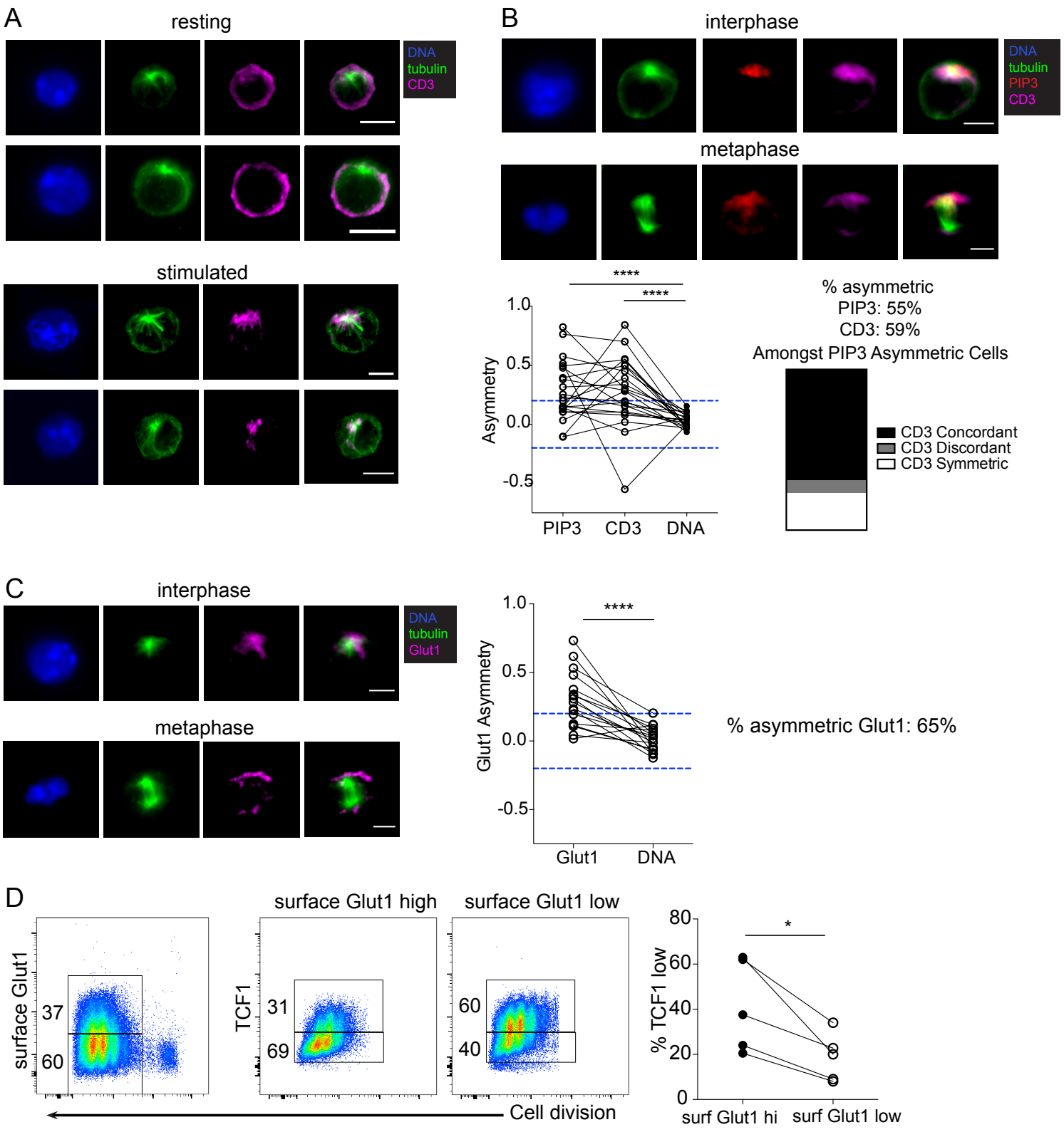

Figure 3.1. Asymmetric division of functional PI3K activity in CD8+ T cells

Figure 3.1. Asymmetric division of functional PI3K activity in CD8+ T cells
(A) Confocal immunofluorescence (IF) microscopy analysis of CD3 localization in unstimulated (N=16) or gp33 peptide-stimulated interphase P14 CD8+ T cells activated for 3 days (N=23).
(B) Top, CD3 and PIP_3 localization in interphase and metaphase P14 blasts at day 3 post-activation. Bottom left, quantification of CD3 and PIP_3 asymmetry in metaphase cells. **** $p<0.001$. Chi Square test with Bonferroni's Correction. Bottom right, amongst PIP_3 asymmetric cells, proportion with CD3 asymmetric concordant (same MTOC), CD3 asymmetric discordant (opposite MTOC), or CD3 symmetric localization.
(C) Left, Glut1 localization in interphase and metaphase P14 blasts. Right, quantification of Glut1 asymmetry in metaphase cells. **** $p<0.001$. Fisher's Exact test.
(D) CD8+ T cells expressing myc-tagged Glut1 were stimulated with anti-CD3/CD28 + IL-2 for 3.5 days. Left, Surface Glut1 versus cell division, gated for high and low populations. Middle, TCF1 expression versus cell division within surface Glut1-high and low populations; Right, quantification of TCF1-low population frequency. * $p<0.05$. Paired T test.
For all panels, dashed blue line denotes asymmetry cutoff value of 0.2, and scale bars = 5 um.

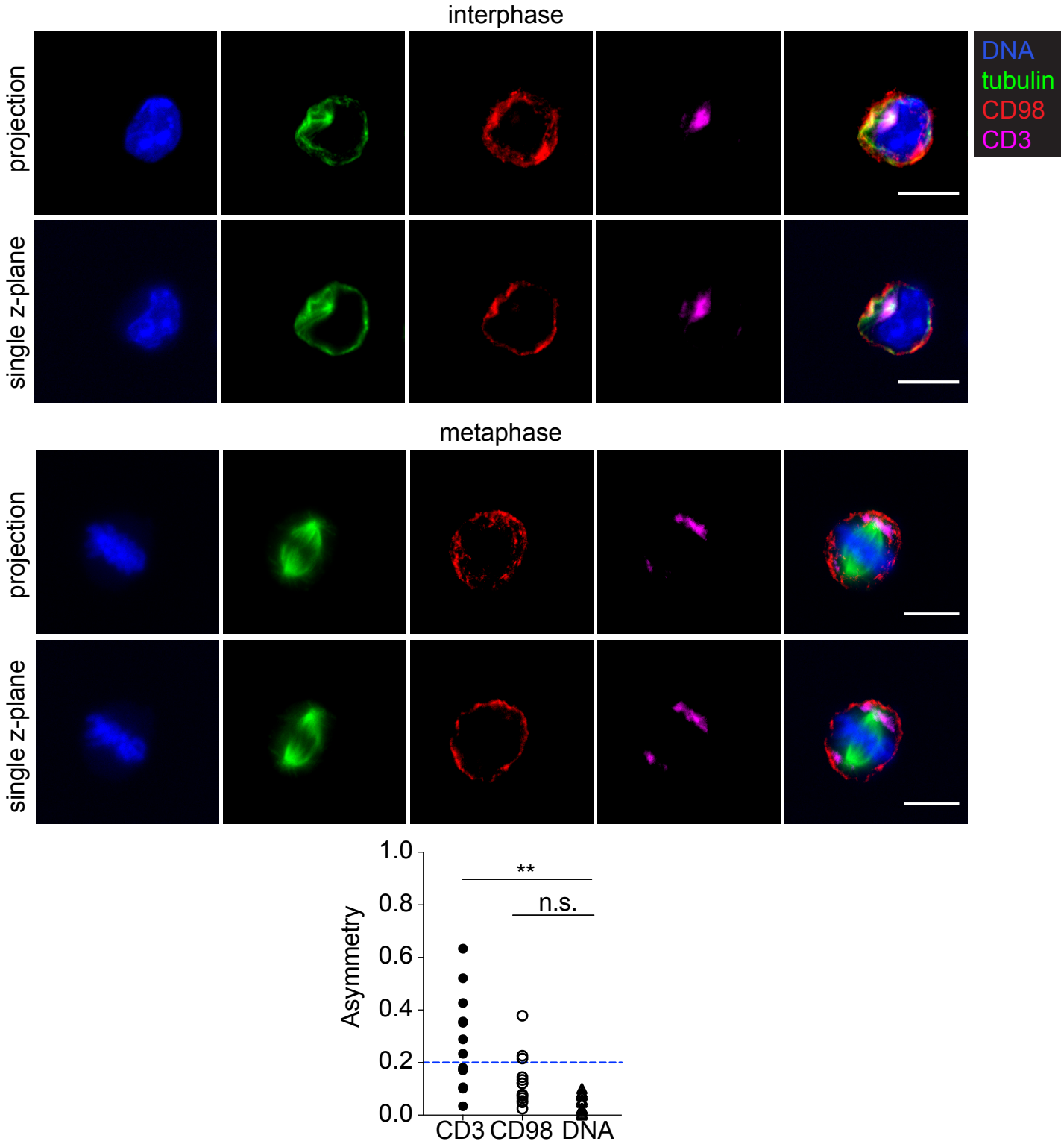

Figure 3.2 Specific receptor polarity and asymmetry is not accompanied by universal receptor polarity

Figure 3.2 Specific receptor polarity and asymmetry is not accompanied by universal receptor polarity Localization of CD98 and CD3 in interphase and metaphase P14 CD8+ T cells activated for 3 days as in Figure 3.1. Both 3-dimensional projection of the entire cell and a single z-slice in the plane of the MTOC or the mitotic spindle are shown. Quantification of CD3 asymmetry relative to DNA in metaphase cells (**$p<0.01$) and CD98 symmetry (n.s. not significantly different than DNA). Chi Square Test with Bonferroni's Correction.

The previously reported observation that activated CD8+ T cells can continue to proliferate and differentiate after transfer to a naïve host led us to examine whether cellular asymmetry was dependent on contact with an antigen presenting cell (Kaech and Ahmed, 2001). We stimulated P14 CD8+ T cells *in vitro* and then sorted cells at 24 hours post-activation (before the first cell division) to obtain a pure population of blasting lymphocytes and remove all APCs/antigen (Figure 3.3). Cells were then re-plated in fresh media containing IL-2 but no peptide and cultured for 3 days followed by IF microscopy analysis. Both CD3 and PIP3 were polarized in interphase cells and asymmetric in mitotic cells, albeit at a lower frequency than during in culture with APCs (Figure 3.3). These data suggest that CD8+ T cells can divide asymmetrically to generate sibling cells with unequal inheritance of endocytosed TCR, independent of contact with an APC.

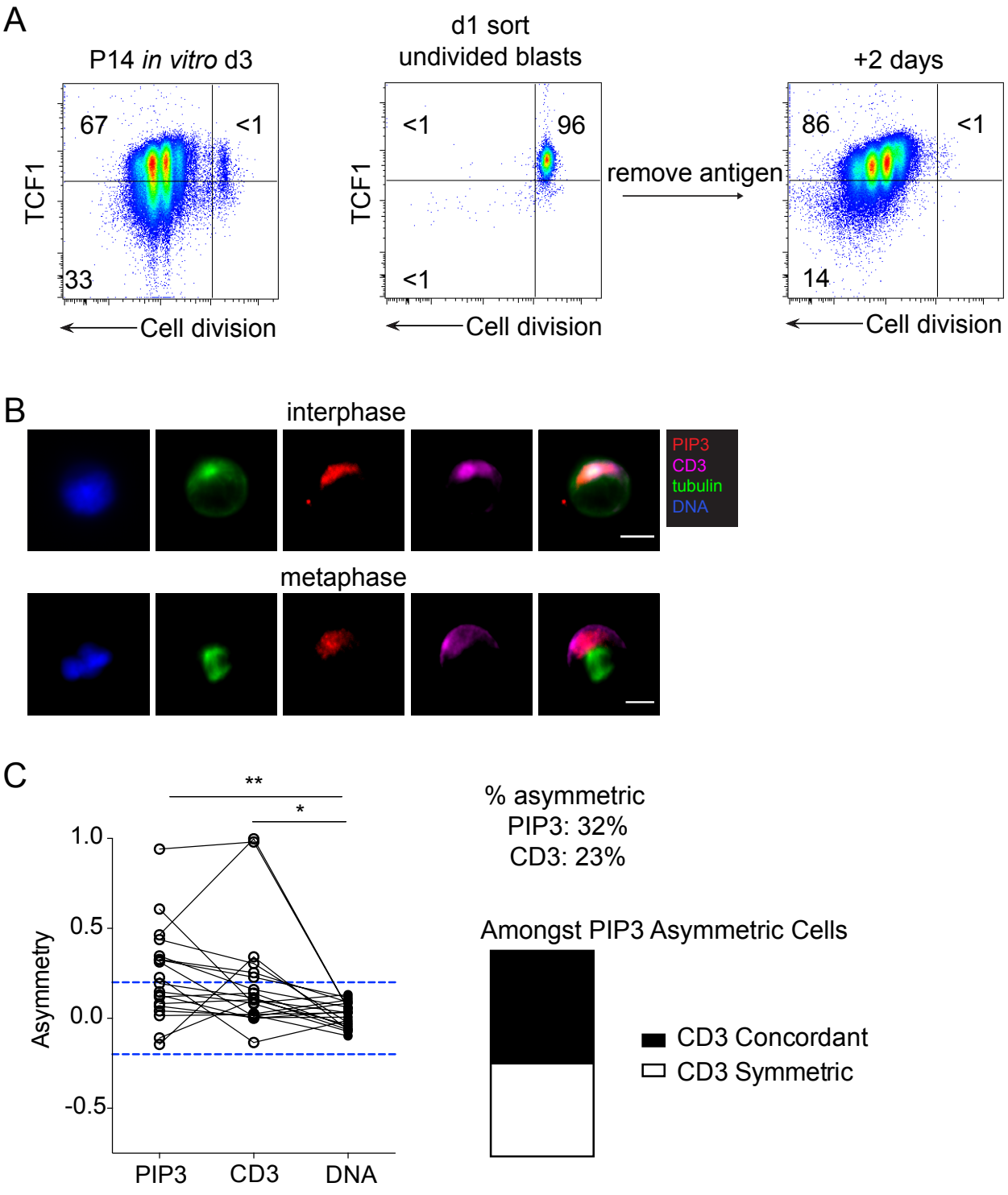

Figure 3.3. Sustained PI3K and antigen receptor polarity in the absence of peptide antigen

Figure 3.3 Sustained PI3K and antigen receptor polarity in the absence of peptide antigen

P14 CD8+ T cells were stimulated with gp33 peptide as in Figure 3.1 for 22 hours. Cells were then sorted before the first cell division to remove antigen and non-P14 splenocytes. Sorted cells were then re-plated in fresh media containing IL-2 without gp33 peptide. A.) Representative FACS plots of TCF1 expression versus cell division for: Left: unsorted P14 cells at day 3, Middle: sorted P14 cells at 22 hours, Right: P14 cells 48 hours post-sort. Left two quadrants indicate divided TCF1 high and low populations. B.) Representative images of PIP3 and CD3 subcellular localization in interphase and metaphase cells 48 hours after sorting and antigen removal. C.) Left: Quantification of PIP3 and CD3 asymmetry in metaphase cells. **$p<0.01$. *$p<0.025$. Chi Square Test with Bonferonni's Correction. Right: Proportion of PIP3 asymmetric cells with concordant CD3 asymmetry or CD3 symmetry. Scale bar, 5 um.

Effector CD8+ T cell differentiation requires sufficient anabolic activation, with concomitant metabolic reprogramming toward aerobic glycolysis (Warburg effect). Glut1 is the principal inducible glucose transporter in T cells and is upregulated upon TCR stimulation. Furthermore, PI3K signaling is essential for trafficking of Glut1 from recycling endosomes to the plasma membrane (Wofford et al., 2008). We examined the subcellular localization of Glut1 in late division CD8+ T cells. Glut1 was primarily found in discrete intracellular puncta, largely polarized to the MTOC, with some transporter also detectable in the plasma membrane (Figure 3.1D). In metaphase cells, Glut1 continued to exhibit an intracellular localization pattern and was frequently asymmetric. To determine whether Glut1 expression is associated with terminal CD8+ T cell differentiation, we used surface Glut1 reporter mice expressing a myc-tag on the extracellular domain of Glut1 (Michalek et al., 2011). Myc-Glut1 CD8+ T cells were activated with TCR stimulation *in vitro*, and the relationship between surface Glut1 and TCF1 expression was analyzed by flow cytometry (Figure 3.1D). Consistent with the previously described role of Glut1 in anabolic activation of CD4+ T cells (Macintyre et al., 2014), cells expressing high levels of surface Glut1 were enriched for TCF1-low effector cells. Asymmetric inheritance of glucose transporters may therefore be associated with TCF1 repression and terminal differentiation of CD8+ T cells. Taken together, these findings suggest that a spatially restricted network of PI3K signals organize polarity and asymmetry of key signaling factors including nutrient receptors and antigen recognition to regulate T cell differentiation.

Asymmetric PI3K activity drives unequal BCR and glucose transporter inheritance in B cells

Given the polarity and asymmetric inheritance of CD3 observed in CD8+ T cells, we sought to determine whether activated B cells also exhibit compartmentalized anabolic signaling. LPS-stimulated B cells transmit PI3K and other critical activating signals through CD19 and IgM (Keppler et al., 2015; Schweighoffer et al., 2017). We therefore first determined whether IgM exhibits asymmetric inheritance during B cell divisions associated with cell fate bifurcations *in vitro*. Terminally differentiated plasmablasts are generated in response to both T-cell dependent and independent antigens. *In vitro*-modeled differentiation of B cells utilizing LPS-stimulation recapitulates the subset dynamics observed during *in vivo* immunization and is characterized by a bifurcation of self-renewing Pax5-hi B cells and differentiated Pax5-lo plasma cells (Lin et al., 2015; Xu et al., 2015a). To determine whether soluble LPS signals can trigger compartmentalized anabolic activity, we performed IF microscopy analysis of IgM in B cells at day 3 post-activation. Compared to unstimulated B cells, B cells receiving tonic TLR stimulation for 3 days had predominantly intracellular IgM, which was polarized to the MTOC (Figure 3.4A). These results are in accordance with previous working documenting rapid internalization of BCR following acute BCR stimulation (Chaturvedi et al., 2011). The polarity of IgM was maintained in dividing B cells, as IgM exhibited an asymmetric distribution from prophase through cytokinesis (Figure 3.4A). Asymmetry of IgM may reflect global unequality in antigen signaling in light of the previously observed asymmetric inheritance of internalized antigen by mitotic B cells (Thaunat et al., 2012).

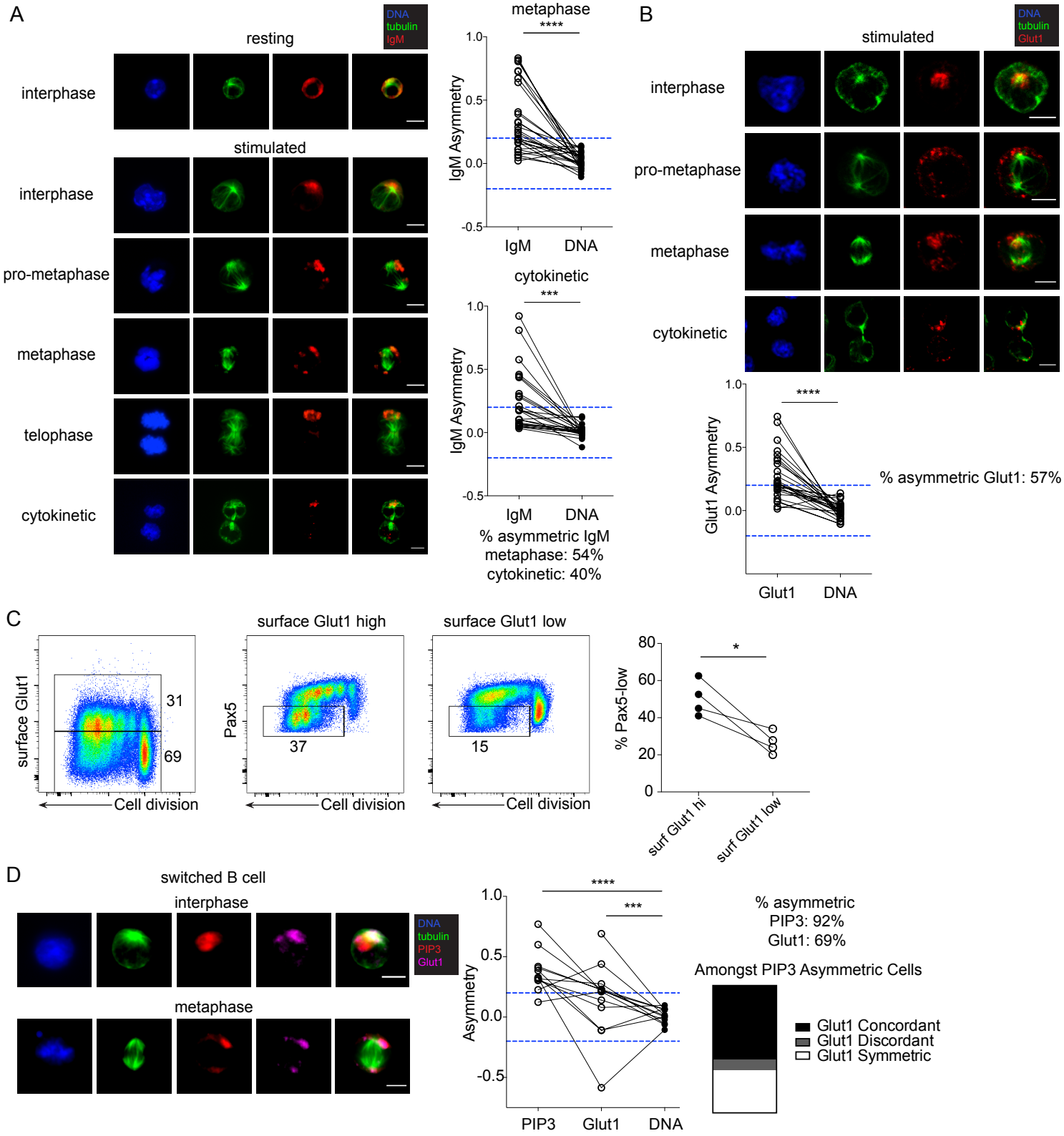

Figure 3.4. Asymmetric division of functional PI3K activity in B cells

Figure 3.4. Asymmetric division of functional PI3K activity in B cells
(A) Confocal IF microscopy analysis of IgM localization in LPS-stimulated B cells at day 3 post-activation. Left, IgM localization in unstimulated (resting) interphase (N=16) or LPS-stimulated interphase and mitotic B cells (N=19). Right, quantification of IgM asymmetry in metaphase and cytokinetic cells. **** $p<0.0001$. *** $p<0.001$. Fisher's Exact test.
(B) Upper, Glut1 localization in LPS-stimulated mitotic B cells at indicated stages of cell cycle. Lower, quantification of Glut1 asymmetry in metaphase cells. **** $p<0.0001$. Fisher's Exact test.
(C) B cells expressing myc-tagged Glut1 stimulated with LPS for 3.5 days. Left, surface Glut1 versus cell division, gated for high and low populations. Middle, Pax5 expression versus cell division within the surface Glut1-high and low populations. Right, quantification of Pax5-low population frequency. *$p<0.05$. Paired T test.
(D) Class-switched (IgM-negative), resting memory B cells stimulated with LPS and analyzed by IF microscopy on day 3 post-activation. Left, subcellular localization of PIP_3 and Glut1 in interphase and metaphase blasts. Middle, quantification of PIP_3 and Glut1 asymmetry in metaphase cells. **** $p<0.0001$. *** $p<0.001$. Chi Square test with Bonferroni's Correction. Right, amongst cells with asymmetric PIP_3, proportion of asymmetric concordant, asymmetric discordant, and symmetric Glut1 localization.

BCR stimulation induces metabolic reprogramming of B cells with increased glycolytic flux and expression of the facultative glucose transporter Glut1, which is required for efficient differentiation of antibody-secreting plasma cells *in vivo* (Caro-Maldonado et al., 2014). We therefore assessed whether differences in active glucose transport are associated with B cell fate bifurcations marked by Pax5 repression *in vitro.* When we examined the subcellular localization of Glut1, we found that LPS-stimulated interphase B cells had polarized Glut1, predominantly localized to intracellular vesicles (Figure 3.4B). Furthermore, intracellular Glut1 was asymmetric in mitotic B cells, indicating that a soluble stimulus can induce polarization of the anabolic machinery. We then sought to correlate Glut1 activity with B cell fate. B cells expressing myc-tagged Glut1 were stimulated with LPS and assessed by flow cytometry on day 3 post-activation for Pax5 expression. As with CD8+ T cells, B cells that expressed high levels of surface Glut1 were enriched for the Pax5-low plasmablast subset (Figure 3.4C). Of note, surface Glut1-high B cells that had passed the third division abruptly became significantly enriched for the Pax5-low subset.

We next asked whether polarized vesicle traffic in activated B cells is associated with spatially restricted PI3K signaling. It has previously been established that the induction of aerobic glycolysis following BCR stimulation relies on PI3K signals (Doughty et al., 2006). We therefore assessed the localization of PIP3+ vesicles in a modified *in vitro* model of differentiating B cells. Due to limitations in antibody clone availability, switched memory (IgM-) B cells were used. Sorted IgM- follicular B cells were stimulated with LPS as for previous experiments and then imaged at day 3 post-activation. Notably, PIP3 was found to be polarized in interphase cells, as for CD8+ T

Cells (Figure 3.4D). Furthermore, polarity of PIP3 was concordant with Glut1, and PIP3 vesicles were often asymmetric in metaphase cells. These findings are compatible with a model where BCR and TLR stimuli both converge on a scaffold of polarized CD19 and IgM to organize intracellular polarity of the anabolism machinery and subsequent asymmetric division.

Inhibition of PI3K activity abolishes compartmentalized anabolic activity

To determine the requirement of PI3K signaling for orchestrating polarity and asymmetry of antigen receptors and Glut1, we performed transient pharmacological inhibition experiments followed by IF imaging in B and T cells. P14 CD8+ T cells were activated in the presence or absence of LY294002, a pan-PI3K inhibitor. We then quantified interphase polarity and metaphase asymmetry of TCR. For interphase cells, a decentralization score was calculated based on the proximity of fluorescent puncta of molecule of interest relative to the MTOC (see Methods). While CD3 was polarized to the MTOC in the majority of the activated T cells, it was highly decentralized from the MTOC in cells that had abolished PI3K activity (Figure 3.5A). Inhibition of PI3K did not impair internalization of CD3, as it was still present in intracellular punctate structures. The decentralized pattern of CD3 in interphase cells lacking intact PI3K activity was phenocopied by treatment with Blebbistatin, an inhibitor of non-muscle myosin II (Figure 3.5A). Myosin II is required for reorientation of the centrosome to the immune synapse upon antigen encounter by T cells (Le Floc'h et al., 2013). Loss of PI3K activity also disrupted CD3 asymmetry in metaphase cells for late-division CD8+ T cells (Figure

3.5B). Inhibition of non-muscle myosin II also disrupted PIP3 polarization to MTOC in interphase T cells (Figure 3.5C).

In view of the importance of class I PI3K activity, particularly PI3Kδ, in antigen receptor signaling (Fruman et al., 2017; Lucas et al., 2016), we tested the effect of Idelalisib, a PI3Kδ-specific inhibitor, and Pictilisib, a pan-class I PI3K inhibitor on T cell fate, nutrient utilization, and polarity. Like LY294002, class I-specific PI3K inhibition resulted in defective silencing of TCF1, reduced cell surface trafficking of Glut1, diminished glucose uptake (Figure 3.5D), and defective CD3 polarity, though the latter defect was more severe in interphase than metaphase cells (Figure 3.5E).

Inhibition of PI3K activity perturbed the asymmetry of endocytosed antigen receptors in both metaphase and cytokinetic B cells (Figure 3.5 F, G). As with CD8+ T cells, inhibition of PI3K activity also led to a disruption of polarity of Glut1 in interphase dividing B cells (Figure 3.5H). Taken together, our data suggest that PI3K activity organizes the polarity of endocytosed antigen receptors and may direct its own cellular asymmetry during cell division.

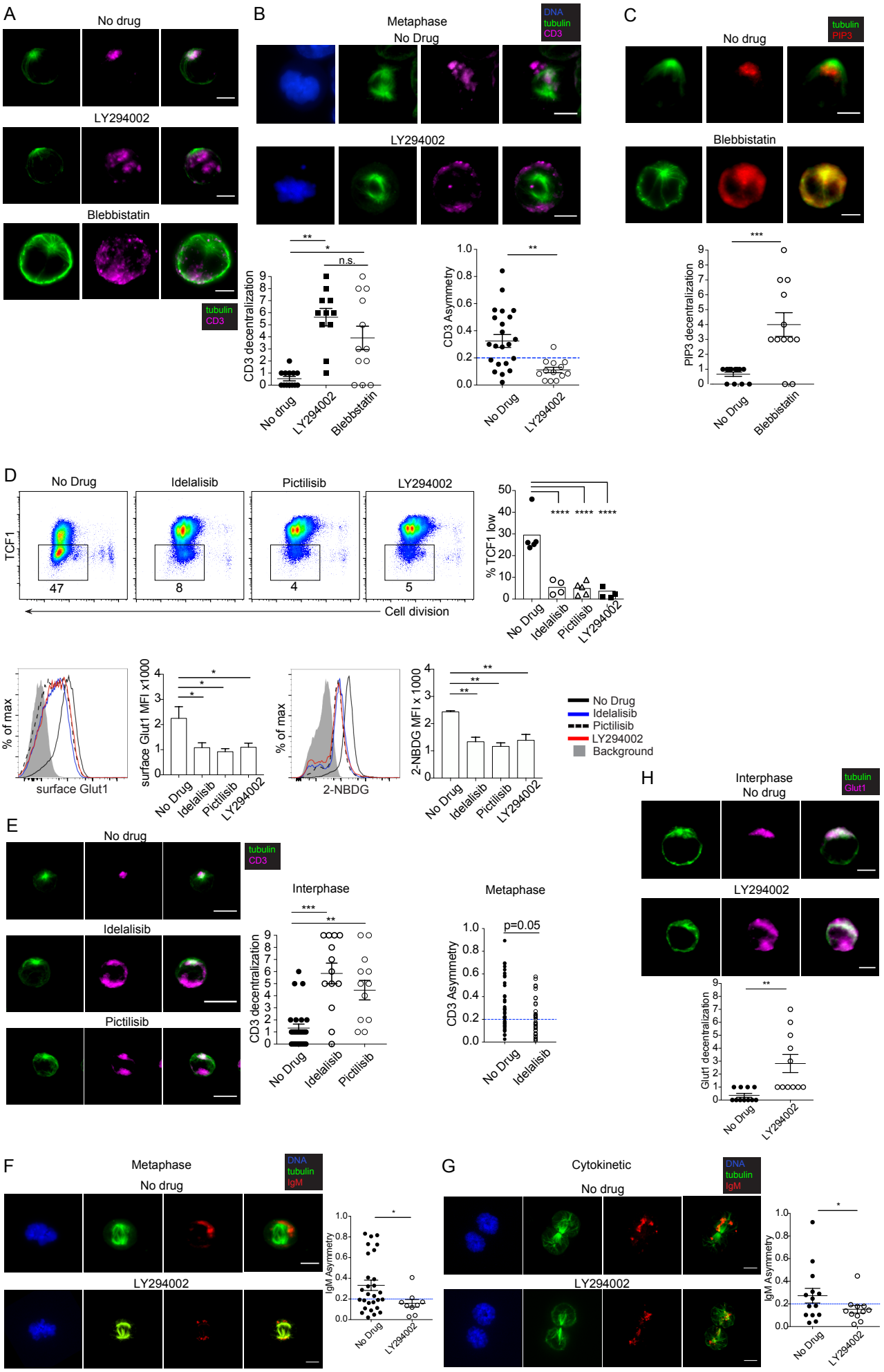

Figure 3.5. PI3K-dependent polarity control of asymmetric PI3K signaling

Figure 3.5. PI3K-dependent polarity control of asymmetric PI3K signaling

(A) P14 CD8+ T cells activated as in Figure 3.1 and treated with the indicated drugs to perturb polarity. Upper: CD3 localization in cells treated with No drug, LY294002, or Myosin II inhibitor (Blebbistatin). Lower right: CD3 decentralization score in indicated treatment groups. *p<0.05. **p<0.01. n.s. not significant. Kruskal-Wallis non-parametric test.

(B) Upper: CD3 localization in metaphase cells treated with No drug or PI3K inhibitor. Lower right: Quantification of CD3 asymmetry in indicated treatment groups. **p<0.01 Fisher's Exact Test.

(C) Upper: PIP_3 localization in interphase CD8+ T cells treated with No drug or Blebbistatin. Lower: PIP_3 decentralization score in indicated treatment groups ***p<0.001 Mann-Whitney U test.

(D) Class I PI3K-driven TCF1 repression and facultative glucose transporter function. Upper row, representative flow cytometry of cell division and TCF1 expression at day 4 in the absence or presence of Idelalisib (PI3Kδ inhibitor), Pictilisib (pan-class I PI3K inhibitor), or LY294002 (pan-PI3K inhibitor). Quantification of frequency of TCF1-repression. Lower left, representative flow cytometry and quantification of surface Glut1 detection in P14 CD8+ T cells 3 days post-activation in the absence or presence of indicated inhibitors. Lower right, representative flow cytometry and quantification of fluorescent glucose analog 2-NBDG uptake in the absence or presence of the indicated inhibitors. *p<0.05 **p<0.01 **** p<0.0001 One way ANOVA.

(E) Representative images of CD3 localization in interphase CD8+ T cells activated in the absence or presence of Idelalisib or Pictilisib. Decentralization score of indicated groups quantified. **p<0.01. ***p<0.001. Kruskal-Wallis non-parametric test. Far right, quantification of CD3 asymmetry in metaphase CD8+ T activated in the absence or presence of Idelalisib p=0.05. Mann-Whitney U test.

(F, G) Representative immunofluorescence images and quantification of IgM asymmetry in LPS-activated B cells in the absence or presence of LY294002 at metaphase (F) and cytokinesis (G). *p<0.05. Fisher's Exact Test.

(H) Representative images of Glut1 localization in interphase LPS-stimulated B cells in the absence or presence of LY294002. Decentralization score of indicated groups quantified. **p<0.01. Mann-Whitney U test.

Asymmetric PI3K signaling and Glut1 inheritance *in vivo*

To examine the compartmentalization and asymmetry of PI3K signaling in CD8+ T cells during an evolving infection *in vivo*, we employed the *Listeria monocytogenes (L. monocytogenes)* model. TCR transgenic P14 CD8+ T cells expressing a *Tcf7*$^{GFP/+}$ reporter were transferred intravenously to naive recipient mice, followed by infection of the recipients with *L. monocytogenes* expressing the LCMV peptide gp33 (LMgp33). Spleens were harvested at day 4-5 post-infection, and *Tcf7*-GFP^{hi} cells were sorted for analysis by confocal immunofluorescence microscopy. The majority of activated P14 cells had undergone 4 or more rounds of division. As with T cells activated *in vitro*, we found that CD3 and PIP3 localized to intracellular puncta, which frequently associated with the MTOC and co-localized. CD3 and PIP3 puncta were also polarized to the MTOC during metaphase in these later-divisions *in vivo* (Figure 3.6A). Furthermore, the asymmetry of intracellular CD3 was concordant with PIP3 asymmetry. We found that Glut1 was also polarized in TCF1-hi interphase cells and asymmetric in metaphase cells *in vivo* (Figure 3.6B). Asymmetric Glut1 exhibited concordant sidedness with asymmetric PIP3 during metaphase (Figure 3.6C). Taken together, these results suggest that CD8+ T cells undergoing late divisions *in vivo* exhibit compartmentalized PI3K activity that correlates with asymmetric inheritance of antigen receptor and facultative glucose transporters.

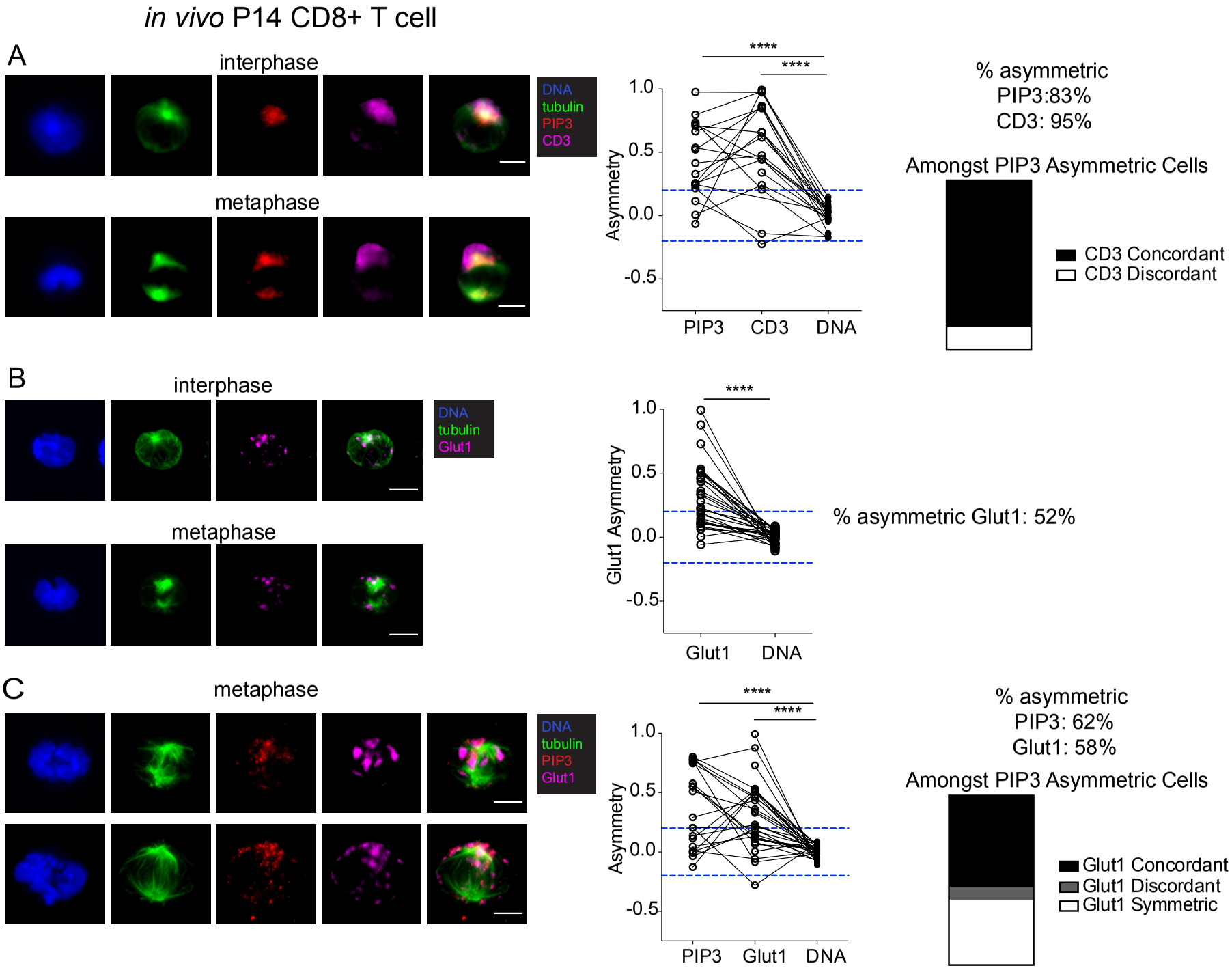

Figure 3.6 Asymmetric PI3K activity organizing unequal inheritance of antigen receptor and glucose transporter in vivo.

Figure 3.6. Asymmetric PI3K activity organizing unequal inheritance of antigen receptor and glucose transporter *in vivo.*
(A) Polarization and asymmetric inheritance of CD3 and PIP_3 in interphase and metaphase P14 CD8+ T cells *in vivo* during *L. monocytogenes* infection. FACS-sorted TCF7-GFP reporter P14 CD8+ T cells at day 4-5 post-infection analyzed by IF microscopy. Left: PIP3 and CD3 localization in interphase and metaphase blasts. Right, quantification of PIP_3 and CD3 asymmetry in metaphase cells. **** $p<0.0001$. Chi Square Test with Bonferroni's Correction.
(B) Polarization and asymmetric inheritance of Glut1 *in vivo*. Left: Glut1 localization in interphase and metaphase P14 CD8+ T cells processed as in A. Right: Quantification of Glut1 asymmetry in metaphase cells. **** $p<0.0001$. Fisher's Exact Test.
(C) Concordant polarity of PIP_3 and Glut1 *in vivo*. Left: PIP_3 and Glut1 localization in metaphase P14 CD8+ T cells. Middle: Quantification of PIP_3 and Glut1 asymmetry in metaphase cells. **** $p<0.0001$. Chi Square Test with Bonferroni's Correction. Right: Proportion of PIP_3 asymmetric cells with CD3 asymmetric concordant (same MTOC), CD3 asymmetric discordant (opposite MTOC), or CD3 symmetric localization.

Discussion

While asymmetric division has been implicated in the diversification of lymphocyte cell fate following clonal selection, the mechanism underlying establishment and maintenance of asymmetry has been controversial. Notably, genetic studies assessing the role of the evolutionarily conserved PAR polarity network have yielded incomplete phenotypes (Nish et al., 2017a). This study provides evidence that class I PI3K phospholipid signaling triggered by antigen and costimulatory receptors, and measured by PIP3 production, is asymmetrically localized such that receptors and downstream protein targets, including Glut1, are unequally trafficked by its activity. Thus, class I PI3K signaling may couple glucose uptake, a requirement for terminal differentiation, with silencing of TCF1, the hallmark of effector T cells. Asymmetric localization of receptors that trigger PI3K activity is at least partly dependent on the Class I PI3K isoform δ. The convergence of PI3K-dependent metabolic, transcriptional, and cell polarity functions during cell division could orchestrate the balanced differentiation program necessary to generate effector and memory cells during differentiation of lymphocytes.

Spatially segregated class I PI3K activity and accompanying cytoskeletal rearrangement is an evolutionarily conserved pathway for responding to environmental cues, including direction cell migration, axon outgrowth of neurons, immunological synapsis, apico-basal polarity, and asymmetric epithelial progenitor division (Dainichi et al., 2016; Engelman et al., 2006; Marat and Haucke, 2016). Endocytic trafficking mediated by class II and III PI3K signaling may potentially cooperate with Class I PI3K-initiated polarity to maintain asymmetry through cell division; this model is consistent

with the finding that endocytosed antigen receptors can propagate anabolic activation (Willinger et al., 2014). Further, we found that inhibition of Class I PI3Kδ perturbed receptor polarity more completely in interphase than metaphase. Previous studies have documented that asymmetric division may be mediated by polarized endocytic trafficking independent of the PAR polarity network (Emery et al., 2005). Whether other PI3K isoforms and classes, mTOR activity, or PAR polarity proteins play complementary or downstream roles alongside class I PI3K, particularly in metaphase, will require further investigation. It also remains possible that a non-canonical extrinsic polarity cue, including T-T and B-B cell synapse, or else a cell-intrinsic lipid cue, may direct PI3K asymmetry in the context of late cell divisions following lymphocyte clonal activation. Nevertheless, these results suggest that PI3K may organize a cell-intrinsic polarity pathway governing lymphocyte differentiation

Methods

Mice

All animal work was conducted in accordance with Institutional Animal Care and Use Guidelines of Columbia University. Mice were housed in specific-pathogen-free conditions. Both male and female mice were used, and all mice were between 6-8 weeks of age. Strains used include: C57BL/6 (wild type), P14 TCR transgenic (P14) recognizing LCMV peptide gp33-41/Db, *TCF7*$^{GFP/+}$ reporter P14 TCR transgenic (Zhou and Xue, 2012), and myc-Glut1 mice expressing Glut1 with a myc tag in the extracellular (surface) domain of the Glut1 transporter (Michalek et al., 2011).

In vitro lymphocyte activation

Spleens from mice of the indicated genotypes were isolated and processed using established protocols. Wild type B cells, myc-tagged Glut1 B cells, or myc-tagged Glut1 CD8+ T cells were enriched from splenocytes using magnetic bead negative selection kits (Miltenyi Biotec). B cells were stimulated with 20ug/mL LPS and polyclonal CD8+ T cells were stimulated with plate-bound anti-CD3/CD28 (1ug/mL) supplemented with 100IU/mL IL2. For experiments with P14 CD8+ T cells, bulk splenocytes were activated with gp33 peptide (1ug/mL) as previously described (Lin et al., 2016). For experiments with switched memory B cells, CD23+, IgD-, IgM-, lineage negative (CD4, CD8, Gr1) cells were first sorted from bulk splenocytes and then stimulated with LPS (20ug/mL). In all experiments, lymphocytes were labeled with Cell Trace Violet (CTV) prior to stimulation according to the manufacturer's instructions to monitor cell division number.

Where indicated, cells were treated with the following drugs: Ly294002 (Cell Signaling Technology, used at 2.5-5uM), Blebbistatin (Abcam, used at 20uM).

In vivo infection

For *in vivo* experiments of CD8+ T cell differentiation, 1-3x10^6 TCF7-GFP reporter P14 CD8+ T cells were adoptively transferred intravenously (i.v.) into allotype-disparate C57Bl/6 wild-type mice, which were subsequently infected with 5x10^3 CFUs of *L. monocytogenes* expressing gp33 (LM-gp33) via i.v. injection. Spleens were harvested at day 4-5 of infection, and CD8+ T cells were then MACS enriched for cell sorting of transferred, TCF7-GFP+ P14 cells. For experiments on tissue homing of Th1 CD4+ T cells, 1-3x10^6 OT-II Thy1.1+ CD4 T cells were purified, pulse-labeled with CTV and MitoTracker Green FM, and then adoptively transferred into Thy1.2+ recipients 24 hr before intranasal infection with 250 50%-tissue culture-infective dose PR8-OVA influenza virus.

FACS staining

Single-cell suspensions were prepared and stained as previously described (Lin Cell Reports 2016). For staining of transcription factors, the eBioscience Foxp3 kit was used. Antibodies used in this study include: rabbit anti-myc tag (71D10, Cell Signaling Technology), mouse anti-myc tag (4A6, Millipore), TCF1 (C63D9, Cell Signaling Technology), Pax5 (1H9, eBioscience), IgM (II/41, eBioscience), IgD, (11-26c.2a), CD23 (B3B4, eBioscience), CD4 (RM405, Biolegend), CD8a (53-6.7, eBioscience), Gr1 (RB6-

8C5, BD Pharmingen). BD LSRII and Fortessa flow cytometers were used to analyze cells. Data were analyzed using FlowJo software (Tree Star).

Confocal Microscopy

Immunofluorescence microscopy of mitotic B and T cells was performed as previously described (Lin et al., 2015). Briefly, cells were adhered to poly-l-lysine (Sigma) coated coverslips and fixed with 3.7% paraformaldehyde followed by permeablization with 0.3% Triton X-100. Cells were then blocked in buffer containing 0.01% saponin and 0.25% fish skin gelatin (Sigma) in PBS+ and stained with antibodies to the indicated proteins. Antibodies used include: α-tubulin (YOL1/34, Abcam), β-tubulin (AA2, Sigma), CD19 (1D3, BD Pharmingen), IgM (II/41, eBioscience), PIP3 (RC6F8, Thermo Fischer), Glut1 (EPR3915, Abcam), anti-CD3ε chain (ebio500A2, eBioscience), goat anti-mouse-IgM (Thermo Fischer). All Alexa Fluor dye-conjugated secondary antibodies were obtained from Thermo Fischer. Imaging was performed on Nikon Ti-Eclipse inverted scanning confocal or spinning disk confocal microscopes. Images were processed with ImageJ software. Metaphase cells were identified by the presence of two microtubule organizing centers (MTOC) with opposed spindle poles. Late telophase/cytokinetic cells were identified by the presence of a characteristic tubulin bridge and cytoplasmic cleft. To quantify polarity in interphase cells, a decentralization score was calculated based on the proximity of fluorescent puncta to the microtubule organizing center. Cells were divided into 6 equal quadrants, and each quadrant that contained at least 1 fluorescent puncta was counted toward the decentralization score. The quadrant containing the MTOC was worth 0 points, the two adjacent quadrants 1 point each, the two further

quadrants 2 points each, and the quadrant directly opposite the MTOC 3 points. Cells with fluorescent puncta entirely localized to the MTOC quadrant therefore received a score of 0 (the most polarized score) while cells with dispersed/decentralized puncta had higher scores. For quantification of asymmetry in mitotic cells, fluorescent signal was thresholded to remove background, and the integrated fluorescence density in each nascent daughter cell or half of the metaphase plate was calculated. Asymmetry was calculated as (fluorescence daughter 1 – fluorescence daughter 2) / (fluorescence daughter 1 + fluorescence daughter 2), with values over 0.2 considered asymmetric. Statistical significance was assessed using GraphPad Prism and specific statistical tests are indicated in each figure legend.

Chapter 4: Metabolic Control of Hematopoietic Progenitor Cell Fate Bifurcations

Portions of this chapter have been adapted from the manuscript

Kratchmarov R, Viragova S, Kim MJ, Rothman NJ, Liu K, Reizis B, and Reiner, SL. (2017). Metabolic control of cell fate bifurcations in a hematopoietic progenitor population. *Immunology & Cell Biology. In revision.*

Abstract

Growth signals drive hematopoietic progenitor cells to proliferate and branch into divergent cell fates, but how unequal outcomes arise from a common progenitor is not fully understood. We used steady-state analysis of in vivo hematopoiesis and Flt3L-induced in vitro differentiation of DCs to understand how growth signals regulate lineage bias. We found that cDC1 versus cDC2 development is characterized by tempered versus unrestrained anabolic metabolism, respectively. Perturbation of AMPK signaling, fatty acid oxidation, or mitochondrial clearance each increased development of cDC2 cells at the expense of cDC1 cells. Conversely, scavenging reactive oxygen species skewed differentiation towards cDC1 cells. Sibling cells of dividing DC progenitors were found to express unequal abundance of the transcription factor IRF8. Retention of IRF8 expression in one of two sibling cells correlated with FoxO3a activity. Unequal transmission of growth signals during cell division may explain how metabolism supports fate branches during expansion of blood progenitors.

Introduction

Hematopoietic progenitor cells undergo spatially and temporally regulated differentiation programs to populate the mature blood lineages. Developmental programs are modulated by external stimuli, including infection and cancer, as well as intrinsic, homeostatic patterns of cell turnover. During cellular differentiation, multi-potent progenitor cells undergo progressive specification into divergent lineages (Pei et al., 2017).

Dendritic cells (DCs) are sentinel immune cells that develop from hematopoietic progenitors and are found in functionally distinct subsets, including cDC1, cDC2, and plasmacytoid dendritic cells (pDC) with distinct transcriptional programs. The developmental pathway of DCs has been defined in both mouse and human, but the mechanisms underlying these developmental cell fate bifurcations are unresolved (Murphy et al., 2016).

Signaling through the Flt3 receptor (Flt3R/CD135) initiates DC differentiation and interferon regulatory factor (IRF)-8 expression to extinguish neutrophil lineage potential (Becker et al., 2012; Kurotaki et al., 2014). IRF8 expression is maintained across DC progenitors until terminal differentiation in the peripheral lymphoid tissue (Liu et al., 2009; Naik et al., 2006), though there is evidence for preliminary specification of cDC1 vs. cDC2 fate in the BM (Schlitzer et al., 2015). In mature DCs, IRF8 is differentially required for the maintenance/function of certain subsets, and cDC1/cDC2s employ divergent transcriptional programs (Sichien et al., 2016). IRF8 and Batf3 direct cDC1 DC differentiation (Grajales-Reyes et al., 2015; Hildner et al., 2008), while tissue-specific transcription factors specify cDC2s (Tussiwand et al., 2015; Vander Lugt et al.,

2014). pDC development is dependent on E2-2 and IRF8 (Cisse et al., 2008). Conversely, FOXO3a restrains terminal differentiation of DC progenitors (Dejean et al., 2009).

Flt3L signaling activates the mTORC pathway (Sathaliyawala et al., 2010; Wang et al., 2013), and PI3K/mTOR as well as their associated regulator subunits may have tissue-specific roles in DC development (Nobs et al., 2015; Scheffler et al., 2014; Sinclair et al., 2017). Emerging evidence implicates the metabolic state of hematopoietic cells as a determinant of cell fate (Chandel et al., 2016; Ito and Ito, 2016). Whether stochastic or deterministic changes in transcription factor expression underlie progenitor cell fate decisions remains unresolved (Hoppe et al., 2016). Asymmetric cell division may regulate stem cell differentiation and enables a cell to generate distinct progeny that either remain quiescent or undergo terminal differentiation (Morrison and Kimble, 2006). Here we examined the role of metabolic signaling in DC progenitor cell differentiation. Our findings are consistent with a model wherein activated progenitors undergo an anabolic switch that is coupled to cell division and asymmetric transcription factor expression to effect pattern formation.

Results

Division-linked differentiation and IRF8 heterogeneity of DC progenitors

We assessed the dynamics of IRF8 expression and DC differentiation through a well-characterized *in vitro* system in which BM hematopoietic progenitor cells cultured in Flt3L undergo differentiation into cDC1-like, cDC2-like, and pDC-like subsets (Naik et al., 2005). Flt3L induced proliferation of progenitors, with upregulation of CD11c, a marker of the DC lineage, occurring after multiple divisions (Figure 4.1A). After 7-9 days in culture, three DC subsets defined by MHCII and B220 expression could be differentiated, including cDCs (CD11c+ MHCII+ B220-), pDCs (CD11c+ MHCII-lo/int B220+) and immature pre-DCs (CD11c+ MHCII- B220-) (Figure 4.1A). Within the cDC compartment, two subsets with reciprocal expression of the transcription factors IRF8 and IRF4 were observed (Figure 4.1B). Surface marker expression, including CD24, Sirp1α, and CD11b, confirmed that the IRF8-high and IRF4-high subsets respectively resembled cDC1 and cDC2 cells. We then assessed the expression of IRF8 in relation to cell division at day 3, 6, and 9 of culture (Figure 4.1C). Expression of IRF8 was heterogeneous, with three distinct populations, IRF8-hi, IRF8-int, and IRF8-lo detectable by day 5 in culture. These populations then resolved to an IRF8hi and low state concomitant with DC maturation. Thus, Flt3L signaling induces cell division in DC progenitors, and terminal DC development with IRF8 heterogeneity is coupled to multiple rounds of cell cycling.

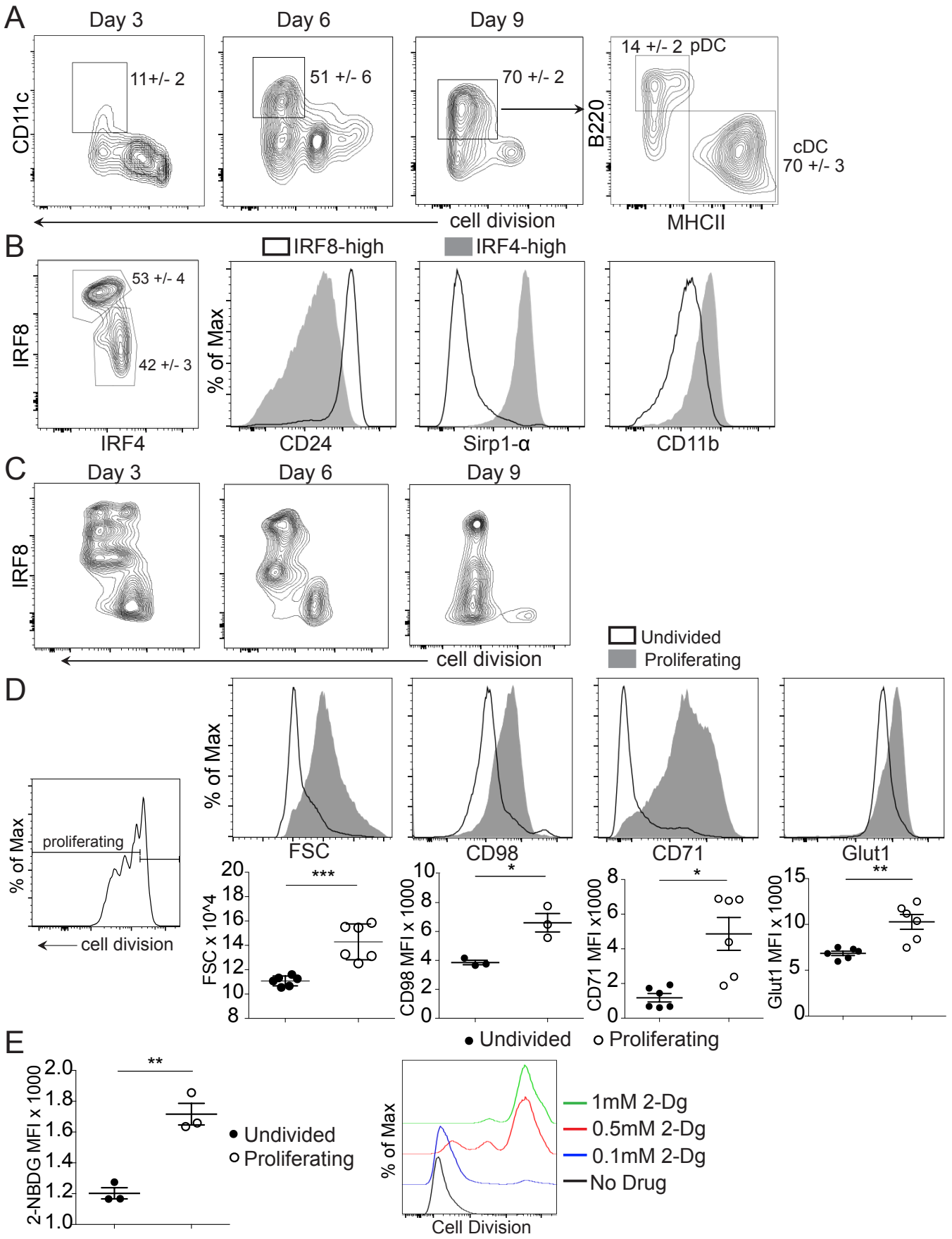

Figure 4.1 Cytokine-induced DC developmental branching accompanying progenitor cell expansion.

Figure 4.1 Cytokine-induced DC developmental branching accompanying progenitor cell expansion. (A) Expression of CD11c versus cell division at day 3, 6, and 9 of culture. Right: cDC (CD11c+ MHCII+) and pDC (CD11c+ B220+ MHCII-) subsets among CD11c+ cells at day 9. Statistic indicates mean +/- standard error the mean (SEM) for gate. (B) Left: Expression of IRF8 and IRF4 marks distinct cDC1 and cDC2 subsets. Statistic indicates mean +/- SEM for gate. Right: Representative histograms of expression of surface markers CD24, Sirp1-α, and CD11b by IRF8-high and IRF4-high cDCs. Histograms are representative of at least 5 independent experiments. (C) Heterogeneity of IRF8 expression by cell division at day 3, 6, and 9 of culture. Representative FACS plots from three independent experiments showing IRF8-low, IRF8-int, and IRF8-high populations at day 3, IRF8-int and IRF8-high at day 6, and IRF8-low and IRF8-high at day 9. (D) Flt3L stimulation increases anabolic signaling in DC progenitors. Left: Representative histogram of CTV dye dilution for gating of undivided and proliferating progenitor cells. Right: Representative histograms and quantification of forward scatter (FSC), an index of cell size, and nutrient transporter expression (CD98, CD71, and Glut1) by proliferating (grey fill) and undivided (black line) progenitors at day 3 of culture. *$p<0.05$. **$p<0.01$. ***$p<0.001$. Student's T test. (E) Glycolysis is required for Flt3L-induced DC progenitor cell proliferation. Left: Increased glucose uptake in proliferating DC progenitors. **$p<0.01$. Student's T test. Right: Cell division with increasing concentrations of glycolysis inhibitor 2-DG. Plots are representative of 3 independent experiments.

Flt3L induces an anabolic switch in DC progenitors

Flt3L signaling activates PI3K/Akt/mTOR (Nobs et al., 2015; Sathaliyawala et al., 2010), and negative regulation of mTOR by Tsc1 is important for regulated DC development (Wang et al., 2013). We asked whether the bifurcating cell fate trajectories of IRF8-hi and IRF4-hi DCs are coupled to a metabolic switch during terminal differentiation. Progenitor cells that had undergone cell division showed a marked increase in size as well as increased expression of CD71, the transferrin receptor, CD98, an amino acid transporter, and Glut1, an Akt-regulated, inducible glucose transporter (Wieman et al., 2007) (Figure 4.1D). These results suggest that terminal differentiation is associated with anabolic activation of progenitor cells.

We then asked whether pharmacologic perturbation of nutritive signaling could alter DC development. Progenitor cells increased glucose uptake following Flt3L stimulation (Figure 4.1E). 2-DG, an irreversible inhibitor of glycolysis, inhibited Flt3L-induced proliferation in a dose-dependent fashion (Figure 4.1E), suggesting that glycolysis is essential for DC progenitor differentiation. We next determined whether fatty acid oxidation, a key regulator of stem cell self-renewal (Ito et al., 2012), was important for progenitor cell fate. Inhibition of fatty acid oxidation with the Cpt1 inhibitor etomoxir did not affect cDC/pDC development but significantly increased the differentiation of IRF4+ cDC2s (Figure 4.2A). These results indicate that the balance of anabolism and catabolism is important for regulated DC progenitor cell differentiation.

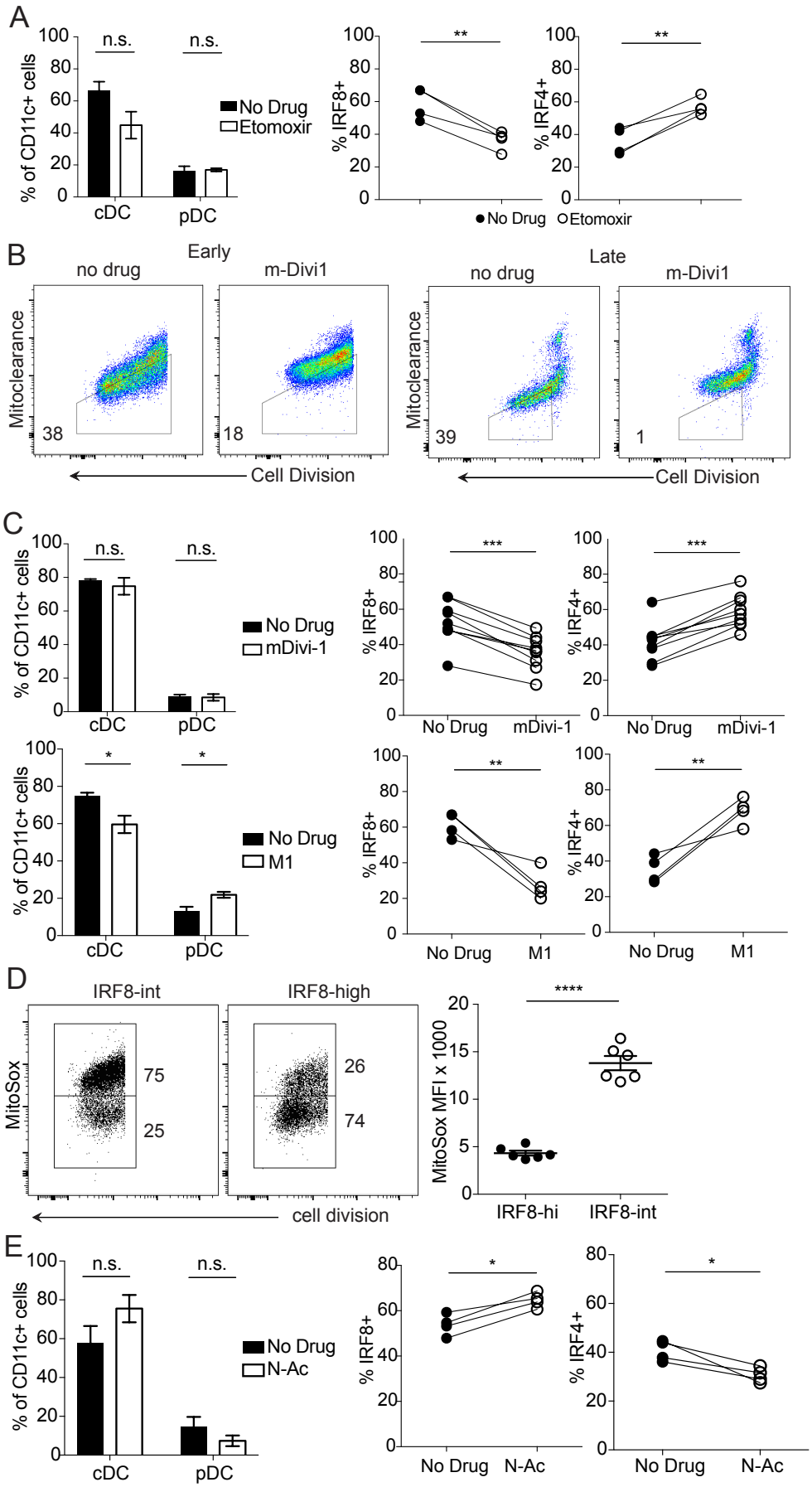

Figure 4.2 Mitochondrial dynamics and metabolism promote selective DC differentiation.

Figure 4.2 Mitochondrial dynamics and metabolism promote selective DC differentiation. (A) Fatty acid oxidation modulates cDC subset development. Left: Frequency of cDC and pDCs amongst CD11c+ DCs following etomoxir treatment. n.s. not significant. Student's T test with Holm-Sidak correction. Right: Development of IRF8+ and IRF4+ DC subsets in cultures treated with etomoxir. **p<0.01. Paired T test. (B) Mitoclearance assay. Progenitors were pulse-labeled with MTGreen at early (day 0) and late (day 4) time points of culture and assessed for decay of fluorescence 3 days later. FACS plots show decaying MTGreen fluorescence per cell division with or without mDivi-1 treatment. Trapezoid gate denotes MTGreen-low population. Plots are representative of 3 independent experiments. (C) Left: Frequency of cDC and pDCs amongst CD11c+ DCs following mDivi-1 or M1 treatment. *p<0.05. n.s. not significant. Student's T test with Holm-Sidak correction. Right: Frequency of IRF8+ and IRF4+ cDC subsets following treatment with mDivi-1 (upper) or M1 (lower). **p<0.01. ***p<0.001. Paired T test. (D) Flt3L induces mROS production in proliferating progenitors. Left: MitoSox levels versus cell division at day 3 of culture in IRF8-int and IRF8-high progenitors. Right: Quantification of MitoSox MFI in IRF8-int and IRF8-high cells. **** p<0.0001. Student's T test. (E) Left: Frequency of cDC and pDCs amongst CD11c+ DCs following treatment with N-Ac. n.s. not significant. Student's T test with Holm-Sidak correction. Right: Frequency of IRF8+ and IRF4+ cDC subsets following treatment with N-Ac. *p<0.05. Paired T test.

Mitochondrial dynamics during DC progenitor differentiation

Changes in mitochondrial function are crucial for supporting the bioenergetic demands of different cell fates, and mitochondria are important for lymphoid/myeloid progenitor cell balance (Luchsinger et al., 2016). Mitophagy is also critical for maintaining self-renewal in hematopoietic stem cells (Ho et al., 2017; Ito et al., 2016). As such, we asked whether mitochondrial function and turnover modulate Flt3L-induced homeostatic DC development. We first assayed mitochondrial clearance at early and late time points following Flt3L stimulation with a fluorescence based pulse-chase assay (Adams et al., 2016). Total mitochondria in progenitors were labeled with Mitotracker dye, and fluorescence was then quantified at day 3 post-activation. Aged mitochondria were passively cleared as well as degraded following Flt3L stimulation (Figure 4.2B). This degradation was dependent on mitochondrial fission, as treatment of cultures with the Drp1 inhibitor mDivi-1 (Cassidy-Stone et al., 2008) resulted in stasis of aged mitochondria across cell divisions (Figure 4.2B). This pattern of mitochondrial clearance was also observed when organelles were pulse labeled at day 4 of culture and then quantified at day 7 (Figure 4.2B). We then assessed whether mitochondrial dynamics and turnover are important for cDC1 vs. cDC2 differentiation. Treatment with m-Divi1, or M1, a mitochondrial fusion promoter (Buck et al., 2016; Wang et al., 2012), did not have significant effects on overall cDC/pDC development but promoted IRF4+ cDC2 differentiation (Figure 4.2C). These results suggest that the clearance of old mitochondria and/or the balance of fission/fusion are important for DC subset specification.

Mitochondria function as signaling organelles during development and homeostasis through the production of mROS (Chandel, 2015). mROS increases PI3K activity and promotes terminal differentiation of hematopoietic progenitor cells and lymphocytes (Chen et al., 2008; Yalcin et al., 2010). We found that Flt3L stimulation of BM progenitors induced mROS production, with cells undergoing division exhibiting elevated, heterogeneous levels with a bimodal distribution (Figure 4.2D). We then determined whether IRF8 expression correlates with mROS production. Progenitor cells from IRF8-eGFP reporter mice were stimulated with Flt3L and labeled with MitoSox. IRF8-int cells exhibited higher levels of mROS (Figure 4.2D). We therefore assessed whether scavenging of mROS could alter the development of DC subsets. When cultures were treated with N-acetyl cysteine (N-Ac), a generalized scavenger of ROS, an increase in IRF8+ cDC1 development was observed (Figure 4.2E). These results suggest that DC progenitor differentiation involves unequal production of mROS and that perturbation of mROS levels can skew subset development.

AMPK-α1 promotes cDC1 differentiation

To determine whether nutritive signaling drives progenitor cell fate bifurcations, we assessed the role of AMPK, an energy sensor that regulates self-renewal in hematopoietic stem cells and lymphocytes (Adams et al., 2016; Blagih et al., 2015; Nakada et al., 2010). We found that Flt3L induces AMPK signaling in BM progenitors (Figure 4.3A). Amongst proliferating cells, a population with phosphorylated, active AMPK was observed as well as phosphorylated acetyl-CoA carboxylase (ACC) and Raptor, key targets of AMPK. To determine whether AMPK is required for differentiation, we assessed the development of cDC1/cDC2 from AMPK-α1 knockout progenitors. AMPK-α1 deficiency resulted in a modest decrease in the total number of CD11c+ cells generated (Figure 4.3B). Within the cDC compartment, we observed a significant increase in IRF4+ cDC2 development from AMPK-α1 deficient progenitors. Loss of AMPK signaling was synergist with inhibition of mitochondrial fission, resulting in a severe loss of IRF8+ cDC1 development (Figure 4.3B). We then determined whether AMPK-α1 was required for regulated cDC1/cDC2 development *in vivo* (Figure 4.3C). While no differences in bone marrow DC progenitor frequencies were observed, we found that AMPK-α1 was required for efficient terminal cDC1 differentiation *in vivo* (Figure 4.3C). In skin-draining lymph nodes, proportions of cDC/pDC were unaffected by loss of AMPK-α1. Resident CD8α+ cDC1s were, however, significantly reduced in AMPK-α1 deficient animals, alongside a lesser reduction in migratory CD8α- CD11b- DCs. Conversely, we observed an increase in CD11b+ cDC2 cells. Thus, catabolic signaling mediated by AMPK-α1 may be involved in DC progenitor cell fate bifurcations and balanced cDC1/cDC2 differentiation *in vitro* and *in vivo.*

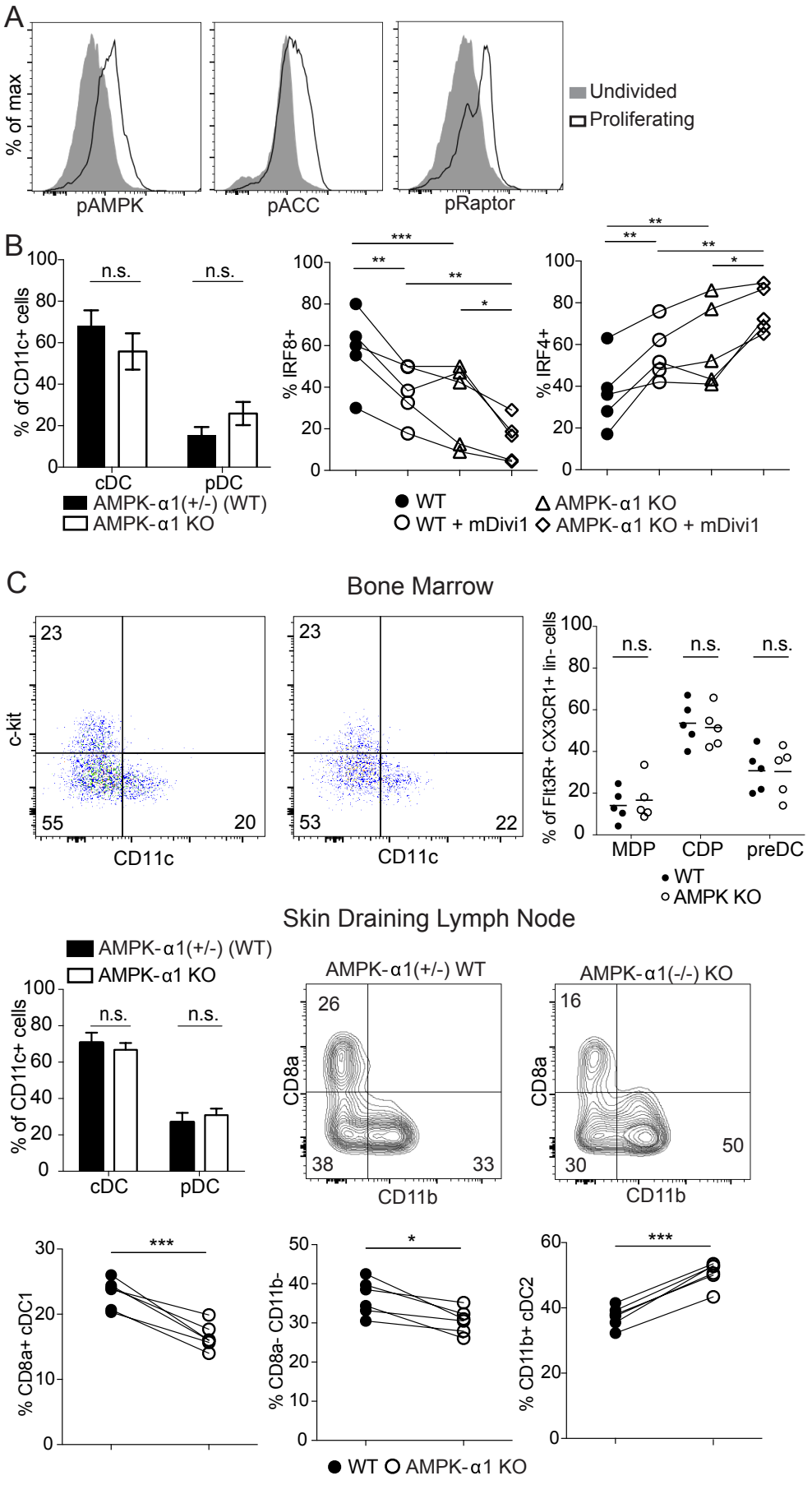

Figure 4.3 Nutrient sensor AMPK promotes selective DC differentiation.

Figure 4.3 Nutrient sensor AMPK promotes selective DC differentiation. (A) Flt3L induces AMPK signaling. Representative histograms of pAMPK, pACC, and pRaptor in proliferating (black line) and undivided (grey fill) progenitor cells stimulated with Flt3L for 3 days. Plots are representative of 2-3 independent experiments. (B) AMPK-α1 deficiency alters DC development *in vitro*. Left: Development of total CD11c+ cells, and cDC/pDCs from AMPK-α1 deficient cells and heterozygote littermate ("WT") controls. n.s. not significant. Student's T test with Holm-Sidak correction. Right: differentiation of IRF8+ and IRF4+ cDC subsets from AMPK-α1 deficient progenitors with or without mDivi-1 treatment. *p<0.05 **p<0.01 ***p<0.001. Repeated measures one way ANOVA with Tukey's correction for multiple comparisons. (C) Steady state *in vivo* bone marrow DC progenitor (upper row), as well as skin draining lymph node cDC/pDC and cDC subset (lower row) frequencies of AMPK-α1 knockout mice and heterozygote littermate (WT) controls. In bone marrow, DC progenitors were gated as lineage (CD3, CD19, B220, NK1.1, Ter119, GR1, CD11b) negative, Flt3R (CD135)+, CX3CR1+ cells. Macrophage dendritic cell progenitors (MDP) were c-kit+ CD11c-. Common dendritic progenitors (CDP) were c-kit- CD11c-. Pre-DCs were c-kit- CD11c+. In lymph nodes, pDCs were lineage- CD11c+ MHCII-int B220+, and amongst lineage- CD11c+ MHCII+ B220- mature cDCs, cDC1 were gated as CD8α+ CD11b-, migratory DCs were CD8α- CD11b-, and cDC2 were CD8α- CD11b+. *p<0.05. ***p<0.001. n.s. not significant. Paired T test.

Asymmetric division of IRF8 in DC progenitors

Hematopoietic progenitor cells can undergo both asymmetric and symmetric divisions (Wu et al., 2007). The pattern of IRF8 transcriptional heterogeneity during DC development suggested that these cell fate bifurcations could be linked to cell division. We therefore assessed the localization of IRF8 in interphase and mitotic cells by immunofluorescence microscopy (Figure 4.4A). In interphase, we observed varying levels of IRF8 expression with a predominantly nuclear localization pattern. During the early stages of mitosis, i.e. prophase/metaphase/anaphase, IRF8 was excluded from condensed chromatin and exhibited a diffuse and symmetric localization (Figure 4.4A). However, robust asymmetry of IRF8 was observed in conjoined daughter cells undergoing cytokinesis. Asymmetry of transcription factors during late cytokinesis suggests that asymmetric signaling may occur during mitosis, as in lymphocytes (Adams et al., 2016; Lin et al., 2015; Pollizzi et al., 2016; Verbist et al., 2016).

The observed effects of metabolic perturbations on DC progenitor differentiation are consistent with a model in which opposing PI3K/AMPK signals modulate cell fate bifurcation. Crosstalk with AMPK regulates FOXO3a transcriptional activity, and FOXO3a conditional knockout mice have increased DC development, with the largest effect on cDC2s (Dejean et al., 2009). FOXO3a has also been implicated in the regulation of mitochondrial function in HSCs (Rimmelé et al., 2015). We found that Flt3L signaling induces phosphorylation of FOXO3a (Figure 4.4B). We then tested whether FOXO3a activity was important for regulating DC subset development. Pharmacologic inhibition of FOXO1/3a resulted in a substantial increase in pDC development with a concomitant decrease in the numbers of cDCs (Figure 4.4B). We examined the

localization and inheritance of FOXO3a in mitotic DC progenitors where both nuclear and cytoplasmic localizations patterns were observed. FOXO3a protein levels were also frequently asymmetric though the magnitude of asymmetry was markedly lower than for IRF8 (Figure 4.4C). Amongst IRF8 asymmetric sibling cell pairs, FOXO3a activity was asymmetric, with nuclear FOXO3a protein predominantly inherited by the IRF8-high daughter. Thus, FOXO3a regulates DC progenitor cell differentiation and exhibits asymmetric activity in cytokinetic sibling cells, coupled to asymmetric IRF8 inheritance.

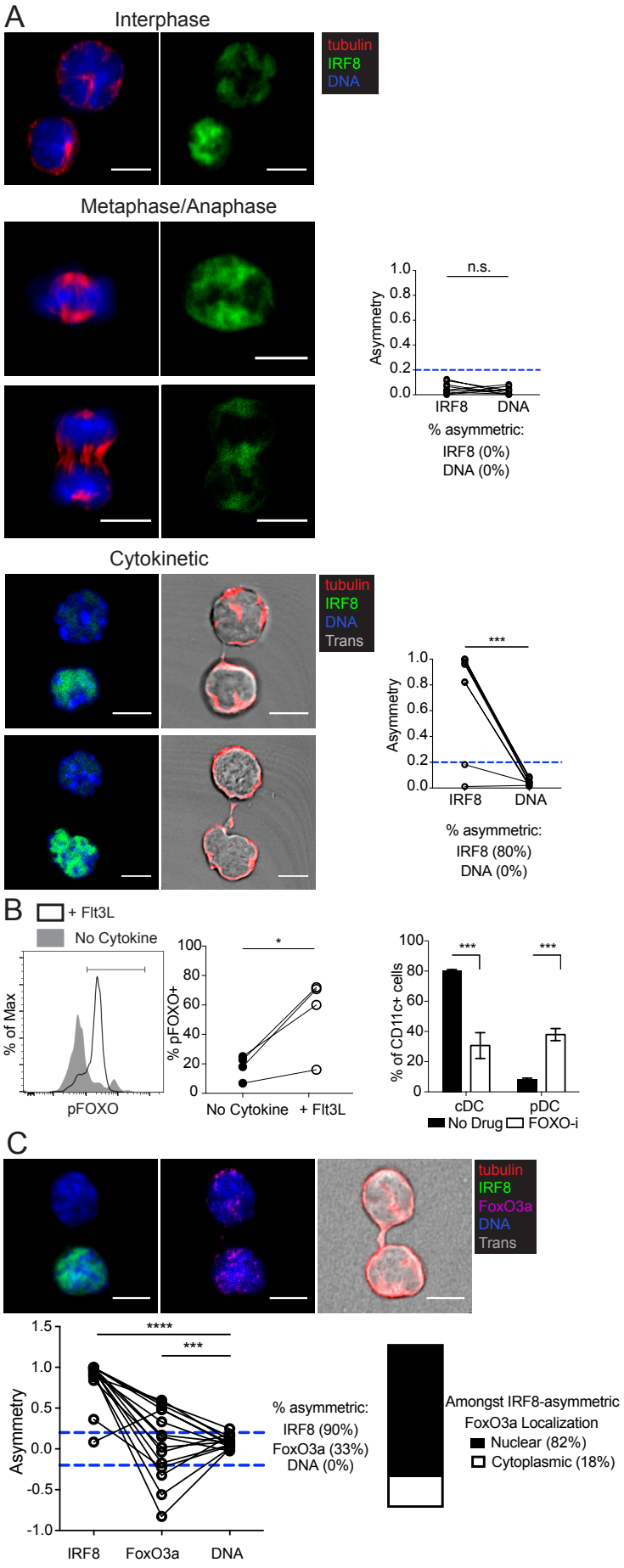

Figure 4.4 Asymmetric division of DC progenitors supporting developmental branching.

Figure 4.4 Asymmetric division of DC progenitors supporting developmental branching. (a) Localization and inheritance of IRF8 in progenitors at day 4-5 of culture with Flt3L. IRF8+ CD11c+ cells were FACS sorted for immunofluorescence (IF) microscopy analysis. Upper: Localization of IRF8 in interphase cells. Middle and lower: Localization of IRF8 in early (metaphase/anaphase) and late (cytokinesis) mitotic cells Left: Representative IF images of IRF8, tubulin, and DNA. Right: Quantification of IRF8 asymmetry ratio as well as % asymmetric cells, as described in methods. *** $p<0.001$. n.s. not significant. Fisher's Exact Test. Scale bar 5uM. (b) Left: Flt3L induces phosphorylation of FoxO1/3a. Representative histograms and quantification of p-FoxO1/3a in IRF8-high progenitors stimulated with Flt3L overnight or rested without cytokine. *$p<0.05$. Paired T test. Right: FOXO inhibitor AS1842856 increases pDC development. Bar graphs indicate frequency of each subset +/- SEM. ***$p<0.001$ Student's T test with Holm-Sidak correction. (c) Nuclear FoxO3a localization in IRF8hi daughter cells. Upper: Representative IF images of IRF8, tubulin, DNA, and transmitted light in conjoined sibling cells. Lower Left: Quantification of IRF8, FoxO3a, and DNA asymmetry and % asymmetric cells amongst cytokinetic cells. ***$p<0.001$ ****$p<0.0001$. Fisher's Exact Test. Lower Right: Amongst IRF8-asymmetric cytokinetic cells, proportion of IRF8-high daughters with nuclear (black fill) or cytoplasmic (white fill) FoxO3a.

Discussion

Emerging evidence indicates that metabolic signaling is coupled to cell fate bifurcations via the action of key transcription factors. These metabolic signals are organized into constellations that exhibit feed-back and feed-forward characteristics to ensure fidelity in cell fate decisions. Perturbation of one element of the constellation, e.g. mitochondrial quality control or ROS production, can induce downstream and upstream effects on the system due to synergy of the individual elements. Here, we should that metabolic signals from anabolic and catabolic pathways can direct specific DC development. Progenitor cells undergoing terminal differentiation following Flt3L signaling diverge in fate due to the effects of growth factor signaling on metabolic pathways and transcription factor expression. Reciprocal expression of IRF8 has been linked to bifurcating cell fates in activated lymphocytes (Xu et al., 2015a), and our work suggests that progenitor cell fate bifurcations across different modes of pattern formation may involve a generalizable mechanism of asymmetric division coupled to unequal nutritive signaling. Asymmetry of IRF8 could promote terminal bifurcations as well as earlier lineage biasing of more primitive progenitor cells (Lee et al., 2017). These results have implications for understanding the detrimental changes in hematopoiesis that accompany aging, malignancy, and infection, and suggest avenues for therapeutic intervention.

Methods

Mice

All animal work was conducted in accordance with the Institutional Animal Care and Use Guidelines of Columbia University. Mice were housed in specific-pathogen-free conditions. Both male and female mice were used, and mice were between 6-8 weeks of age. C57BL/6 wild type, IRF8-eGFP reporter (Wang et al., 2014), and AMPK-α1 knockout mice (Jørgensen et al., 2004) were used. Spleens, skin-draining lymph nodes, and long bones were harvested based on experimental needs.

DC Differentiation Assay and Drug Treatments

BM progenitors were cultured in RPMI 1640 supplemented with 10% FBS, 1% penicillin/streptomycin, and human recombinant Flt3L (Celldex or Peprotech) at 100ng/mL to induce DC development. Drugs used for pharmacologic perturbation of DC development were all added at the beginning of culture and included: mDivi-1 (Cayman, used at 10uM), M1 (Sigma, used at 5uM), FoxO1/3a inhibitor (AS1842856; Calbiochem, used at 1uM), N-Acetyl cysteine (N-Ac, Sigma, used at 5mM), 2-deoxyglucose (2-DG, Sigma, used at 100uM-1mM), and etomoxir (Cayman, used at 100uM).

Flow Cytometry

Staining for flow cytometry analysis was performed as described (3, 4). Antibodies used in this study include: B220 (RA3-6B2, eBioscience), MHCII (M5/114.15.2, Biolegend and Tonbo Biosciences), CD3 (2C11, BD Pharmingen), CD8a (53-6.7, Biolegend), CD11b (M1/70, Biolegend), CD11c (N418, Biolegend), CD19 (1D3, BD Pharmingen),

CD24 (M1/69, Biolegend), CD71 (RI7217, Biolegend), CD98 (RI388; Biolegend), CD117 (c-Kit, 2B8, eBioscience), CD135 (Flt3R, A2F10, eBioscience), Glut1 (EPR3915; Abcam), phospho-S6 (S235/236; Cell Signaling Technology), p-AMPK (40H9, Cell Signaling Technology), p-ACC (D7D11, Cell Signaling Technology), phospho-FOXO1/3a (9464; Cell Signaling Technology), p-Raptor (24C12, Cell Signaling Technology), IRF8 (V3GYWCH, eBioscience), IRF4 (3E4, eBioscience), Gr1 (RB6-8C5, BD Pharmingen), Nk1.1 (PK136, Biolegend), Ter119 (TER-119, BD Pharmingen), and goat anti-rabbit Alexa Fluor 647 secondary (Thermo Fischer). Samples were acquired on a BD LSRII or BD Fortessa, and analysis was performed with FlowJo software (Treestar, San Carlos, CA). Glucose uptake was measured by incubating cells in 2-NBDG (Cayman; 100 μM) for 45 minutes at 37 °C in glucose free RPMI supplemented with 10% dialyzed FBS. Mitoclearance was assessed by labeling progenitor cells with Mitotracker Green (Thermo Fisher; 200nM per 1x10^^{6} cells) followed by two washes with complete media. Cells were then labeled with Cell Trace Violet according to the manufacturer's instructions (CTV, Thermo Fischer). Mitochondrial ROS was detected by labeling cells with MitoSox (Thermo Fischer) according to the manufacturer's instructions.

Immunofluorescence Microscopy

Immunofluorescence microscopy was performed as previously described (Lin et al., 2015). Antibodies used include: α-tubulin (YOL1/34, Abcam), β-tubulin (AA2, Sigma), IRF8 (V3GYWCH, eBioscience), and FOXO3a (75D8, Cell Signaling Technology). Alexa Fluor dye-conjugated secondary antibodies (Thermo Fischer) were used at

1:1000. All imaging was performed on Nikon Ti-Eclipse inverted scanning or spinning disk confocal microscopes. Images were processed with ImageJ software. Metaphase cells were identified by the presence of two microtubule organizing centers (MTOC) with opposed spindle poles. Nascent cytokinetic daughter cell pairs were identified by their residual connection, i.e. the tubulin bridge and cytoplasmic cleft. For quantification of asymmetry in mitotic cells, fluorescent signal was thresholded to remove background, and the integrated fluorescence density in each nascent daughter cell or half of the metaphase plate was calculated. Asymmetry was calculated as (fluorescence daughter 1 – fluorescence daughter 2) / (fluorescence daughter 1 + fluorescence daughter 2), with values over 0.2 considered asymmetric.

Statistical analyses

Statistical analyses were performed using GraphPad Prism (version 6). P-values and significance cut-offs are specified in each figure legend.

Conclusions and Future Directions

While it has been previously established that distinct types of metabolism are required for the function of mature cells (Buck et al., 2017), our results establish metabolic signals as a critical node for regulating the differentiation and cell fate of progenitors in the immune and hematopoietic systems. Preserving the fidelity of lineage trees in the hematopoietic system as well as effector versus memory cell fate decisions in lymphocytes is critical for maintain homeostasis in the context of cellular turnover. By connecting metabolism with cell fate through the action of key transcription factors, self-renewal is ensured through a feed-forward feed-back mechanism that dampens activation/differentiation in certain progeny. Our results may explain the observed deficiencies in self-renewal observed during chronic infections and cancer, wherein excessive terminal effector cell differentiation precipitates the collapse of protective immunity.

Further work will be necessary to characterize the intracellular pathway that facilitates asymmetric metabolic signaling. Our results suggest that polarized traffic of endocytosed membranes as well as intracellular organelles can direct the asymmetric division of cells, with important functional consequences including the asymmetric expression of fate determining transcription factors occurring downstream. The trafficking of these subcellular compartments may be independent of the PAR polarity network (Emery et al., 2005), potentially explaining the modest phenotypes observed in both lymphocytes and hematopoietic cells for PAR knockout mice (Nish et al., 2017a). The asymmetry of Rab11 recycling endosomes has been described previously (Emery et al., 2005), and it will be important to establish whether the asymmetry pathway

described here involves Rab11+ structures. Of note, Class II PI3K activity has been implicated in endosomal trafficking and recycling (Marat and Haucke, 2016) and may explain why inhibition of Class I PI3K does not fully abolish mitotic asymmetry. Perturbation of the recycling endosome pathway with dominant negative Rab11 constructs will clarify the contribution of these vesicles to the asymmetric division of lymphocytes.

The observation that this asymmetry pathway is functional in cells activated by soluble stimuli, i.e. LPS, as well as cells no longer receiving antigen receptor stimulation, i.e. sorted T cells, raises a critical question regarding the initiating receptor or protein that organizes the subsequent cascade of polarized signals. It is possible that PI3K activity may self-aggregate, particularly in the context of lipid raft microdomains which have been implicated in the clustering of antigen receptor signaling scaffolds (Sezgin et al., 2017). Alternatively, the existence of homotypic T-T cell and B-B cell synapses has been described, and it is possible that direct contact between lymphocytes subsequent to initial activation by an APC may be sufficient to drive polarity of the observed factors (Gérard et al., 2013; Severinson and Westerberg, 2003).

The ability to modulate cell fate bifurcations via metabolic perturbations presents an attractive avenue for therapeutic intervention during infection, cancer, and aging. Key pharmacologic agents that alter cellular metabolic pathways, including the mTOR inhibitor rapamycin, AMPK agonist metformin, and PI3K inhibitor idelalisib, are all FDA approved for the treatment of other conditions and have manageable side-effect profiles. Metformin, in particular, is taken regularly by large portions of the general population and has minimal side-effects; it will be critical to determine its effects on

immune function. Several studies have already demonstrated the feasibility of combining checkpoint blockade with drugs targeting metabolic pathways in mouse models of cancer (Bowers et al., 2017; Pedicord et al., 2015). This body of work supports the idea that maintaining progenitor cell function could improve outcomes for the treatment of conditions that strain the regenerative capacity of the immune system. Similarly, it is well-known that the aging hematopoietic system becomes myeloid-biased, with alterations in the lymphoid-biased progenitor compartment (Dykstra et al., 2011; Pang et al., 2011; Snoeck, 2013). It is possible that altering the metabolic signaling environment within certain bone marrow niches may be sufficient to redirect key progenitor populations and restore the balance of differentiation programs. Scavenging of ROS, which are known to modulate PI3K activity in progenitors, presents a candidate pharmacological intervention.

The successful metabolic intervention on immune and hematopoietic cells is partially predicated on the assumption that deterministic differentiation programs govern the dynamics of these cells. If key inflection points govern the bifurcation of effector/memory cells, then it is formally possible to alter the balance of these decisions via extrinsic modulation of the signaling pathways that underlie each branch point. However, if stochastic differentiation and competition underlie the acquisition of distinct cell fates, it is more difficult to predict the effect of extrinsic perturbations on the outcome of the system. Unambiguous resolution of the question of deterministic versus stochastic differentiation will therefore be critical for informing the design of next generation therapies. Advances in cellular barcoding techniques that render such assays more tractable and reproducible may facilitate such advances (Pei et al., 2017),

as current technologies present major barriers to entry. Improvements in live cell imaging systems as well as *in situ* imaging techniques via two-photon microscopy will also be critical for studying the immune response *in vivo*. The application of such techniques to mouse models of lymphocyte differentiation can clarify the contribution of asymmetric division to cell fate bifurcations. Nevertheless, it is possible that a combination of noise/stochastic differentiation and deterministic lineage trees more fully describe the behavior of such cells than more constrained individual models. A combination of improved mouse experimentation as well as proof-of-concept studies in humans will ultimately drive the improvement of immunotherapies for currently intractable conditions.

References

Adams, W.C., Chen, Y.-H., Kratchmarov, R., Bonnie, Y., Nish, S.A., Lin, W.-H.W., Rothman, N.J., Luchsinger, L.L., Klein, U., Busslinger, M., et al. (2016). Anabolism-Associated Mitochondrial Stasis Driving Lymphocyte Differentiation over Self-Renewal. Cell Reports *17*, 3142–3152.

Arsenio, J., Kakaradov, B., Metz, P.J., Kim, S.H., Yeo, G.W., and Chang, J.T. (2014). Early specification of CD8+ T lymphocyte fates during adaptive immunity revealed by single-cell gene-expression analyses. Nat Immunol *15*, 365–372.

Becattini, S., Latorre, D., Mele, F., Foglierini, M., De Gregorio, C., Cassotta, A., Fernandez, B., Kelderman, S., Schumacher, T.N., Corti, D., et al. (2015). Functional heterogeneity of human memory CD4⁺ T cell clones primed by pathogens or vaccines. Science *347*, 400–406.

Becker, A.M., Michael, D.G., Satpathy, A.T., Sciammas, R., Singh, H., and Bhattacharya, D. (2012). IRF-8 extinguishes neutrophil production and promotes dendritic cell lineage commitment in both myeloid and lymphoid mouse progenitors. Blood *119*, 2003–2012.

Blagih, J., Coulombe, F., Vincent, E.E., Dupuy, F., Galicia-Vázquez, G., Yurchenko, E., Raissi, T.C., van der Windt, G.J.W., Viollet, B., Pearce, E.L., et al. (2015). The energy sensor AMPK regulates T cell metabolic adaptation and effector responses in vivo. Immunity *42*, 41–54.

Bollig, N., Brüstle, A., Kellner, K., Ackermann, W., Abass, E., Raifer, H., Camara, B., Brendel, C., Giel, G., Bothur, E., et al. (2012). Transcription factor IRF4 determines germinal center formation through follicular T-helper cell differentiation. Proc. Natl. Acad. Sci. U.S.a. *109*, 8664–8669.

Bowers, J.S., Majchrzak, K., Nelson, M.H., Aksoy, B.A., Wyatt, M.M., Smith, A.S., Bailey, S.R., Neal, L.R., Hammerbacher, J.E., and Paulos, C.M. (2017). PI3Kδ Inhibition Enhances the Antitumor Fitness of Adoptively Transferred CD8(+) T Cells. Front Immunol *8*, 1221.

Brüstle, A., Heink, S., Huber, M., Rosenplänter, C., Stadelmann, C., Yu, P., Arpaia, E., Mak, T.W., Kamradt, T., and Lohoff, M. (2007). The development of inflammatory T(H)-17 cells requires interferon-regulatory factor 4. Nat Immunol *8*, 958–966.

Buchholz, V.R., Flossdorf, M., Hensel, I., Kretschmer, L., Weissbrich, B., Gräf, P., Verschoor, A., Schiemann, M., Höfer, T., and Busch, D.H. (2013). Disparate individual fates compose robust CD8+ T cell immunity. Science *340*, 630–635.

Buck, M.D., O'Sullivan, D., Klein Geltink, R.I., Curtis, J.D., Chang, C.-H., Sanin, D.E., Qiu, J., Kretz, O., Braas, D., van der Windt, G.J.W., et al. (2016). Mitochondrial Dynamics Controls T Cell Fate through Metabolic Programming. Cell *166*, 63–76.

Buck, M.D., Sowell, R.T., Kaech, S.M., and Pearce, E.L. (2017). Metabolic Instruction of Immunity. Cell *169*, 570–586.

Caro-Maldonado, A., Wang, R., Nichols, A.G., Kuraoka, M., Milasta, S., Sun, L.D., Gavin, A.L., Abel, E.D., Kelsoe, G., Green, D.R., et al. (2014). Metabolic reprogramming is required for antibody production that is suppressed in anergic but exaggerated in chronically BAFF-exposed B cells. J. Immunol. *192*, 3626–3636.

Cassidy-Stone, A., Chipuk, J.E., Ingerman, E., Song, C., Yoo, C., Kuwana, T., Kurth, M.J., Shaw, J.T., Hinshaw, J.E., Green, D.R., et al. (2008). Chemical inhibition of the mitochondrial division dynamin reveals its role in Bax/Bak-dependent mitochondrial outer membrane permeabilization. Dev. Cell *14*, 193–204.

Chan, L.L.-Y., Shen, D., Wilkinson, A.R., Patton, W., Lai, N., Chan, E., Kuksin, D., Lin, B., and Qiu, J. (2012). A novel image-based cytometry method for autophagy detection in living cells. Autophagy *8*, 1371–1382.

Chandel, N.S. (2015). Evolution of Mitochondria as Signaling Organelles. Cell Metab. *22*, 204–206.

Chandel, N.S., Jasper, H., Ho, T.T., and Passegué, E. (2016). Metabolic regulation of stem cell function in tissue homeostasis and organismal ageing. Nat. Cell Biol. *18*, 823–832.

Chang, J.T., Ciocca, M.L., Kinjyo, I., Palanivel, V.R., McClurkin, C.E., Dejong, C.S., Mooney, E.C., Kim, J.S., Steinel, N.C., Oliaro, J., et al. (2011). Asymmetric proteasome segregation as a mechanism for unequal partitioning of the transcription factor T-bet during T lymphocyte division. Immunity *34*, 492–504.

Chang, J.T., Palanivel, V.R., Kinjyo, I., Schambach, F., Intlekofer, A.M., Banerjee, A., Longworth, S.A., Vinup, K.E., Mrass, P., Oliaro, J., et al. (2007). Asymmetric T lymphocyte division in the initiation of adaptive immune responses. Science *315*, 1687–1691.

Chaturvedi, A., Martz, R., Dorward, D., Waisberg, M., and Pierce, S.K. (2011). Endocytosed BCRs sequentially regulate MAPK and Akt signaling pathways from intracellular compartments. Nat Immunol *12*, 1119–1126.

Chen, C., Liu, Y., Liu, R., Ikenoue, T., Guan, K.-L., Liu, Y., and Zheng, P. (2008). TSC-mTOR maintains quiescence and function of hematopoietic stem cells by repressing mitochondrial biogenesis and reactive oxygen species. Journal of Experimental Medicine *205*, 2397–2408.

Chen, M., Hong, M.J., Sun, H., Wang, L., Shi, X., Gilbert, B.E., Corry, D.B., Kheradmand, F., and Wang, J. (2014). Essential role for autophagy in the maintenance of immunological memory against influenza infection. Nat. Med. *20*, 503–510.

Choi, Y.S., Gullicksrud, J.A., Xing, S., Zeng, Z., Shan, Q., Li, F., Love, P.E., Peng, W.,

Xue, H.-H., and Crotty, S. (2015). LEF-1 and TCF-1 orchestrate T(FH) differentiation by regulating differentiation circuits upstream of the transcriptional repressor Bcl6. Nat Immunol *16*, 980–990.

Cisse, B., Caton, M.L., Lehner, M., Maeda, T., Scheu, S., Locksley, R., Holmberg, D., Zweier, C., Hollander, den, N.S., Kant, S.G., et al. (2008). Transcription factor E2-2 is an essential and specific regulator of plasmacytoid dendritic cell development. Cell *135*, 37–48.

Crotty, S., Johnston, R.J., and Schoenberger, S.P. (2010). Effectors and memories: Bcl-6 and Blimp-1 in T and B lymphocyte differentiation. Nat Immunol *11*, 114–120.

Dainichi, T., Hayden, M.S., Park, S.-G., Oh, H., Seeley, J.J., Grinberg-Bleyer, Y., Beck, K.M., Miyachi, Y., Kabashima, K., Hashimoto, T., et al. (2016). PDK1 Is a Regulator of Epidermal Differentiation that Activates and Organizes Asymmetric Cell Division. Cell Reports *15*, 1615–1623.

Dejean, A.S., Beisner, D.R., Ch'en, I.L., Kerdiles, Y.M., Babour, A., Arden, K.C., Castrillon, D.H., DePinho, R.A., and Hedrick, S.M. (2009). Transcription factor Foxo3 controls the magnitude of T cell immune responses by modulating the function of dendritic cells. Nat Immunol *10*, 504–513.

Dey-Guha, I., Wolfer, A., Yeh, A.C., G Albeck, J., Darp, R., Leon, E., Wulfkuhle, J., Petricoin, E.F., Wittner, B.S., and Ramaswamy, S. (2011). Asymmetric cancer cell division regulated by AKT. Proc. Natl. Acad. Sci. U.S.a. *108*, 12845–12850.

Doughty, C.A., Bleiman, B.F., Wagner, D.J., Dufort, F.J., Mataraza, J.M., Roberts, M.F., and Chiles, T.C. (2006). Antigen receptor-mediated changes in glucose metabolism in B lymphocytes: role of phosphatidylinositol 3-kinase signaling in the glycolytic control of growth. Blood *107*, 4458–4465.

Duffy, K.R., Wellard, C.J., Markham, J.F., Zhou, J.H.S., Holmberg, R., Hawkins, E.D., Hasbold, J., Dowling, M.R., and Hodgkin, P.D. (2012). Activation-induced B cell fates are selected by intracellular stochastic competition. Science *335*, 338–341.

Dykstra, B., Olthof, S., Schreuder, J., Ritsema, M., and de Haan, G. (2011). Clonal analysis reveals multiple functional defects of aged murine hematopoietic stem cells. Journal of Experimental Medicine *208*, 2691–2703.

Eiyama, A., and Okamoto, K. (2015). PINK1/Parkin-mediated mitophagy in mammalian cells. Curr. Opin. Cell Biol. *33*, 95–101.

Emery, G., Hutterer, A., Berdnik, D., Mayer, B., Wirtz-Peitz, F., Gaitan, M.G., and Knoblich, J.A. (2005). Asymmetric Rab 11 endosomes regulate delta recycling and specify cell fate in the Drosophila nervous system. Cell *122*, 763–773.

Engelman, J.A., Luo, J., and Cantley, L.C. (2006). The evolution of phosphatidylinositol 3-kinases as regulators of growth and metabolism. Nat. Rev. Genet. *7*, 606–619.

Fruman, D.A., Chiu, H., Hopkins, B.D., Bagrodia, S., Cantley, L.C., and Abraham, R.T. (2017). The PI3K Pathway in Human Disease. Cell *170*, 605–635.

Fuxa, M., and Busslinger, M. (2007). Reporter gene insertions reveal a strictly B lymphoid-specific expression pattern of Pax5 in support of its B cell identity function. J. Immunol. *178*, 3031–3037.

García-Prat, L., Martinez-Vicente, M., Perdiguero, E., Ortet, L., Rodríguez-Ubreva, J., Rebollo, E., Ruiz-Bonilla, V., Gutarra, S., Ballestar, E., Serrano, A.L., et al. (2016). Autophagy maintains stemness by preventing senescence. Nature *529*, 37–42.

Gerlach, C., Rohr, J.C., Perié, L., van Rooij, N., van Heijst, J.W.J., Velds, A., Urbanus, J., Naik, S.H., Jacobs, H., Beltman, J.B., et al. (2013). Heterogeneous differentiation patterns of individual CD8+ T cells. Science *340*, 635–639.

Gerriets, V.A., Kishton, R.J., Nichols, A.G., Macintyre, A.N., Inoue, M., Ilkayeva, O., Winter, P.S., Liu, X., Priyadharshini, B., Slawinska, M.E., et al. (2015). Metabolic programming and PDHK1 control CD4+ T cell subsets and inflammation. J. Clin. Invest. *125*, 194–207.

Gérard, A., Khan, O., Beemiller, P., Oswald, E., Hu, J., Matloubian, M., and Krummel, M.F. (2013). Secondary T cell-T cell synaptic interactions drive the differentiation of protective CD8+ T cells. Nat Immunol *14*, 356–363.

Goldstein, B., and Macara, I.G. (2007). The PAR proteins: fundamental players in animal cell polarization. Dev. Cell *13*, 609–622.

Grajales-Reyes, G.E., Iwata, A., Albring, J., Wu, X., Tussiwand, R., Kc, W., Kretzer, N.M., Briseño, C.G., Durai, V., Bagadia, P., et al. (2015). Batf3 maintains autoactivation of Irf8 for commitment of a CD8α(+) conventional DC clonogenic progenitor. Nat Immunol *16*, 708–717.

Green, D.R., Galluzzi, L., and Kroemer, G. (2011). Mitochondria and the autophagy-inflammation-cell death axis in organismal aging. Science *333*, 1109–1112.

Guo, S., Liang, Y., Murphy, S.F., Huang, A., Shen, H., Kelly, D.F., Sobrado, P., and Sheng, Z. (2015). A rapid and high content assay that measures cyto-ID-stained autophagic compartments and estimates autophagy flux with potential clinical applications. Autophagy *11*, 560–572.

Gwinn, D.M., Shackelford, D.B., Egan, D.F., Mihaylova, M.M., Mery, A., Vasquez, D.S., Turk, B.E., and Shaw, R.J. (2008). AMPK phosphorylation of raptor mediates a metabolic checkpoint. Mol. Cell *30*, 214–226.

Habib, S.J., Chen, B.-C., Tsai, F.-C., Anastassiadis, K., Meyer, T., Betzig, E., and Nusse, R. (2013). A localized Wnt signal orients asymmetric stem cell division in vitro. Science *339*, 1445–1448.

Hawkins, E.D., Oliaro, J., Kallies, A., Belz, G.T., Filby, A., Hogan, T., Haynes, N., Ramsbottom, K.M., Van Ham, V., Kinwell, T., et al. (2013). Regulation of asymmetric cell division and polarity by Scribble is not required for humoral immunity. Nat Commun *4*, 1801.

Hildner, K., Edelson, B.T., Purtha, W.E., Diamond, M., Matsushita, H., Kohyama, M., Calderon, B., Schraml, B.U., Unanue, E.R., Diamond, M.S., et al. (2008). Batf3 deficiency reveals a critical role for CD8alpha+ dendritic cells in cytotoxic T cell immunity. Science *322*, 1097–1100.

Ho, T.T., Warr, M.R., Adelman, E.R., Lansinger, O.M., Flach, J., Verovskaya, E.V., Figueroa, M.E., and Passegué, E. (2017). Autophagy maintains the metabolism and function of young and old stem cells. Nature *543*, 205–210.

Hoppe, P.S., Schwarzfischer, M., Loeffler, D., Kokkaliaris, K.D., Hilsenbeck, O., Moritz, N., Endele, M., Filipczyk, A., Gambardella, A., Ahmed, N., et al. (2016). Early myeloid lineage choice is not initiated by random PU.1 to GATA1 protein ratios. Nature *535*, 299–302.

Huber, M., and Lohoff, M. (2014). IRF4 at the crossroads of effector T-cell fate decision. Eur. J. Immunol. *44*, 1886–1895.

Inoki, K., Zhu, T., and Guan, K.-L. (2003). TSC2 mediates cellular energy response to control cell growth and survival. Cell *115*, 577–590.

Ito, K., Carracedo, A., Weiss, D., Arai, F., Ala, U., Avigan, D.E., Schafer, Z.T., Evans, R.M., Suda, T., Lee, C.-H., et al. (2012). A PML–PPAR-δ pathway for fatty acid oxidation regulates hematopoietic stem cell maintenance. Nat. Med. *18*, 1350–1358.

Ito, K., and Ito, K. (2016). Metabolism and the Control of Cell Fate Decisions and Stem Cell Renewal. Annu. Rev. Cell Dev. Biol. *32*, 399–409.

Ito, K., Turcotte, R., Cui, J., Zimmerman, S.E., Pinho, S., Mizoguchi, T., Arai, F., Runnels, J.M., Alt, C., Teruya-Feldstein, J., et al. (2016). Self-renewal of a purified Tie2+ hematopoietic stem cell population relies on mitochondrial clearance. Science *354*, 1156–1160.

Jang, K.-J., Mano, H., Aoki, K., Hayashi, T., Muto, A., Nambu, Y., Takahashi, K., Itoh, K., Taketani, S., Nutt, S.L., et al. (2015). Mitochondrial function provides instructive signals for activation-induced B-cell fates. Nat Commun *6*, 6750.

Jørgensen, S.B., Viollet, B., Andreelli, F., Frøsig, C., Birk, J.B., Schjerling, P., Vaulont, S., Richter, E.A., and Wojtaszewski, J.F.P. (2004). Knockout of the alpha2 but not alpha1 5'-AMP-activated protein kinase isoform abolishes 5-aminoimidazole-4-carboxamide-1-beta-4-ribofuranosidebut not contraction-induced glucose uptake in skeletal muscle. J. Biol. Chem. *279*, 1070–1079.

Kaech, S.M., and Ahmed, R. (2001). Memory CD8+ T cell differentiation: initial antigen

encounter triggers a developmental program in naïve cells. Nat Immunol *2*, 415–422.

Katajisto, P., Döhla, J., Chaffer, C.L., Pentinmikko, N., Marjanovic, N., Iqbal, S., Zoncu, R., Chen, W., Weinberg, R.A., and Sabatini, D.M. (2015). Asymmetric apportioning of aged mitochondria between daughter cells is required for stemness. Science *348*, 340–343.

Keppler, S.J., Gasparrini, F., Burbage, M., Aggarwal, S., Frederico, B., Geha, R.S., Way, M., Bruckbauer, A., and Batista, F.D. (2015). Wiskott-Aldrich Syndrome Interacting Protein Deficiency Uncovers the Role of the Co-receptor CD19 as a Generic Hub for PI3 Kinase Signaling in B Cells. Immunity *43*, 660–673.

Klein, U., Casola, S., Cattoretti, G., Shen, Q., Lia, M., Mo, T., Ludwig, T., Rajewsky, K., and Dalla-Favera, R. (2006). Transcription factor IRF4 controls plasma cell differentiation and class-switch recombination. Nat Immunol *7*, 773–782.

Kurotaki, D., Yamamoto, M., Nishiyama, A., Uno, K., Ban, T., Ichino, M., Sasaki, H., Matsunaga, S., Yoshinari, M., Ryo, A., et al. (2014). IRF8 inhibits C/EBPα activity to restrain mononuclear phagocyte progenitors from differentiating into neutrophils. Nat Commun *5*, 4978.

Le Floc'h, A., Tanaka, Y., Bantilan, N.S., Voisinne, G., Altan-Bonnet, G., Fukui, Y., and Huse, M. (2013). Annular PIP3 accumulation controls actin architecture and modulates cytotoxicity at the immunological synapse. Journal of Experimental Medicine *210*, 2721–2737.

Lee, J., Zhou, Y.J., Ma, W., Zhang, W., Aljoufi, A., Luh, T., Lucero, K., Liang, D., Thomsen, M., Bhagat, G., et al. (2017). Lineage specification of human dendritic cells is marked by IRF8 expression in hematopoietic stem cells and multipotent progenitors. Nat Immunol *18*, 877–888.

Lin, W.-H.W., Adams, W.C., Nish, S.A., Chen, Y.-H., Bonnie, Y., Rothman, N.J., Kratchmarov, R., Okada, T., Klein, U., and Reiner, S.L. (2015). Asymmetric PI3K Signaling Driving Developmental and Regenerative Cell Fate Bifurcation. Cell Reports *13*, 2203–2218.

Lin, W.-H.W., Nish, S.A., Bonnie, Y., Chen, Y.-H., Adams, W.C., Kratchmarov, R., Rothman, N.J., Bhandoola, A., Xue, H.-H., and Reiner, S.L. (2016). CD8(+) T Lymphocyte Self-Renewal during Effector Cell Determination. Cell Reports *17*, 1773–1782.

Liu, K., Victora, G.D., Schwickert, T.A., Guermonprez, P., Meredith, M.M., Yao, K., Chu, F.-F., Randolph, G.J., Rudensky, A.Y., and Nussenzweig, M. (2009). In vivo analysis of dendritic cell development and homeostasis. Science *324*, 392–397.

Lohoff, M., Mittrücker, H.-W., Brüstle, A., Sommer, F., Casper, B., Huber, M., Ferrick, D.A., Duncan, G.S., and Mak, T.W. (2004). Enhanced TCR-induced apoptosis in interferon regulatory factor 4-deficient CD4(+) Th cells. J. Exp. Med. *200*, 247–253.

Lohoff, M., Mittrücker, H.-W., Prechtl, S., Bischof, S., Sommer, F., Kock, S., Ferrick, D.A., Duncan, G.S., Gessner, A., and Mak, T.W. (2002). Dysregulated T helper cell differentiation in the absence of interferon regulatory factor 4. Proc. Natl. Acad. Sci. U.S.a. *99*, 11808–11812.

Lucas, C.L., Chandra, A., Nejentsev, S., Condliffe, A.M., and Okkenhaug, K. (2016). PI3Kδ and primary immunodeficiencies. Nat Rev Immunol *16*, 702–714.

Luchsinger, L.L., de Almeida, M.J., Corrigan, D.J., Mumau, M., and Snoeck, H.-W. (2016). Mitofusin 2 maintains haematopoietic stem cells with extensive lymphoid potential. Nature *529*, 528–531.

Macintyre, A.N., Gerriets, V.A., Nichols, A.G., Michalek, R.D., Rudolph, M.C., Deoliveira, D., Anderson, S.M., Abel, E.D., Chen, B.J., Hale, L.P., et al. (2014). The glucose transporter Glut1 is selectively essential for CD4 T cell activation and effector function. Cell Metab. *20*, 61–72.

Mahnke, J., Schumacher, V., Ahrens, S., Käding, N., Feldhoff, L.M., Huber, M., Rupp, J., Raczkowski, F., and Mittrücker, H.-W. (2016). Interferon Regulatory Factor 4 controls TH1 cell effector function and metabolism. Sci Rep *6*, 35521.

Man, K., Miasari, M., Shi, W., Xin, A., Henstridge, D.C., Preston, S., Pellegrini, M., Belz, G.T., Smyth, G.K., Febbraio, M.A., et al. (2013). The transcription factor IRF4 is essential for TCR affinity-mediated metabolic programming and clonal expansion of T cells. Nat Immunol *14*, 1155–1165.

Marat, A.L., and Haucke, V. (2016). Phosphatidylinositol 3-phosphates-at the interface between cell signalling and membrane traffic. Embo J. *35*, 561–579.

Masopust, D., Vezys, V., Marzo, A.L., and Lefrançois, L. (2001). Preferential localization of effector memory cells in nonlymphoid tissue. Science *291*, 2413–2417.

Metz, P.J., Arsenio, J., Kakaradov, B., Kim, S.H., Remedios, K.A., Oakley, K., Akimoto, K., Ohno, S., Yeo, G.W., and Chang, J.T. (2015). Regulation of Asymmetric Division and CD8+ T Lymphocyte Fate Specification by Protein Kinase Cζ and Protein Kinase Cλ/ι. J. Immunol. *194*, 2249–2259.

Metz, P.J., Lopez, J., Kim, S.H., Akimoto, K., Ohno, S., and Chang, J.T. (2016). Regulation of Asymmetric Division by Atypical Protein Kinase C Influences Early Specification of CD8(+) T Lymphocyte Fates. Sci Rep *6*, 19182.

Michalek, R.D., Gerriets, V.A., Jacobs, S.R., Macintyre, A.N., MacIver, N.J., Mason, E.F., Sullivan, S.A., Nichols, A.G., and Rathmell, J.C. (2011). Cutting edge: distinct glycolytic and lipid oxidative metabolic programs are essential for effector and regulatory CD4+ T cell subsets. J. Immunol. *186*, 3299–3303.

Mishra, P., and Chan, D.C. (2014). Mitochondrial dynamics and inheritance during cell division, development and disease. Nat. Rev. Mol. Cell Biol. *15*, 634–646.

Morrison, S.J., and Kimble, J. (2006). Asymmetric and symmetric stem-cell divisions in development and cancer. Nature *441*, 1068–1074.

Murphy, T.L., Grajales-Reyes, G.E., Wu, X., Tussiwand, R., Briseño, C.G., Iwata, A., Kretzer, N.M., Durai, V., and Murphy, K.M. (2016). Transcriptional Control of Dendritic Cell Development. Annu. Rev. Immunol. *34*, 93–119.

Naik, S.H., Metcalf, D., van Nieuwenhuijze, A., Wicks, I., Wu, L., O'Keeffe, M., and Shortman, K. (2006). Intrasplenic steady-state dendritic cell precursors that are distinct from monocytes. Nat Immunol *7*, 663–671.

Naik, S.H., Perié, L., Swart, E., Gerlach, C., van Rooij, N., de Boer, R.J., and Schumacher, T.N. (2013). Diverse and heritable lineage imprinting of early haematopoietic progenitors. Nature *496*, 229–232.

Naik, S.H., Proietto, A.I., Wilson, N.S., Dakic, A., Schnorrer, P., Fuchsberger, M., Lahoud, M.H., O'Keeffe, M., Shao, Q.-X., Chen, W.-F., et al. (2005). Cutting edge: generation of splenic CD8+ and CD8- dendritic cell equivalents in Fms-like tyrosine kinase 3 ligand bone marrow cultures. J. Immunol. *174*, 6592–6597.

Nakada, D., Saunders, T.L., and Morrison, S.J. (2010). Lkb1 regulates cell cycle and energy metabolism in haematopoietic stem cells. Nature *468*, 653–658.

Nish, S.A., Lin, W.-H.W., and Reiner, S.L. (2017a). Lymphocyte Fate and Metabolism: A Clonal Balancing Act. Trends in Cell Biology *27*, 946–954.

Nish, S.A., Zens, K.D., Kratchmarov, R., Lin, W.-H.W., Adams, W.C., Chen, Y.-H., Bonnie, Y., Rothman, N.J., Bhandoola, A., Xue, H.-H., et al. (2017b). CD4+ T cell effector commitment coupled to self-renewal by asymmetric cell divisions. Journal of Experimental Medicine *214*, 39–47.

Nobs, S.P., Schneider, C., Dietrich, M.G., Brocker, T., Rolink, A., Hirsch, E., and Kopf, M. (2015). PI3-Kinase-γ Has a Distinct and Essential Role in Lung-Specific Dendritic Cell Development. Immunity *43*, 674–689.

O'Sullivan, D., van der Windt, G.J.W., Huang, S.C.-C., Curtis, J.D., Chang, C.-H., Buck, M.D., Qiu, J., Smith, A.M., Lam, W.Y., DiPlato, L.M., et al. (2014). Memory CD8(+) T cells use cell-intrinsic lipolysis to support the metabolic programming necessary for development. Immunity *41*, 75–88.

O'Sullivan, T.E., Johnson, L.R., Kang, H.H., and Sun, J.C. (2015). BNIP3- and BNIP3L-Mediated Mitophagy Promotes the Generation of Natural Killer Cell Memory. Immunity *43*, 331–342.

Owusu-Ansah, E., and Banerjee, U. (2009). Reactive oxygen species prime Drosophila haematopoietic progenitors for differentiation. Nature *461*, 537–541.

Pang, W.W., Price, E.A., Sahoo, D., Beerman, I., Maloney, W.J., Rossi, D.J., Schrier,

S.L., and Weissman, I.L. (2011). Human bone marrow hematopoietic stem cells are increased in frequency and myeloid-biased with age. Proc. Natl. Acad. Sci. U.S.a. *108*, 20012–20017.

Pearce, E.L., Walsh, M.C., Cejas, P.J., Harms, G.M., Shen, H., Wang, L.-S., Jones, R.G., and Choi, Y. (2009). Enhancing CD8 T-cell memory by modulating fatty acid metabolism. Nature *460*, 103–107.

Pedicord, V.A., Cross, J.R., Montalvo-Ortiz, W., Miller, M.L., and Allison, J.P. (2015). Friends not foes: CTLA-4 blockade and mTOR inhibition cooperate during CD8+ T cell priming to promote memory formation and metabolic readiness. J. Immunol. *194*, 2089–2098.

Pei, W., Feyerabend, T.B., Rössler, J., Wang, X., Postrach, D., Busch, K., Rode, I., Klapproth, K., Dietlein, N., Quedenau, C., et al. (2017). Polylox barcoding reveals haematopoietic stem cell fates realized in vivo. Nature *548*, 456–460.

Pham, K., Shimoni, R., Charnley, M., Ludford-Menting, M.J., Hawkins, E.D., Ramsbottom, K., Oliaro, J., Izon, D., Ting, S.B., Reynolds, J., et al. (2015). Asymmetric cell division during T cell development controls downstream fate. The Journal of Cell Biology *210*, 933–950.

Pollizzi, K.N., and Powell, J.D. (2014). Integrating canonical and metabolic signalling programmes in the regulation of T cell responses. Nat Rev Immunol *14*, 435–446.

Pollizzi, K.N., Sun, I.-H., Patel, C.H., Lo, Y.-C., Oh, M.-H., Waickman, A.T., Tam, A.J., Blosser, R.L., Wen, J., Delgoffe, G.M., et al. (2016). Asymmetric inheritance of mTORC1 kinase activity during division dictates CD8(+) T cell differentiation. Nat Immunol *17*, 704–711.

Powell, J.D., Lerner, C.G., and Schwartz, R.H. (1999). Inhibition of cell cycle progression by rapamycin induces T cell clonal anergy even in the presence of costimulation. J. Immunol. *162*, 2775–2784.

Ray, J.P., Staron, M.M., Shyer, J.A., Ho, P.-C., Marshall, H.D., Gray, S.M., Laidlaw, B.J., Araki, K., Ahmed, R., Kaech, S.M., et al. (2015). The Interleukin-2-mTORc1 Kinase Axis Defines the Signaling, Differentiation, and Metabolism of T Helper 1 and Follicular B Helper T Cells. Immunity *43*, 690–702.

Reiner, S.L., and Adams, W.C. (2014). Lymphocyte fate specification as a deterministic but highly plastic process. Nat Rev Immunol *14*, 699–704.

Reinhardt, R.L., Khoruts, A., Merica, R., Zell, T., and Jenkins, M.K. (2001). Visualizing the generation of memory CD4 T cells in the whole body. Nature *410*, 101–105.

Rimmelé, P., Liang, R., Bigarella, C.L., Kocabas, F., Xie, J., Serasinghe, M.N., Chipuk, J., Sadek, H., Zhang, C.C., and Ghaffari, S. (2015). Mitochondrial metabolism in hematopoietic stem cells requires functional FOXO3. EMBO Rep. *16*, 1164–1176.

Sallusto, F., Geginat, J., and Lanzavecchia, A. (2004). Central memory and effector memory T cell subsets: function, generation, and maintenance. Annu. Rev. Immunol. *22*, 745–763.

Sathaliyawala, T., O'Gorman, W.E., Greter, M., Bogunovic, M., Konjufca, V., Hou, Z.E., Nolan, G.P., Miller, M.J., Merad, M., and Reizis, B. (2010). Mammalian target of rapamycin controls dendritic cell development downstream of Flt3 ligand signaling. Immunity *33*, 597–606.

Scheffler, J.M., Sparber, F., Tripp, C.H., Herrmann, C., Humenberger, A., Blitz, J., Romani, N., Stoitzner, P., and Huber, L.A. (2014). LAMTOR2 regulates dendritic cell homeostasis through FLT3-dependent mTOR signalling. Nat Commun *5*, 5138.

Schlitzer, A., Sivakamasundari, V., Chen, J., Sumatoh, H.R.B., Schreuder, J., Lum, J., Malleret, B., Zhang, S., Larbi, A., Zolezzi, F., et al. (2015). Identification of cDC1- and cDC2-committed DC progenitors reveals early lineage priming at the common DC progenitor stage in the bone marrow. Nat Immunol *16*, 718–728.

Schweighoffer, E., Nys, J., Vanes, L., Smithers, N., and Tybulewicz, V.L.J. (2017). TLR4 signals in B lymphocytes are transduced via the B cell antigen receptor and SYK. Journal of Experimental Medicine *214*, 1269–1280.

Sena, L.A., Li, S., Jairaman, A., Prakriya, M., Ezponda, T., Hildeman, D.A., Wang, C.-R., Schumacker, P.T., Licht, J.D., Perlman, H., et al. (2013). Mitochondria are required for antigen-specific T cell activation through reactive oxygen species signaling. Immunity *38*, 225–236.

Sengupta, A., Duran, A., Ishikawa, E., Florian, M.C., Dunn, S.K., Ficker, A.M., Leitges, M., Geiger, H., Diaz-Meco, M., Moscat, J., et al. (2011). Atypical protein kinase C (aPKCzeta and aPKClambda) is dispensable for mammalian hematopoietic stem cell activity and blood formation. Proc. Natl. Acad. Sci. U.S.a. *108*, 9957–9962.

Severinson, E., and Westerberg, L. (2003). Regulation of adhesion and motility in B lymphocytes. Scand. J. Immunol. *58*, 139–144.

Sezgin, E., Levental, I., Mayor, S., and Eggeling, C. (2017). The mystery of membrane organization: composition, regulation and roles of lipid rafts. Nat. Rev. Mol. Cell Biol. *18*, 361–374.

Sichien, D., Scott, C.L., Martens, L., Vanderkerken, M., Van Gassen, S., Plantinga, M., Joeris, T., De Prijck, S., Vanhoutte, L., Vanheerswynghels, M., et al. (2016). IRF8 Transcription Factor Controls Survival and Function of Terminally Differentiated Conventional and Plasmacytoid Dendritic Cells, Respectively. Immunity *45*, 626–640.

Sinclair, C., Bommakanti, G., Gardinassi, L., Loebbermann, J., Johnson, M.J., Hakimpour, P., Hagan, T., Benitez, L., Todor, A., Machiah, D., et al. (2017). mTOR regulates metabolic adaptation of APCs in the lung and controls the outcome of allergic inflammation. Science *357*, 1014–1021.

Sinclair, L.V., Rolf, J., Emslie, E., Shi, Y.-B., Taylor, P.M., and Cantrell, D.A. (2013). Control of amino-acid transport by antigen receptors coordinates the metabolic reprogramming essential for T cell differentiation. Nat Immunol *14*, 500–508.

Snoeck, H.-W. (2013). Aging of the hematopoietic system. Curr. Opin. Hematol. *20*, 355–361.

Staudt, V., Bothur, E., Klein, M., Lingnau, K., Reuter, S., Grebe, N., Gerlitzki, B., Hoffmann, M., Ulges, A., Taube, C., et al. (2010). Interferon-regulatory factor 4 is essential for the developmental program of T helper 9 cells. Immunity *33*, 192–202.

Taylor, J.J., Pape, K.A., Steach, H.R., and Jenkins, M.K. (2015). Apoptosis and antigen affinity limit effector cell differentiation of a single naïve B cell. Science *347*, 784–787.

Thaunat, O., Granja, A.G., Barral, P., Filby, A., Montaner, B., Collinson, L., Martinez-Martin, N., Harwood, N.E., Bruckbauer, A., and Batista, F.D. (2012). Asymmetric segregation of polarized antigen on B cell division shapes presentation capacity. Science *335*, 475–479.

Ting, S.B., Deneault, E., Hope, K., Cellot, S., Chagraoui, J., Mayotte, N., Dorn, J.F., Laverdure, J.-P., Harvey, M., Hawkins, E.D., et al. (2012). Asymmetric segregation and self-renewal of hematopoietic stem and progenitor cells with endocytic Ap2a2. Blood *119*, 2510–2522.

Tominaga, N., Ohkusu-Tsukada, K., Udono, H., Abe, R., Matsuyama, T., and Yui, K. (2003). Development of Th1 and not Th2 immune responses in mice lacking IFN-regulatory factor-4. Int. Immunol. *15*, 1–10.

Tubo, N.J., Pagán, A.J., Taylor, J.J., Nelson, R.W., Linehan, J.L., Ertelt, J.M., Huseby, E.S., Way, S.S., and Jenkins, M.K. (2013). Single Naive CD4(+) T Cells from a Diverse Repertoire Produce Different Effector Cell Types during Infection. Cell *153*, 785–796.

Tussiwand, R., Everts, B., Grajales-Reyes, G.E., Kretzer, N.M., Iwata, A., Bagaitkar, J., Wu, X., Wong, R., Anderson, D.A., Murphy, T.L., et al. (2015). Klf4 expression in conventional dendritic cells is required for T helper 2 cell responses. Immunity *42*, 916–928.

van der Windt, G.J.W., O'Sullivan, D., Everts, B., Huang, S.C.-C., Buck, M.D., Curtis, J.D., Chang, C.-H., Smith, A.M., Ai, T., Faubert, B., et al. (2013). CD8 memory T cells have a bioenergetic advantage that underlies their rapid recall ability. Proc. Natl. Acad. Sci. U.S.a. *110*, 14336–14341.

Vander Lugt, B., Khan, A.A., Hackney, J.A., Agrawal, S., Lesch, J., Zhou, M., Lee, W.P., Park, S., Xu, M., DeVoss, J., et al. (2014). Transcriptional programming of dendritic cells for enhanced MHC class II antigen presentation. Nat Immunol *15*, 161–167.

Verbist, K.C., Guy, C.S., Milasta, S., Liedmann, S., Kamiński, M.M., Wang, R., and Green, D.R. (2016). Metabolic maintenance of cell asymmetry following division in

activated T lymphocytes. Nature *532*, 389–393.

Wang, D., Wang, J., Bonamy, G.M.C., Meeusen, S., Brusch, R.G., Turk, C., Yang, P., and Schultz, P.G. (2012). A small molecule promotes mitochondrial fusion in mammalian cells. Angew. Chem. Int. Ed. Engl. *51*, 9302–9305.

Wang, H., Yan, M., Sun, J., Jain, S., Yoshimi, R., Abolfath, S.M., Ozato, K., Coleman, W.G., Ng, A.P., Metcalf, D., et al. (2014). A reporter mouse reveals lineage-specific and heterogeneous expression of IRF8 during lymphoid and myeloid cell differentiation. J. Immunol. *193*, 1766–1777.

Wang, Y., Huang, G., Zeng, H., Yang, K., Lamb, R.F., and Chi, H. (2013). Tuberous sclerosis 1 (Tsc1)-dependent metabolic checkpoint controls development of dendritic cells. Proc. Natl. Acad. Sci. U.S.a. *110*, E4894–E4903.

Wieman, H.L., Wofford, J.A., and Rathmell, J.C. (2007). Cytokine stimulation promotes glucose uptake via phosphatidylinositol-3 kinase/Akt regulation of Glut1 activity and trafficking. Mol. Biol. Cell *18*, 1437–1446.

Willinger, T., Ferguson, S.M., Pereira, J.P., De Camilli, P., and Flavell, R.A. (2014). Dynamin 2-dependent endocytosis is required for sustained S1PR1 signaling. Journal of Experimental Medicine *211*, 685–700.

Wofford, J.A., Wieman, H.L., Jacobs, S.R., Zhao, Y., and Rathmell, J.C. (2008). IL-7 promotes Glut1 trafficking and glucose uptake via STAT5-mediated activation of Akt to support T-cell survival. Blood *111*, 2101–2111.

Wu, M., Kwon, H.Y., Rattis, F., Blum, J., Zhao, C., Ashkenazi, R., Jackson, T.L., Gaiano, N., Oliver, T., and Reya, T. (2007). Imaging hematopoietic precursor division in real time. Cell Stem Cell *1*, 541–554.

Wu, T., Shin, H.M., Moseman, E.A., Ji, Y., Huang, B., Harly, C., Sen, J.M., Berg, L.J., Gattinoni, L., McGavern, D.B., et al. (2015). TCF1 Is Required for the T Follicular Helper Cell Response to Viral Infection. Cell Reports *12*, 2099–2110.

Xu, H., Chaudhri, V.K., Wu, Z., Biliouris, K., Dienger-Stambaugh, K., Rochman, Y., and Singh, H. (2015a). Regulation of bifurcating B cell trajectories by mutual antagonism between transcription factors IRF4 and IRF8. Nat Immunol *16*, 1274–1281.

Xu, L., Cao, Y., Xie, Z., Huang, Q., Bai, Q., Yang, X., He, R., Hao, Y., Wang, H., Zhao, T., et al. (2015b). The transcription factor TCF-1 initiates the differentiation of T(FH) cells during acute viral infection. Nat Immunol *16*, 991–999.

Xu, X., Araki, K., Li, S., Han, J.-H., Ye, L., Tan, W.G., Konieczny, B.T., Bruinsma, M.W., Martinez, J., Pearce, E.L., et al. (2014). Autophagy is essential for effector CD8(+) T cell survival and memory formation. Nat Immunol *15*, 1152–1161.

Yalcin, S., Marinkovic, D., Mungamuri, S.K., Zhang, X., Tong, W., Sellers, R., and

Ghaffari, S. (2010). ROS-mediated amplification of AKT/mTOR signalling pathway leads to myeloproliferative syndrome in Foxo3(-/-) mice. Embo J. *29*, 4118–4131.

Yao, S., Buzo, B.F., Pham, D., Jiang, L., Taparowsky, E.J., Kaplan, M.H., and Sun, J. (2013). Interferon regulatory factor 4 sustains CD8(+) T cell expansion and effector differentiation. Immunity *39*, 833–845.

Zheng, Y., Chaudhry, A., Kas, A., deRoos, P., Kim, J.M., Chu, T.-T., Corcoran, L., Treuting, P., Klein, U., and Rudensky, A.Y. (2009). Regulatory T-cell suppressor program co-opts transcription factor IRF4 to control T(H)2 responses. Nature *458*, 351–356.

Zhou, X., and Xue, H.-H. (2012). Cutting edge: generation of memory precursors and functional memory CD8+ T cells depends on T cell factor-1 and lymphoid enhancer-binding factor-1. J. Immunol. *189*, 2722–2726.

Zhu, J., Yamane, H., and Paul, W.E. (2010). Differentiation of effector CD4 T cell populations. Annu. Rev. Immunol. *28*, 445–489.

Zimdahl, B., Ito, T., Blevins, A., Bajaj, J., Konuma, T., Weeks, J., Koechlein, C.S., Kwon, H.Y., Arami, O., Rizzieri, D., et al. (2014). Lis1 regulates asymmetric division in hematopoietic stem cells and in leukemia. Nat. Genet. *46*, 245–252.